SCIENTIFIC COMMITTEE
TWENTY-FIRST REGULAR SESSION

Nuku'alofa, Tonga

13–21 August 2025

Stock Assessment of Oceanic Whitetip Shark in the Western and Central Pacific Ocean: 2025

WCPFC-SC21-2025/SA-WP-08
July 2025

Philipp Neubauer[1], **Kath Large**[1]

[1] **Dragonfly Data Science, Wellington, Aotearoa/New Zealand**

Stock assessment of oceanic whitetip shark in the Western and Central Pacific Ocean 2025

Authors:
Philipp Neubauer
Kath Large

DRAGONFLY
Data Science

Cover Notes

To be cited as:

Neubauer, Philipp; Large, Kath (2025). Stock assessment of oceanic whitetip shark in the Western and Central Pacific Ocean 2025, 82 pages. WCPFC-SC21-2025/SA-WP-08. Report to the WCPFC Scientific Committee. Twenty-first Regular Session, 13–21 August 2025.

CONTENTS

EXECUTIVE SUMMARY

The present analysis assessed the oceanic whitetip shark (*Carcharhinus longimanus*; OCS) stock in the Western and Central Pacific Ocean (WCPO), marking the third stock assessment of this stock. The analysis incorporated updated data inputs through 2023 and used methodologies building upon recent WCPFC shark stock assessments to address the challenges and uncertainties inherent in assessing OCS and sharks in general. A central challenge, acknowledged throughout the assessment process, is the paradoxical effect of the primary conservation measure CMM-2011-04 which, while intended to reduce mortality through a non-retention policy, has simultaneously degraded the quality of the scientific data required to monitor its effectiveness.

For this assessment, all data inputs were re-evaluated, and redeveloped. The historical catch series supporting the model was reconstructed using a refined approach for imputing hooks-between-floats (HBF), a critical proxy for fishing depth. Previous assessments treated reported zero-HBF values as true data, which likely inflated early catch estimates. By treating these zeros as missing data, the updated catch history for the early period was markedly lower and less variable than catch estimates used for the previous stock assessment for OCS. Despite improvements in methodologies, a conflict persisted between the standardised catch-per-unit-effort (CPUE) index, which shows a steep historical decline, and the length-composition data, which did not show the expected corresponding decline in the mean size of caught sharks.

In recognition of this data conflict and other structural uncertainties, the 2025 assessment applied a dual-model approach to ensure the robustness of its conclusions. The primary assessment was conducted using an ensemble over integrated, age-structured population models in Stock Synthesis (SS3), which built on the framework of the 2019 assessment. In parallel, a more parsimonious dynamic surplus production model (DSPM) was used. The DSPM relied primarily on catch and CPUE time series, and did not use the conflicting length-composition data. This approach served as a crucial structural sensitivity analysis, and provides an additional perspective on stock status. This multi-model inference strengthens the scientific basis for management advice in a data-limited context.

The multi-model analysis showed that the OCS stock remains in a severely depleted state but is showing signs of recovery. The stock synthesis ensemble estimated that the stock biomass reached a low point around 2013–2014, at approximately 4% of its unfished level. Since then, the biomass was estimated to have experienced a subtle but steady increase, reaching approximately 6% of the unfished level in recent years (i.e., 2022–2023). This trajectory aligned with expectations from previous projection studies, and indicates that the steep decline observed in prior decades has likely been halted. Nevertheless, fundamental uncertainties remain, and recent signs of improvement need to be considered with caution given the subtlety of the estimated increase.

Considering fishing pressure, the largest historical source of fishing mortality was estimated to be from longline fisheries. The significant reduction in interactions resulting from changes in fishing practices over the last decade appears to have been

effective in reducing this pressure. The assessment concluded with high confidence that recent fishing mortality has been below biological limit reference points that would preclude stock rebuilding. The ensemble of models indicates that recent fishing mortality rates are below both F_{lim} and F_{crash} (the fishing mortality that would lead to long-term extinction), and the probability of exceeding these limits was near zero in recent years (i.e., 2022–2023) under the considered models.

Main assessment conclusions

- Based on the precedent of using SS3 for the OCS assessment, and on advances in Bayesian methodologies used for the present assessment (relative to the 2024 silky shark assessment), we suggest that the ensemble of SS3 models be used for management advice.
- The multi-model approach for assessing OCS resulted in a low stock status, but with high confidence that recent fishing mortality is below levels that would preclude stock rebuilding.
- The largest fishing mortality of OCS was estimated to be in longline fisheries. Reductions in OCS interactions as a result of changes in fishing practices over the last decade may have substantially reduced this source of mortality, likely halting the previously observed steep decline, and possibly leading to some (albeit slow) rebuilding.
- Recent fishing mortality rates were below biological limit reference points for the ensemble (Diagnostic F_{recent}/F_{crash}: 0.54 [0.37–0.74]; P(F_{recent}/F_{crash} >1)=0; P(F_{recent}/F_{lim} >1)=0).
- Recent biomass was estimated to have had a subtle increase from a low-point in 2013–14 near 4% of unfinished biomass, to 6% of unfished biomass in recent years (2022–23).

Given some of the fundamental uncertainties highlighted above, we recommend:

- **Improve observer data protocols:** To counter the degradation of data quality resulting from the non-retention conservation measure (CMM-2011-04), it is recommended that longline observer programmes implement clear and consistent directives for recording all capture events, especially unobserved "discarded-cut-free" (DCF) individuals. Furthermore, recording approximate length measurements for sharks released in the water, a practice already in place in some programmes, should be standardised across the Western and Central Pacific Ocean.
- **Prioritise research on stock structure and connectivity:** Fundamental uncertainty remains regarding the stock structure of OCS in the Pacific Ocean. It is recommended that CCMs prioritise and support planned work under the

WCPFC's Shark Research Plan (SRP) involving satellite tagging and expanded genetic/genomics studies to address questions of regional residency, mixing, and stock boundaries.

- **Resolve conflicting life history parameters:** The significant divergence between available growth studies remains a considerable factor for the uncertainty in stock productivity. To build a more robust understanding of this species' life history, it is recommended that work scheduled under the SRP to conduct additional growth studies and validate ageing methods from a range of locations be prioritised.

- **Continue multi-model assessment frameworks:** Given the persistent conflict between CPUE and length data, it is recommended that future assessments continue to use multi-model approaches. The use of simpler models, such as the Dynamic Surplus Production Model, alongside integrated age-structured models, provides a vital cross-assessment, and ensures management advice is robust to structural uncertainty.

- **Refine historical catch estimates:** Although progress has been made, the catch history for the longline fishery remains uncertain with considerable discrepancies between studies. It is recommended that shark catch reconstructions be reviewed, and these discrepancies be explored to gain an improved understanding of core uncertainties.

- **Review and document recent improvements in shark assessment methodologies:** With the present assessment, a full cycle of assessments has now been undertaken for blue, mako, silky and oceanic whitetip sharks, using consistent assessment methods, consistently refined over time. A review workshop and summary paper to capture recent progress and outstanding challenges is recommended to provide a solid basis for upcoming work, and provide an opportunity to share these advances across RFMOs. We recommend this workshop be considered by the Informal Small Working Group: Sharks for inclusion and prioritisation in the Shark Research Plan update at SC21.

1. INTRODUCTION

The Oceanic whitetip shark (*Carcharhinus longimanus*; OCS), is a large, circumglobal pelagic species found predominantly in tropical and warm-temperate oceanic waters (Bonfil et al. 2008, Brouwer et al. 2024). Within the Western and Central Pacific Ocean (WCPO), the species is considered a single stock for assessment purposes (Tremblay-Boyer et al. 2019). Historically regarded as one of the most common sharks in offshore tropical ecosystems, its populations are understood to have undergone significant declines in recent decades (Tremblay-Boyer et al. 2019). In the WCPO, oceanic whitetip sharks are caught almost exclusively as bycatch in the primary commercial fisheries targeting tunas. These interactions occur across two main gear types: the tropical and sub-tropical longline fisheries, which target tunas, billfish, and blue sharks; and, to a lesser degree, the tropical purse seine fisheries (Brouwer et al. 2024). Unlike some other shark species, such as blue shark in the South Pacific, there are no directed commercial fisheries for oceanic whitetip shark in the WCPO in recent years.

The management of oceanic whitetip shark in the WCPO is principally governed by Conservation and Management Measures (CMMs) established by the Western and Central Pacific Fisheries Commission (WCPFC). In response to scientific advice from the first stock assessment in 2012, which indicated a severely depleted stock, the WCPFC adopted CMM-2011-04, effective from 1 January 2013 (Tremblay-Boyer et al. 2019). This measure fundamentally altered the operational context of the fisheries by prohibiting WCPFC Members, Cooperating Non-Members, and Participating Territories (CCMs) from retaining on board, transshipping, storing, or landing any oceanic whitetip shark. The CMM mandated that all individuals caught must be released as soon as possible and in a manner that maximizes their survival. This non-retention policy was later incorporated into the more comprehensive shark management framework of CMM-2019-04, which consolidated measures for multiple shark species.

The implementation of this management framework precipitated a significant and observable shift in fishery operations. Analysis of observer data by Brouwer et al. (2024) documented a substantial change in the fate of captured oceanic whitetip sharks, particularly in the longline fishery. Prior to the 2013–2015 period, the majority of observed individuals were retained. Following the CMM's implementation, there was an abrupt transition, and since 2015, almost all observed oceanic whitetip sharks have been assigned fate codes corresponding to "discarded" or "cut-free" (Brouwer et al. 2024). A similar trend was observed in the purse seine fishery, where retention rates declined steadily over time, with nearly all individuals being discarded since 2015.

This management-driven change in operational practice, while intended to reduce fishing mortality, has created a significant challenge for the scientific assessment of the stock. The shift to a non-retention fishery has paradoxically introduced new sources of potential bias and uncertainty into the very data streams required to evaluate the effectiveness of the conservation measure. As sharks are increasingly released without being brought on board, often by cutting the branchline, observers face considerable difficulty in accurately identifying the species, measuring its length, or even consistently recording the interaction event itself. This issue was highlighted as

a major concern in the 2019 assessment (Tremblay-Boyer et al. 2019), which noted that the quality of both catch-per-unit-effort (CPUE) and length-composition time series is compromised in the post-CMM period. Consequently, the scientific process must now account for a management action that, while beneficial for the stock, simultaneously degrades the data required to monitor it.

The 2025 assessment is the third comprehensive evaluation of the oceanic whitetip shark stock in the WCPO. The two preceding assessments established the scientific consensus regarding the stock's depleted status. The inaugural stock assessment for oceanic whitetip shark in the WCPO (Rice & Harley 2012) covered the period from 1995 to 2009. It provided the first quantitative evaluation of the stock's status, concluding that it was severely depleted. The assessment estimated that the spawning biomass had declined by 86% from its 1995 level and that fishing mortality was approximately 6.5 times the level associated with maximum sustainable yield (F_{MSY}), indicating the stock was both overfished and subject to overfishing.

The second and most recent assessment (Tremblay-Boyer et al. 2019) extended the model time series to 2016, incorporating the first four years of data collected after the implementation of CMM-2011-04. This assessment was notable for its use of a comprehensive structural uncertainty grid, which explored 648 different model configurations to characterize the high degree of uncertainty in data and biological parameters. Despite these methodological advancements and the inclusion of data from the non-retention period, the assessment upheld the conclusions of the 2012 assessment, finding that the stock remained overfished and was still undergoing overfishing.

The 2019 assessment documented several critical uncertainties and data conflicts that have shaped the direction of subsequent research and the design of the 2025 assessment. The most significant technical challenge identified was a persistent conflict between the two primary sources of information on stock trends. The standardized longline CPUE index showed a steep and continuous decline in relative abundance from the late 1990s. However, this trend was not corroborated by the length-composition data, which lacked a corresponding decline in the mean length of caught sharks. Such a decline in size would be the expected demographic signature of a heavily exploited population losing its older, larger individuals. This inconsistency suggested that at least one of the primary data inputs was providing a biased signal of the stock's dynamics.

In addition, the historical catch series was identified as a key source of uncertainty. Due to poor historical logsheet reporting for bycatch species, particularly before it became mandatory, the assessment relied on catches reconstructed from observer data. The sparse and non-representative distribution of observer effort, especially in the early years of the fishery, introduced considerable uncertainty into the magnitude and trend of total fishery removals.

The 2019 assessment outcomes were demonstrated to be sensitive to assumptions regarding key life history parameters. The choice of growth model (e.g., the faster growth profile from Seki et al. (1998) versus the slower, less productive profiles from

Joung et al. (2016) or D'Alberto et al. (2017)), natural mortality (M), and the steepness (h) of the stock-recruitment relationship, all had substantial impacts on the estimates of stock status and productivity.

The 2019 assessment was also the first assessment to grapple with the interpretation of data from the post-CMM-2011-04 era. It highlighted the difficulty in reliably interpreting CPUE and length data from 2013 onwards, given the unquantified effects of non-retention practices on observer reporting protocols and the potential for unrecorded release events.

Projections using the 2019 stock assessment model under alternative assumptions of recent fishing and post-release mortalities highlighted the likely importance of recent non-retention and release practices on the ability of the stock to rebuild from recent low levels (Bigelow & Carvalho 2021, Bigelow et al. 2022). Whether non-retention measures and handling/release practices in years since CMM2011-04 have been sufficient to stop the decline of the oceanic whitetip stock and allow for rebuilding was therefore a central question for the present stock assessment.

The 2025 stock assessment was based upon a re-evaluation and redevelopment of all key data inputs (Brouwer et al. 2024, Hill-Moana et al. 2024). This preparatory work, refined through discussions at the 2025 Pre-Assessment Workshop (PAW; Hamer 2025), incorporated methodological advancements from other recent WCPO shark assessments to address the specific uncertainties associated with oceanic whitetip shark.

In recognition of the significant uncertainties in the input data, particularly for the post-CMM period, the 2025 assessment employed a dual-model approach. This strategy, recommended by the Scientific Committee and endorsed at the PAW (Hamer 2025), was designed to ensure the robustness of management advice by evaluating the consistency of results across different model structures. The primary assessment was conducted using an integrated, age-structured population model implemented in Stock Synthesis (SS3), and proceeds in a stepwise fashion, building from the structure of the 2019 assessment and incorporating the updated data inputs and methodological refinements. A dynamic surplus production model, also known as a biomass dynamic model (BDM), was run in parallel. This type of model is more parsimonious, relying primarily on a time series of catch and an index of relative abundance (CPUE), and is therefore less sensitive to the the conflicting length-composition data. The BDM served as a crucial structural sensitivity, providing an alternative perspective on stock productivity and status.

The primary objective of the 2025 assessment was to provide the WCPFC with updated and robust scientific advice on the status of the oceanic whitetip shark stock, including estimates of stock status relative to potential biological reference points. A specific objective, highlighted in the preparatory work, was to explicitly test the hypothesis that fishing-related mortality has decreased since 2015, and to provide commentary on recent trends in stock status since the full implementation of the non-retention CMMs. This directly addresses the critical management question regarding the efficacy of the

primary conservation measure for this species.

2. METHODS

2.1 Data inputs

2.1.1 Catch assumptions

Catches were reconstructed in Hill-Moana et al. (2024) for years between 1995 and 2022 using an ensemble of spatial GLMM models that included effects for oceanographic predictors as well as targeting and total effort per stratum (5x5 degree grid, flag, year, month). A key difference between updated catch estimates produced in Hill-Moana et al. (2024) was a markedly lower estimate of over-all catch-levels in the late 1990s and early 2010s. Although these estimates were in line with estimates produced in Peatman et al. (2018b), the difference in estimates was not fully explained.

For the present assessment, the analysis presented in Hill-Moana et al. (2024) was updated with data up to 2023. As part of this process, we aimed to more conclusively resolve differences between catches used in Tremblay-Boyer et al. (2019) and the updated catch time-series. While the difference in the use of spatial model terms was put forward initially as a source of differences, another difference was that recent models have used proxies for gear depth, because hooks-between-floats (HBF), the most informative gear characteristic in that respect, is not fully reported for WCPFC longline effort. Tremblay-Boyer et al. (2019) used random forests based on effort data with reported HBF and target catch composition to impute (predict) deep (>10 HBF) vs shallow (<10 HBF) fishing effort. In models used since 2021 (i.e., the blue shark stock assessment), an alternative proxy for targeting and gear configuration in terms of catch proportions of other species was used. To enable a more direct comparison between analyses in Tremblay-Boyer et al. (2019) and in Hill-Moana et al. (2024), we repeated our analysis using HBF instead of species compositions.

Our analysis of CPUE (Hill-Moana et al. 2024) showed that hooks between floats are an important predictor of OCS catch rates (Figure 1), but that catch rates decline abruptly around HBF numbers higher than 8, consistent with findings that most OCS captures occur at low hook numbers (i.e., close to floats; Brouwer et al. 2024). In addition, the slow but consistent decline in catch rates for sets with HBF>8 may be important in driving over-all catch rates. We therefore chose to directly impute HBF (as opposed to imputing HBF categories) using a model based on a boosted-regression tree (BRT) with a Poisson loss function.

Importantly, we found that many reported HBF in the HBF-disaggregated effort dataset were reported as zeros; sometimes in a pattern (e.g., all early Korean effort reported zero HBF), sometimes at random (e.g., 5x5xfleet strata with zero HBF recorded; Figure 2). In most cases, these zeros almost certainly reflect an absence of data rather than an actual HBF value, but were treated as actual data (i.e., zero HBF) in the previous catch-reconstruction for OCS by Tremblay-Boyer et al. (2019). Coupled with high estimated

catch-rates at low HBF, and large amounts of effort in strata with reported zeros, this treatment of HBF explained the difference in scale in predicted catches compared to the 2024 catch reconstructions presented in Hill-Moana et al. (2024). Applying our catch reconstruction methods to a dataset with similar assumptions (treating zero HBF as data) to Tremblay-Boyer et al. (2019) yielded estimates on the same scale (Figure A-1). For the following, we treated zeros as missing data, and imputed HBF across any effort with missing HBF or reported zeros (Table 1).

Our initial predictions using the BRT approach to impute HBF for missing or zero records were mainly driven by differences in average HBF between flags, with changes over time and by area (Figure 3). However, the relative importance of predictors was strongly dependent on the treatment of predictors. We initially used target species catch rates as predictors. Changing this to catch proportions for target substantially changed the relative importance of predictors in the BRT model. However, this change made hardly any difference to the predicted HBF and ultimately to total predicted catches, suggesting strong aliasing of different factors in the HBF imputation model. For consistency with previous analyses, we used the species proportion formulation in subsequent analyses.

The BRT model was able to predict HBF reasonably well (Figure 4), although low HBF tended to be slightly over-predicted, and at high HBF the model often under-predicted HBFs. The latter case is less problematic since catch-rates are generally low for sets with high HBF. Predicted HBF for missing data generally aligned well with observed HBF in most cases (Figures 5, 6), predicting consistently high HBF for Korean effort for missing years, for example. Most of the imputed effort was deep (>=10 HBF), although some effort from Chinese Taipei and Tonga was predicted as using low numbers of HBFs (Figure 6).

Total catches estimated using HBF were on a similar level to those estimated previously in Hill-Moana et al. (2024) without the use of HBF (Figure 7), but lacked the large spikes in predicted catches seen in the earlier analysis. They also suggest slightly lower catches early in the time-series than initial estimates, but were otherwise comparable.

2.1.2 Discards and survival

Given the likely importance of discard and survival rates for contemporary dynamics of OCS (Bigelow & Carvalho 2021, Bigelow et al. 2022), we aimed to construct a range of plausible catch trajectories based on levels of handling and discard mortality. The time-series were constructed based on models developed in Neubauer et al. (2021a). Briefly, we assumed 100% mortality for retained and/or finned sharks. In addition, for discarded sharks, any sharks that had a condition at release of 'Dead' or 'Alive - dying' were classified as dead/retained.

Although information about condition at release is frequently recorded in recent years, records prior to 2015 often had fate codes indicating discard (e.g., "Discarded - other reason", or "Discarded - shark damage"), but had missing condition-at-release information. Nevertheless, these data often had information on the condition at

capture. In order to obtain a better picture of discard mortality prior to 2015, we used a binomial GLMM to infer the condition at release (i.e., dead or likely dying vs. alive and healthy) from the condition at capture (cond code), species, vessel and flag. Unlike analyses for blue shark developed in Neubauer et al. (2021a), recent analyses have been conducted across all shark species to allow for borrowing of information across species, but included a species factor to adjust for species specific differences. We also included flag-year interactions to account for potential changes in handling by fleets. All but the condition effects were fitted as random effects, and the final model for the expected number of mortalities for a given number of records in each stratum was then:

```
condD.num | trials(records) ~ (1 | flag_id) +(1 | yy) + (1 |
flag_id:yy) + (1 | species) + (1 | vessel_id) + cond_code
```

where condD.num was the number of sharks classified as dead out of the total number of records. The fate of captured individuals was largely driven by the condition at capture (injured or dying individuals were mostly likely dead on discard), but also varied by flag, year, and species (Figure 8), as well as by vessel. Oceanic whitetip shark had the lowest estimated rate of handling mortality of all shark species, leading to estimates of low mortality for individuals in good condition (A0–A2; Figure 8). The model above allowed us to predict the expected condition at release (dead or alive) of discarded individuals for which the condition at release was not recorded.

To estimate trends in discarding, we used the recorded and imputed discard status to estimate trends in proportions of live-discarded individuals by flag and year. The main purpose of this model was to estimate a live-discard rate by year and fleet that could be applied to estimated catches. The model was largely similar to the condition model, and was written as:

```
FateD.num | trials(records) ~ (1 | flag_id) + (1 | flag_id:yy) + (1 | species) +
(1 | vessel_id) + s(year)
```

Models were fitted using MCMC sampling in 'brms' as outlined above. Year was the largest estimated effect (Figure 9), resulting in an estimate of high recent live-discards of between 50 and 75%. We applied the 25%, 50% (median) and 75% percentiles of the posterior distribution of predicted live-discards, to predicted catches (posterior median and 90^{th} percentile of predicted catches) to derive the total fishing related mortality used in the stock assessment.

Interaction estimates for longline and purse-seine were combined with the model for annual discard rates per flag (Figures 10, 11), which was used to produce scenarios of total fishing-induced mortality. Due to high discard uncertainties, especially before increased observer coverage in the 2010s, we considered the possibility of high and low discards alongside the base assumption of the median discard estimate from the discard model (Figures 12, 13, 14, 15). Post-release mortality was included at a rate of 8% (Bigelow et al. 2022) in the calculations of total fishing-related mortality for longline fisheries, and was applied at a rate of 85% for purse-seine fisheries. Given relatively

low catches in purse-seine fisheries, the latter value was unlikely to play a role in the stock assessment.

We only considered median estimates of total captures as the estimates had relatively low uncertainty, but we considered the 25th and 75th percentile for predicted discard fate predictions, as the latter determines how many sharks are assumed to survive capture.

2.1.3 CPUE indices

Observer-based CPUE indices were presented in Hill-Moana et al. (2024). Upon examination, we found that the large peaks in CPUE across all indices were largely driven by very few records in the observer dataset with very high catch-rates (Figure 16). It was considered likely that these high catch rates represent data errors, or shark targeting that was not identifiable as such (recorded shark target sets or sets using shark lines were excluded from CPUE). We therefore updated the analyses presented in Hill-Moana et al. (2024) using a threshold of 0.5 OCS per 1000 hooks as a cutoff. The resulting index is very similar in terms of over-all trends, but early catch rates were lower than those predicted without the threshold (Figure 17). In addition, extending the CPUE to 2023 showed a more marked uptick in CPUE since about 2016, mirroring CPUE increases seen in purse-seine catch rates in recent years (Hill-Moana et al. 2024). The sensitivity to these successive CPUE developments was tested within the step-wise updates of the 2019 assessment.

2.1.4 Length compositions

The previous stock assessment used raw, un-scaled or standardised length compositions, and noted a conflict between indices and length compositions in the model, with compositions not reflecting the steep decline in CPUE. For the present assessment, length compositions were standardised and scaled using model-based methods (Hill-Moana et al. 2024). As for the 2024 silky shark assessment, we separated compositions for capture and index fleets, scaling the former by catch and the latter by CPUE. However, even when standardising for observer programme, latitude and year, the scaled length compositions for longline fisheries lacked a clear trend (Figure 18); the sparse compositions for purse seine were used only to derive a selectivity in the stock assessment, and contain little other information given the small number of OCS measured from PS captures (Figure 19).

2.2 Biological assumptions

2.2.1 Biological and stock structure assumptions

The extent of biological knowledge about oceanic whitetip sharks in the Pacific Ocean and beyond was summarised by Tremblay-Boyer et al. (2019). The authors' found little evidence for sub-stocks within the Pacific, and it is generally thought that OCS

travel long distances in open water, potentially leading to long-range connectivity (Bonfil et al. 2008). There is also little evidence of significant population structure in biological data collected by observers on WCPFC longline vessels (Brouwer et al. 2024), other than a slight north to south gradient in reported mean size. In addition, sparse observer coverage and composition data make it difficult to infer definitive patterns from lengths that might highlight substantial differences in selectivity between fleets operating in different regions. We therefore maintained the one-stock assumption from the previous stock assessments (Figure 20), but chose to split the assessment into three fisheries (longline, object-associated and free-school purse-seine) as opposed to four, as there was insufficient length-composition data to adequately characterise the previously-used longline target fishery. In addition, the target fishery, which is no longer operational, was found to have a negligible effect in the models. Catch estimates for associated flags and strata were therefore rolled into the catch estimates for the longline fleet.

2.2.2 Productivity

Productivity of oceanic whitetip sharks remains poorly understood, and divergent growth estimates between studies and regions suggest that growth cannot be considered known. Tremblay-Boyer et al. (2019) used two sets of growth estimates based on Joung et al. (2016) and Seki et al. (1998), with the latter suggesting faster growth ($k = 0.11$) and a more productive stock (lower age at maturity) than the former ($k = 0.08$). We considered natural mortality independently of growth in the axis of uncertainty. We developed an informed prior for natural mortality on the basis of each growth study, using natural mortality estimators based on life-history correlation (Cope & Hamel 2022). The resulting priors reflected the over-all difference in productivity between these two studies (Figure 21), with respective means of 0.135 and 0.175. Both prior means were lower than M used in the previous stock assessment.

2.3 Reference points

Clarke and Hoyle (2014) and Zhou et al. (2018) evaluated methods to derive reference points for elasmobranches in the Western and Central Pacific Ocean (WCPO). However, to date, there are no formally agreed reference points for sharks in the WCPO. Tremblay-Boyer et al. (2019) compared fishing mortality to F_{lim} as a tentative limit reference point for sharks, and to F_{crash}, the fishing mortality that would lead to extinction in the long-term. If one assumes a simple Schaefer surplus production model, then $F_{crash} = R_{max}$, the maximum population growth rate (intuitively, a population cannot be sustained if fishing removes more individuals than the population can maximally produce), and $F_{lim} = 0.75R_{max}$.

2.4 Stock synthesis assessment

2.4.1 Model setup

The model used Stock Synthesis (Version 30.23.01 Methot et al. 2021). CPUE data were included from 1995 (when suitable CPUE data became available) up to and including 2023 (Figure 22). Models were run from 1995 to 2023, and outputs were analysed with respect to stock status in 2023.

2.4.2 Step-wise model updates

Models were updated in a step-wise manner from the 2019 diagnostic model, starting with the version update for Stock Synthesis, and amalgamating the target and non-target longline fleets in the model. We then proceeded to include 2023 catch estimates, followed by 2023 CPUE without and with high CPUE filters (cutoff). We lastly switched to the setup described below for estimating productivity parameters (termed "FAL setup" for it's proximity to silky shark assumptions made in Neubauer et al. (2024)). This setup also included a switch to considering length compositions separately for index and capture fisheries.

2.4.3 Natural mortality

The previous assessment for OPS fixed M at 0.18 for the diagnostic model, and then used a wide range of sensitivities (0.1, to 0.26) to reflect large uncertainties about M. Given well-documented correlations between growth and natural mortality, and slow growth and low fecundity of OCS, we attempted to specify a growth-model specific prior for M as described above, and to estimate M within the assessment, as was done for silky shark in 2024 (Neubauer et al. 2024).

2.4.4 Reproductive output and recruitment

Taylor et al. (2013) suggested that standard stock-recruit relationships such as the Beverton-Holt model can make unreasonable assumptions about pre-recruit survival at low biomass (i.e., lead to survival greater than 1), especially if pre-recruit survival is high (a condition that is likely for many sharks). These authors proposed a survival-based stock recruit (SBSR) relationship as a three-parameter model with a shape parameter controlling the shape of the stock recruitment relationship. With a shape parameter $\beta < 1$, the model can emulate the shape of the Beverton-Holt (BH) SRR, whereas a shape of $\beta > 1$ leads to an over-compensatory SRR, with maximum recruitment at intermediate stock sizes. A second parameter (z_{frac}) determines the rate of density-dependent increase in survival as the stock is depleted (i.e., the strength of density dependence).

Although the previous OCS stock assessment used a Beverton-Holt (BH) model, more recent assessments for sharks in the WCPFC have employed the survival relationship (Neubauer et al. 2021b, ISC 2017), deriving parameters for the function based on

simulations run in the context of a Beverton-Holt (BH) model, whereas the most recent assessment for silky shark attempted to estimate the parameters of the SBSR model. As shown for silky shark, the BH model is essentially equivalent to a model with a low value for the shape parameter ($\beta < 1$; Taylor et al. (2013)), which assumes that density dependence is greatest near stock collapse, leading to an assumed high resilience at very low stock size, but limited density dependence at larger stock sizes. This is likely unrealistic for sharks if cannibalism and intra-specific competition are important (Neubauer et al. 2024). We used a range of fixed β values to ensure that uncertainty in the location of peak recruitment was considered as part of our key uncertainties, while z_{frac} was estimated using a vague beta distribution prior with slight doming towards values of 0.5.

As in the previous stock assessment, recruitment variability was assumed to be low, with σ_R fixed at 0.1.

2.4.5 Selectivity

Although we included the previous target longline fishery in the single longline fishery considered for the present model, we maintained the same selectivity assumption for the longline fishery; a double normal selectivity that allows for a dome-shaped selectivity, assuming that the largest sharks are less vulnerable to capture, with highest selectivity at intermediate sizes. The largest proportion of large OCS occur in the occasional purse seine captures. We therefore assumed asymptotic logistic selectivity for the purse-seine fisheries, noting that these fisheries catch few individuals, but provide a test if model assumptions can be reconciled with a population where large individuals are fully vulnerable to purse-seine gear.

2.4.6 Initial fishing mortality

We estimated initial F by assuming the population is at equilibrium with mortality from the longline fleet. In an attempt to provide some curvature (information) to the model to aid estimation of initial fishing mortality, we set a log-normal normal prior with mean 0.135, the prior mean of our M prior, and a CV of 100%, meaning the initial F was assumed to be within one standard deviation of both F_{MSY} and F_{crash}.

2.4.7 Data weighting

Data weighting in recent assessments for sharks followed Francis (2011), first fitting a smoother through the CPUE index, and calculating the expected CV for CPUE from this fit on the basis of the SD of the residuals. The latter was found to be near 0.18, and the input SE for CPUE was initially set to this level. However, iterative reweighing of length frequencies tended to give excessive weight to length frequencies, leading to increasingly optimistic stock status estimates, further up-weighting LFs relative to CPUE at every step of the process. We therefore did not use this process, forcing a tighter CV on CPUE (0.1) to force a closer fit to CPUE, and set arbitrarily low weights

for LFs ($N = 1$) while exploring the sensitivity to this value as part of the uncertainty grid.

2.4.8 Priors

We employed prior predictive/push-forward checks in order to avoid potential bias from regions of parameter-space that are *a priori* implausible (Kim & Neubauer 2025). The latter are parameter combination that lead to stock collapse in the past (the stock is still present, even if it may be at a very low relative biomass), or combinations that consider the stock to be near unfished levels. For this test, we simulated 2000 trajectories from the model, removing only the catch but without evaluating the likelihood (i.e., simulating under the prior only). We used wide priors for $log(R_0)$ for the initial simulation, as well as the stated priors for M and z_{frac}, although Kim and Neubauer (2025) showed that the scale parameter $log(R_0)$ is the most important to consider.

From the 2000 simulations, we retained all draws that led to a non-zero stock status as well as a terminal relative biomass of <0.6. The updated prior for $log(R_0)$ was derived by fitting a log-normal distribution to the retained $log(R_0)$ draws after filtering (Figure 26).

2.4.9 Diagnostic model

For the diagnostic model, we fixed growth at estimates from Joung et al. (2016), and β at a value of 2. For catches, we assumed the median estimated discard level. The resulting model was fitted using maximum likelihood, all gradients were inspected and jittering was done from 10 starting values to ensure convergence was achieved. We then conducted retrospective analysis and profiled key parameters (M, $log(R_0)$, z_{frac}, and initial F).

2.4.10 MCMC

While stepwise updates and the initial diagnostic model were run using MAP estimates only, uncertainty for the diagnostic model and key sensitivities in the uncertainty grid was estimated using full Bayesian inference, using the No-U-Turn sampler as implemented for ADMB (Monnahan & Kristensen 2018). We ran eight chains with different random seeds, and used 200 iterations for adaptation starting from the MAP estimate; these iterations were subsequently discarded as burn-in. We used adaptation based on the dense covariance matrix in order to minimise divergent iterations, rather than the diagonal of the covariance matrix (the default), to minimise issues with the sampler.

As with the silky shark assessment, we were unable to achieve consistent models without divergences. However, as for silky shark, models had relatively few divergent iterations and appeared to show good convergence and mixing. For silky shark, we discarded the stock synthesis models on the basis that divergent transitions can bias

inference, and management quantities from these models may therefore me biased. Here, we explicitly tested for this bias using simulation-based calibration (SBC; Talts et al. 2018, Kim & Neubauer 2025). SBC works by first simulating data from the model under the prior (i.e., simulating CPUE and length compositions), and then fitting the model to each simulated dataset using Bayesian inference. It is straightforward to demonstrate that the combined posterior across fits to all simulated datasets should recover the priors for parameters and the implied priors over management quantities – provided the inference is unbiased. We tested this premise by simulating 400 datasets and fitting the model, using full MCMC, to each dataset. We then compared the combined posterior draws over datasets to the prior draws from the model for key parameters and management quantities.

2.4.11 Uncertainty grid

While we aimed to consider uncertainty as part of model fitting - estimating productivity where possible, data and structural uncertainty are not easily represented in the form of estimable parameters. Key uncertainties remain in terms of productivity assumptions, data weighting and inputs (catch data). We therefore ran a full factorial grid across four axes:

Growth and M prior While the diagnostic model considered the Joung et al. (2016) growth model, the grid integrates over uncertainty by also considering the Seki et al. (1998) growth parameters and associated M prior.

Data weighting Due to conflicts between CPUE and length data with regards to mortality and stock size, as well as the dubious performance of the Francis re-weighting method, we employed a sensitivity to decrease or increase our (arbitrary) LF weights by an order of magnitude.

Alternative values for β The shape of the stock-recruit function is inherently uncertain. We ran three alternative options with beta fixed at 1 (close to a BH model) and 4, in addition to diagnostic model runs with $\beta = 2$.

Discard mortality We used the 25th and 75th percentiles of the predicted live discards as alternatives to the mean assumption in the grid. Given the percentiles for discard mortality represent regions of lower likelihood from the fate model, a corresponding weight of 0.75 was applied to models using these inputs, relative to a weight of 1 for the median discard assumption.

The uncertainty grid was fitted using full MCMC, and posterior samples were combined. For each model, 8 independent chains were run, with 200 iterations used for adaptation and discarded as burn-in, and 100 independent draws kept per chain

and combined. Inference was based on a total of 28800 draws from the joint posterior distribution across the grid of 36 models.

2.5 Dynamic surplus production model

Length frequency data provide little information for OCS, and even conflicted with relative abundance trends. We sought to check trends found with the integrated assessment model against a simpler dynamic surplus production model (biomass dynamics model; BDM) to verify that the estimates are not unduly influenced by the conflict between LFs and CPUE. We applied the Schaefer surplus production model implemented in the *bdm* R package (Edwards 2017) to aggregated catch across fisheries and CPUE from the longline time series as used in the integrated assessment model.

Neubauer et al. (2019) provided context for the application of dynamic surplus production models (DSPM) to sharks in the WCPFC, and other recent assessments have applied these models when the available information lead to difficulties with integrated stock assessment models (ISC 2024). For silky shark in 2024, this type of model was used to provide management advice (Neubauer et al. 2024). DSPM are fitted based on state-space equations (McAllister & Edwards 2016, Froese et al. 2017) and do not require equilibrium assumptions that make traditional approaches to surplus production assessments difficult to justify (Bonfil 2005). Examples of packages that implement DSPMs are JABBA ("Just Another Bayesian Biomass Assessment"; Winker et al. 2018) and BDM ("Bayesian biomass dynamics model"; Edwards 2017). As such, the DSPM operates similarly to integrated assessments, where recruitment essentially functions as a process error term. The DSPMs tend to use an index of abundance (usually CPUE) to constrain the time series of abundance. Although productivity is usually estimated within DSPMs, it is useful to also constrain productivity via an informative prior (Edwards 2017).

We used a classic Schaefer production model implemented in the BDM package (although other hybrid production functions can be used with this R package). The population dynamics are parameterised in terms of the relative depletion ($x_t = N_t/K$), with harvest H_t also expressed in relative terms ($H_t = C_t/K$):

$$x_{t+1} = x_t + g(x_t) - H_t \tag{1}$$

$$g(x_t) = R_{max} x_t \left(1 - x_t\right). \tag{2}$$

2.5.1 Priors for dynamic surplus production models

Population growth R_{max} was calculated from methods in Pardo et al. (2018) based on the Euler-Lotka equation (see also Zhou et al. 2018), adjusted for survival to age at first maturity (Pardo et al. 2016). Estimating R_{max} serves a dual purpose here: it can act as a reference point for methods that cannot estimate stock productivity independently (e.g., risk assessments), but can also act as a prior for a DSPM for which R_{max} is the

productivity parameter.

Life history input values for the Euler-Lotka equation were compiled from ranges and point estimates reported in Clarke et al. (2015) and the most recent stock assessment report (Tremblay-Boyer et al. 2019). Specifically, growth rate k was simulated with sufficient variability to encompass uncertainty (Tremblay-Boyer et al. 2019, Figure 23) to reflect this uncertainty in the resulting values of R_{max} (Figure 24). When only ranges were reported, the distributions were constructed to encompass those ranges as extreme quantiles (i.e., near the 5th and 95th percentile).

Priors for the carrying capacity, K, and initial population depletion in 1995 were formulated as vague log-normal distributions, encompassing scenarios of high initial depletion as well as high initial biomass (i.e., $> B_0$). In order to ensure that these priors made sense in the context of observed catch, we simulated from the model using the prior for R_{max}, a wide prior for carrying capacity and initial depletion ([0.01;0.6], and applied the catch to obtain a prior predictive/pushforward distribution for recent depletion (Kim & Neubauer 2025). The obtained recent depletion values were then subset to values between 0.05% and 60% of carrying capacity, and only prior draws which led to these outcomes were retained (Figure 25). We used the retained simulations to estimate the parameters of a log-normal prior distributions for R_{max}, K and initial depletion. We subsequently manipulated the prior for initial depletion to investigate the sensitivity of the model to mis-specification of this prior. We fitted the model based on three sets of priors for the initial depletion level, with sensitivities assuming higher and lower levels of *a priori* initial depletion in 1995 (multiplying or dividing the prior mean of initial depletion by a factor of two). The process error standard deviation was fixed at 0.01.

Catch was summed across predicted purse seine and longline catches, as this appeared most appropriate for the assumption inherent in dynamic surplus production models that the population indexed by the CPUE index is fully vulnerable and affected by the specified catch.

2.5.2 Implementation

All estimation was done within the BDM package, with Markov Chain Monte Carlo (MCMC) in the underlying Bayesian estimation software Stan (Stan Development Team 2018) used to estimate parameters. We ran the MCMC for 25 000 iterations, discarding the first 5 000 iterations as burn-in, and keeping 2000 samples from each of 4 chains. All model were checked to ensure that $\hat{R}$ values were <1.01, and did not show any divergent iterations. Retrospectives were run with 10 peels, and Mohn's rho and predictive coverage were calculated as the proportion of the posterior for year y that is contained within the predictive distribution for that year from the retrospective model ending in year $y - 1$.

3. ASSESSMENT RESULTS

3.1 Stock synthesis assessment

3.1.1 Step-wise updates

Initial steps in the step-wise update did not lead to large changes - updating the SS version, and combining the longline target and non-target fleets did not lead to any perceivable differences in models (Figure 27). The updated catch history initially led to a more continuous estimated decline in biomass to a low at the end of the time-series, but including recent CPUE led to an upwards correction of biomass trends in recent years, with trajectories not reaching the same low-points as in the 2019 assessment. Estimating initial F (rather than fixing it as in 2019), and estimating productivity, led to an increase in uncertainty, and a decrease in the trajectory to similar levels as the 2019 stock assessment during the low period around 2013–14 (Figure 27). The attempted Francis re-weighting moved the trajectories towards higher biomass; however, the procedure did not converge and produced spurious results in this model, and the last model in this stepwise update was therefore not used.

3.1.2 Diagnostic model fits

The diagnostic model run showed reasonable fit to CPUE (Figure 28), although, given large variability in the early part of the time series,the residuals reflected the model's propensity to fit through the index rather than follow the rapid peaks and troughs of the CPUE index (Figure 29), with correspondingly high standard deviation of normalised residuals (SDNR). The model produced a relatively good fit to over-all length composition data (Figures 31), despite the simplified selectivity assumptions (Figure 30).

3.1.3 Retrospectives

Retrospectives showed only slight retrospective patterns in fishing mortality, CPUE fits and estimated stock size (Figure 33). For stock status, recent estimates showed only very slight retrospective patterns, but the initial estimated fishing mortality declined with more recent data included in the model. This pattern does not affect management advice, however, and was therefore judged to be acceptable.

3.1.4 Profiles

Negative log-Likelihood profiles of R_0 suggested that the lower bounds of R_0 and M were largely driven by the compositions data, while the upper bound was given by the CPUE index (Figure 32). Juvenile survival (z_{frac}) was strongly constrained at the lower bound by the composition data, and only the prior keeping it away from 100% survival. The initial F estimate was driven by a combination of composition data and indices trading off against the prior.

3.1.5 Estimation uncertainty from MCMC

Simulation-based calibration confirmed that the MCMC estimation of model parameters, and the derived management quantities, was unbiased (Figure 34: especially for management quantities, the prior and joint SBC posterior overlapped near perfectly; only the estimation of M seemed potentially biased with a difference of less than 1%. Given this confirmation of bias-free estimation, we proceeded to calculate assessment outputs across the MCMC model ensemble across the uncertainty grid.

Models with the low discard assumption universally failed to converge, and were therefore not used. The reason for this convergence failure could not be straightforwardly determined. The ensemble across the remaining uncertainty grid (36 models) showed little variability with respect to β and length-composition weights (Figures 35, 36); most of the variation in estimated parameters and management quantities derived from the growth/productivity assumptions (for status; Figures 37, 38) and discard assumptions (Figures 39, 40), with the latter leading to a bi-modal posterior with respect to $F_{recent}/F_{\text{MSY}}$.

3.1.6 Estimated stock recruit relationship

The stock recruit relationship of the diagnostic model can be compared to the alternative β assumptions using estimated values for pre-recruit survival and z_{frac} (Figure 41). At $beta$ = 2, the diagnostic model, pre-recruit survival remains high across a wide range of depletion levels from 0 to 0.5, before dropping steeply towards relatively low ($\sim$0.1) survival at high stock biomass. When $beta$ is increased to 4, this plateau of high survival is slightly lower, but extends to higher biomass levels. Conversely, at $beta$ = 1, the relationship between depletion and pre-recruit survival is near-linear. The corresponding stock-recruit functions mirror these differences with the function for $beta$ = 1 showing no doming in the stock-recruit function.

3.1.7 Model ensemble population trajectory

The model suggested an over-all high fishing mortality up to the mid 2010's (Figures 42), driven by high longline catches (Figure 43). Recent fishing mortality was estimated to have declined sharply since 2013, to levels well near F_{MSY}, from levels exceeding F_{crash} (the fishing mortality that would lead to population collapse in the long term). Given declining trends in fishing mortality F, the diagnostic model estimated a slow and steady increase in biomass over this period (Figure 44) from low around 5% of unfished biomass to 6% of unfished biomass (Figure 44). The model did not require large recruitment deviations to fit the over-all trends, with little recruitment variation estimated across the ensemble (Figure 45).

3.1.8 Stock status

The ensemble mirrored the range of model outcomes for the respective sensitivities (Figure 45), with recent (2022–2023) stock status showing relatively low levels of uncertainty despite a diversity of assumptions. Fishing mortality estimates were more uncertain, with estimates based on high levels of discarding leading to F estimates below F_{MSY}, but median discard rates suggesting F remains above F_{MSY}. Given the weighting towards the somewhat higher F assumption, the mean fishing mortality is estimated to have remained above F_{MSY} (Figure 46. Table 2).

3.2 Dynamic surplus production model

Dynamic surplus production models converged rapidly, and showed good MCMC mixing for all key parameters (Figure 47), and good convergence diagnostics and effective sample size (Table 3, Figure 48).

Dynamic surplus production models were largely in agreement with the integrated assessment in terms of recent stock trajectories as well as fishing mortality rates relative to proposed reference points (Figures 49 – 52). Models without discards could not fit trends in recent CPUE (Figure 50), and had higher residuals (Figure 53). The initial starting assumption could not be distinguished in the fits to CPUE, all providing identical fits to CPUE, but divergent recent status estimates due to differing starting conditions. The estimated process error by year showed a similar pattern to the estimated recruitment deviations from the integrated stock assessment (Figure 54).

Retrospective patterns were small for biomass (Mohn's $\rho = 0.10$) and harvest rate ($\rho = 0.07$; Figure 55). Uncertainty in all years includes upwards of 94% of updated trajectories, with high predictive coverage of around 95% confirming that the posterior distribution of each new year in the retrospectives is 95% contained within the predictive distribution from the previous fit (Table 4).

The model estimated the stock to be similarly productive to the SS3 model, with U above U_{crash} between the early 2000s. Recent depletion levels, however, were estimated to be below U_{crash}, and likely below U_{lim}. Recent depletion levels were were also comparable to those estimated from the integrated stock assessment across the median assumption of starting depletion, which most closely matched the estimated initial depletion in the SS model. The base assumption led to an estimated status in 2023 of 7% (95% CI: 3%–13%) of unfished abundance, with alternative depletion priors leading to estimates of 2% (95% CI: 1%–4%) for a prior suggesting a lower initial abundance, and 12% (95% CI: 5%–23%) for a model with *a priori* high initial stock status in 1995 (Table 3).

Given the aligned outcomes between the median initial depletion prior models and the stock-synthesis ensemble, we considered only the base starting prior as a candidate model for management advice. In addition, because low discard assumptions led to poor CPUE fit, we also discarded this set of models. The resulting stock status calculated across the ensemble of remaining discard assumptions is 7% of unfished abundance and recent harvest rates below U_{MSY} (Figure 56).

3.3 Model comparison

Stock status (SB_{recent}/SB_0), measured as recent (2022–2023) relative depletion, was highly consistent across models, with mean estimates ranging from 0.06 (95% CI: 0.04–0.08) for the ensemble across stock synthesis models (Table 5; Figure 57), to 0.07 (95% CI: 0.02–0.16) for an ensemble across dynamic surplus production model assumptions of discard mortalities. Uncertainty about recent relative depletion across the range of models was low, despite considerable uncertainty about initial population status in both ensembles. Fishing mortality was consistently estimated to be below possible limit reference points with high probability (P(F_{recent}/F_{crash} >1)=0 for dynamic surplus production and Stock Synthesis models.

4. DISCUSSION

The 2025 assessment for oceanic whitetip shark (*Carcharhinus longimanus*) in the Western and Central Pacific Ocean (WCPO), like most shark assessments, required us to consider a range of uncertainties associated with reporting, data availability, and knowledge about key population parameters and processes. The core issue remains providing robust management advice for a stock confirmed to be in a severely depleted state, while grappling with significant data limitations and structural uncertainties that are, paradoxically, exacerbated by the primary conservation measure in place. Nevertheless, the current assessment lines up very closely with the previous stock assessment, despite a number of changes to the catch-history, model methods and assumptions, and uncertainty treatment. The low-point in biomass estimated by the 2019 diagnostic model is almost exactly replicated by the present assessment, and the recent slow increase aligns with expectations from simulation work under intermediate mortality scenarios (Bigelow et al. 2022).

The foundation of any stock assessment is a reliable history of fishery removals, a particular challenge for bycatch species like oceanic whitetip shark. Due to historically poor and inconsistent logbook reporting, all shark assessments rely on reconstructing catch histories by modelling and extrapolating from observer data (e.g., Tremblay-Boyer et al. 2019). The 2025 assessment process continued to refine this approach by re-evaluating a key model covariate, hooks-between-floats (HBF), which is a proxy for fishing depth. The analysis showed that previous treatment of reported zero-HBF values as true data likely inflated early catch estimates, as low HBF values are associated with high catch rates for this surface-oriented species. By treating these zeros as missing data and imputing HBF using a boosted-regression tree model, the updated 2025 catch series is markedly lower and less variable in the early part of the time series, thereby reconciling differences with other historical estimates. Ultimately, however, the update in catch estimates had only have a minor impact on the stock assessment.

Despite refinements in catch estimation, a fundamental conflict between the primary data streams used to infer population trends persists. Standardized catch-per-unit-effort (CPUE) from the longline fishery, the main index of relative abundance, has historically shown a steep decline, forming the principal evidence for the stock's severe

depletion (Rice & Harley 2012, Tremblay-Boyer et al. 2019). Conversely, the length-composition data have failed to show a corresponding decline in the mean size of sharks caught, a demographic signature that would be expected as fishing pressure removes larger, older individuals from a population. The 2019 assessment hypothesized this disconnect could be due to a confounding north-south spatial gradient in mean shark size or other sampling biases. This unresolved conflict suggests at least one of these key data inputs is providing a biased signal of the stock's dynamics.

This data integrity issue is compounded by the primary management measure for the species, CMM-2011-04, which mandated a non-retention policy beginning in 2013. While designed to reduce fishing mortality, this policy has created a conservation paradox by systematically degrading the data required to monitor its own effectiveness. The shift to releasing sharks, often by cutting them free without bringing them on board, means that observers are frequently unable to confirm species identification, take length measurements, or even consistently record the interaction itself. This practice introduces an unquantified negative bias into the CPUE and length time series in the most recent years, undermining confidence in observed trends. Consequently, accurately estimating total fishing mortality (F) now hinges on assumptions about post-release survival rates, a key source of uncertainty that was formally incorporated in the 2019 assessment and further refined with updated models of discard practices in the 2025 analysis.

In response to these uncertainties, the scientific approach has evolved significantly. The 2019 assessment employed a comprehensive structural uncertainty grid, running 648 model configurations to explore the impact of disparate assumptions regarding growth, natural mortality (M), and recruitment dynamics. This effectively mapped the plausible range of stock trajectories. The 2025 assessment advances this by adopting a dual-model approach to directly confront the data conflict. It paired the complex, age-structured Stock Synthesis (SS3) model with a simpler dynamic surplus production model (DSPM) that is less reliant on the problematic length-composition data, thus providing a crucial structural sensitivity analysis. This dual-model approach represents a pragmatic and scientifically defensible strategy. It acknowledges that while the new data processing methods are an improvement, the underlying data streams may still be too compromised to fully support a complex, data-hungry integrated model without corroboration. This multi-model inference strengthens the foundation for management advice in a data-limited context.

Furthermore, the present assessment proposes more biologically coherent priors, such as linking natural mortality estimates directly to specific growth model assumptions (e.g., faster growth from Seki et al. (1998) versus slower growth from Joung et al. (2016)), rather than treating them as independent sources of uncertainty. This treatment, coupled with estimation of key quantities, over a fixed grid approach, provides increased confidence in the model conclusions and uncertainty estimates. Nevertheless, substantial and under-represented uncertainties likely remain; including, the variability among predicted catch time-series between assessments, as well as irreducible uncertainties due to insufficient historic data on sharks, which point to a potential under-representation of uncertainty in most shark assessments. While

methodological updates provides a clearer picture, recent stock trends should still be regarded as uncertain.

The 2019 assessment, which included the first four years post-CMM, concluded that while fishing mortality-based reference points like F/F_{MSY} had improved, the stock remained overfished and subject to overfishing, with the spawning biomass (SB) at a critically low median of 3.7% of its unfished level (SB_0) in 2016. The 2025 assessment, benefiting from nearly a decade of additional data under the non-retention CMM, offers a slightly more optimistic outlook. The analysis of observer data confirmed a definitive operational shift in the fishery, with almost all oceanic whitetip sharks being released since 2015. The updated and filtered CPUE index showed a more pronounced uptick since 2016, suggesting a potential positive response in the stock. The 2025 assessment concludes with high confidence that recent fishing mortality has been reduced to a level below biological limit reference points (e.g., F_{lim} and F_{crash}) that would preclude stock rebuilding. While the stock likely remains severely depleted, the evidence increasingly suggests that the management measures have been sufficient to halt the decline and may now be allowing for the initial stages of recovery.

4.1 Main Assessment Conclusions

- Based on the precedent of using SS3 for the OCS assessment, and on advances in Bayesian methodologies used for the present assessment (relative to the 2024 silky shark assessment), we suggest that the ensemble of SS3 models be used for management advice.
- The multi-model approach for assessing OCS resulted in a low stock status, but with high confidence that recent fishing mortality is below levels that would preclude stock rebuilding.
- The largest fishing mortality of OCS was estimated to be in longline fisheries. Reductions in OCS interactions as a result of changes in fishing practices over the last decade may have substantially reduced this source of mortality, likely halting the previously observed steep decline, and possibly leading to some (albeit slow) rebuilding.
- Recent fishing mortality rates were below biological limit reference points for the ensemble (Diagnostic F_{recent}/F_{crash}: 0.54 [0.37–0.74]; P(F_{recent}/F_{crash} >1)=0; P(F_{recent}/F_{lim} >1)=0).
- Recent biomass was estimated to have had a subtle increase from a low-point in 2013–14 near 4% of unfinished biomass, to 6% of unfished biomass in recent years (2022–23).

Given some of the fundamental uncertainties highlighted above, we recommend:

- **Improve observer data protocols:** To counter the degradation of data quality resulting from the non-retention conservation measure (CMM-2011-04), it

is recommended that longline observer programmes implement clear and consistent directives for recording all capture events, especially unobserved "discarded-cut-free" (DCF) individuals. Furthermore, recording approximate length measurements for sharks released in the water, a practice already in place in some programmes, should be standardised across the Western and Central Pacific Ocean.

- **Prioritise research on stock structure and connectivity:** Fundamental uncertainty remains regarding the stock structure of OCS in the Pacific Ocean. It is recommended that CCMs prioritise and support planned work under the WCPFC's Shark Research Plan (SRP) involving satellite tagging and expanded genetic/genomics studies to address questions of regional residency, mixing, and stock boundaries.

- **Resolve conflicting life history parameters:** The significant divergence between available growth studies remains a considerable factor for the uncertainty in stock productivity. To build a more robust understanding of this species' life history, it is recommended that work scheduled under the SRP to conduct additional growth studies and validate ageing methods from a range of locations be prioritised.

- **Continue multi-model assessment frameworks:** Given the persistent conflict between CPUE and length data, it is recommended that future assessments continue to use multi-model approaches. The use of simpler models, such as the Dynamic Surplus Production Model, alongside integrated age-structured models, provides a vital cross-assessment, and ensures management advice is robust to structural uncertainty.

- **Refine historical catch estimates:** Although progress has been made, the catch history for the longline fishery remains uncertain with considerable discrepancies between studies. It is recommended that shark catch reconstructions be reviewed, and these discrepancies be explored to gain an improved understanding of core uncertainties.

- **Review and document recent improvements in shark assessment methodologies:** With the present assessment, a full cycle of assessments has now been undertaken for blue, mako, silky and oceanic whitetip sharks, using consistent assessment methods, consistently refined over time. A review workshop and summary paper to capture recent progress and outstanding challenges is recommended to provide a solid basis for upcoming work, and provide an opportunity to share these advances across RFMOs. We recommend this workshop be considered by the Informal Small Working Group: Sharks for inclusion and prioritisation in the Shark Research Plan update at SC21.

5. ACKNOWLEDGEMENTS

The authors would like to thank SPC, particularly Tiffany Vidal for providing the WCPFC members' data for these analyses. We would also like to thank Paul Hamer and the stock assessment team at SPC for constructive discussions throughout this work, and for comments on earlier drafts of this report. Thanks also to the members of the SPC Pre-Assessment Workshop for their helpful feedback on the revised data inputs and the preliminary runs of the integrated stock assessment and the biomass dynamics models.

Funding for this project was provided by the WCPFC.

6. REFERENCES

Bigelow, K. & Carvalho, F. (2021). *Review of potential mitigation measures to reduce fishing-related mortality on silky and oceanic whitetip sharks (Project 101)*. WCPFC-SC17-2021/EB-WP-01. Report to the Western and Central Pacific Fisheries Commission Scientific Committee. Seventeenth Regular Session. Electronic Meeting, 11–19 August 2021.

Bigelow, K.; Rice, J., & Carvalho, F. (2022). *Future stock projections of oceanic whitetip sharks in the Western and Central Pacific Ocean*. PIFSC (Pacific Islands Fisheries Science Center) data report DR-22-33.

Bonfil, R.; Clarke, S. C., & Nakano, H. (2008). The biology and ecology of the oceanic whitetip shark, *Carcharhinus longimanus*. In *Sharks of the open ocean: Biology, fisheries and conservation* (pp. 128–139). Oxford: Blackwell Science.

Bonfil, R. (2005). Fishery stock assessment models and their application to sharks. In R. Bonfil & J. A. Musick (Eds.), (p. 154). Rome: FAO.

Brouwer, S.; Hill-Moana, T.; Neubauer, P., & Large, K. (2024). *Characterisation of the fisheries catching oceanic whitetip sharks (*Carcharhinus longimanus*) in the Western and Central Pacific Ocean*. WCPFC-SC20-2024/SA-IP-23 (Rev.01). Report to the Western and Central Pacific Fisheries Commission Scientific Committee. Twentieth Regular Session, 14–21 August 2024, Manila, Philippines. 51 p.

Clarke, S.; Coelho, R.; Francis, M.; Kai, M.; Kohin, S.; Liu, K. M.; Simpfendorfer, C.; Tovar-Avila, J.; Rigby, C., & Smart, J. (2015). *Report of the Pacific shark life history expert panel workshop, 28-30 April 2015*. WCPFC-SC11-EB-IP-13. Report to the Western and Central Pacific Fisheries Commission Scientific Committee. Eleventh Regular Session, 5–15 August 2015, Pohnpei, Federated States of Micronesia.

Clarke, S. & Hoyle, S. (2014). *Development of limit reference points for elasmobranchs*. WCPFC-SC10-2014/MI-WP-07. Report to the Western and Central Pacific Fisheries Commission Scientific Committee. Tenth Regular Session, 6–14 August 2014, Majuro, Republic of the Marshall Islands.

Cope, J. & Hamel, O. (2022). Upgrading from M version 0.2: An application-based method for practical estimation, evaluation and uncertainty characterization of natural mortality. *Fisheries Research*, *256*, 106493.

Edwards, C. T. T. (2017). *Bdm: Bayesian biomass dynamics model*. R package version 0.0.0.9022.

Francis, R. I. C. (2011). Data weighting in statistical fisheries stock assessment models. *Canadian Journal of Fisheries and Aquatic Sciences*, *68*(6), 1124–1138.

Froese, R.; Demirel, N.; Coro, G.; Kleisner, K. M., & Winker, H. (2017). Estimating fisheries reference points from catch and resilience. *Fish and Fisheries*, *18*(3), 506–526.

Hamer, P. (2025). *Summary report from the SPC Pre-assessment Workshop – April 2025*. WCPFC-SC21-2025/SA-IP-01. Report to the Western and Central Pacific Fisheries Commission Scientific Committee. Twenty-first Regular Session, 13–21 August 2025, Nuku'alofa, Tonga.

Hill-Moana, T.; Neubauer, P.; Large, K., & Brouwer, S. (2024). *Analysing potential inputs to the 2025 stock assessment of Western and Central Pacific oceanic whitetip shark (*Carcharhinus longimanus*)*. WCPFC-SC20-2024/SA-WP-11-Rev2. Report to the Western and Central Pacific Fisheries Commission Scientific Committee. Twentieth Regular Session,14–21 August 2024, Manila, Philippines. 174 p.

ISC (2017). *Stock assessment and future projections of blue shark in the North Pacific Ocean through 2015*. WCPFC-SC13-2017/SA-WP-10. Report to the Western and Central Pacific Fisheries Commission Scientific Committee. Thirteenth Regular Session, 9–17 August 2017, Rarotonga, Cook Islands.

ISC (2024). *Stock assessment of Shortfin Mako Shark in the North Pacific Ocean through 2022*. WCPFC-SC20-2024/SA-WP-14. Report to the Western and Central Pacific Fisheries Commission Scientific Committee. Twentieth Regular Session, 14–21 August 2024, Manilla, Phillipines.

Joung, S.-J.; Chen, N.-F.; Hsu, H.-H., & Liu, K.-M. (2016). Estimates of life history parameters of the oceanic whitetip shark, *Carcharhinus longimanus*, in the western North Pacific Ocean. *Marine Biology Research*, *12*(7), 758–768.

Kim, K. & Neubauer, P. (2025). Examining potential biases through prior predictive checks: Prior mis-specifications and their impact on Bayesian stock assessments. *Fisheries Research*, *107405*.

McAllister, M. & Edwards, C. (2016). Applications of a Bayesian surplus production model to New Zealand fish stocks. *New Zealand Fisheries Assessment Report*, *52*. 79 p

Methot, R. D.; Wetzel, C. R.; Taylor, I. G.; Doering, K. L., & Johnston, K. F. (2021). *Stock Synthesis User Manual Version 3.30.17*. NOAA Fisheries, Seattle, WA.

Monnahan, C. & Kristensen, K. (2018). No-U-Turn Sampling for fast Bayesian Inference in ADMB and TMB: Introducing the adnuts and tmbstan R packages. *PloS One*, *13*(5), e0197954.

Neubauer, P.; Kim, K.; Large, K., & Brouwer, S. (2024). *Stock assessment of silky shark in the Western and Central Pacific Ocean 2024*. WCPFC-SC20-2024/SA-WP-04-Rev2. Report to the Western and Central Pacific Fisheries Commission Scientific Committee. Twentieth Regular Session,14–21 August 2024, Manila, Philippines. 131 p.

Neubauer, P.; Large, K.; Brouwer, S.; Kai, M.; Tasi, W. P., & Liu, K. M. (2021a). *Input data for the 2021 South Pacific blue shark (*Prionace glauca*) stock assessment*. WCPFC-SC17-2021/SA-IP-18. Report to the Western and Central Pacific Fisheries Commission Scientific Committee. Seventeenth Regular Session, 11–19 August 2021. Electronic meeting.

Neubauer, P.; Large, K., & Brouwer, S. (2021b). *Stock assessment for South Pacific blue shark in the Western and Central Pacific Ocean*. WCPFC-SC17-2021/SA-WP-03. Report to the Western and Central Pacific Fisheries Commission Scientific Committee. Seventeenth Regular Session, 11–19 August 2021, Pohnpei, Federated States of Micronesia.

Neubauer, P.; Richard, Y., & Tremblay-Boyer, L. (2019). *Alternative assessment methods for oceanic white-tip shark*. WCPFC-SC15-2019/SA-IP-13. Report to the Western and Central Pacific Fisheries Commission Scientific Committee. Nineteenth Regular Session, 12–20 August 2019, Pohnpei, Federated States of Micronesia.

Pardo, S. A.; Kindsvater, H. K.; Reynolds, J. D., & Dulvy, N. K. (2016, August). Maximum intrinsic rate of population increase in sharks, rays, and chimaeras: The importance of survival to maturity. *Canadian Journal of Fisheries and Aquatic Sciences*, *73*(8), 1159–1163. doi:10.1139/cjfas-2016-0069

Pardo, S. A.; Cooper, A. B.; Reynolds, J. D., & Dulvy, N. K. (2018, January 5). Quantifying the known unknowns: Estimating maximum intrinsic rate of population increase in the face of uncertainty. *ICES Journal of Marine Science*. doi:10.1093/icesjms/fsx220

Peatman, T.; Bell, L.; Allain, V.; Caillot, S.; Williams, P.; Tuiloma, I.; Panizza, A.; Tremblay-Boyer, L.; Fukofuka, S., & Smith, N. (2018a). *Summary of longline bycatch at a regional scale, 2003–2017*. WCPFC-SC14-2018/ST-WP-03 Rev 3 (15 April 2019). Report to the Western and Central Pacific Fisheries Commission Scientific Committee. Fourteenth Regular Session, 8–16 August 2018, Busan, Korea.

Peatman, T.; Bell, L.; Allain, V.; Caillot, S.; Williams, P.; Tuiloma, I.; Panizza, A.; Tremblay-Boyer, L.; Fukofuka, S., & Smith, N. (2018b). *Summary of longline fishery bycatch at a regional scale, 2003-2017*. WCPFC-SC14-2018/ST-WP-03. Report to the Western and Central Pacific Fisheries Commission Scientific Committee. Fourteenth Regular Session, 8–16 August 2018, Busan, Republic of Korea.

Rice, J. & Harley, S. (2012). Stock assessment of oceanic whitetip sharks in the western and central Pacific Ocean. WCPFC-SC8-2012/SA-WP-06-Rev1. Report to the Western and Central Pacific Fisheries Commission Scientific Committee. Eighth Regular Session. Busan, Republic of Korea, 7–15 August 2012.

Seki, T.; Taniuchi, T.; Nakano, H., & Shimizu, M. (1998). Age, growth and reproduction of the oceanic whitetip shark from the Pacific Ocean. *Fisheries Science*, *64*(1), 14–20.

Stan Development Team (2018). RStan: the R interface to Stan. R package version 2.17.3. Retrieved from http://mc-stan.org/.

Talts, S.; Betancourt, M.; Simpson, D.; Vehtari, A., & Gelman, A. (2018). Validating bayesian inference algorithms with simulation-based calibration. *arXiv preprint arXiv:1804.06788*.

Taylor, I. G.; Gertseva, V.; Methot Jnr., R. D., & Maunder, M. N. (2013). A stock–recruitment relationship based on pre-recruit survival, illustrated with application to spiny dogfish shark. *Fisheries Research*, (142), 15–21.

Tremblay-Boyer, L.; Carvalho, F.; Neubauer, P., & Pilling, G. (2019). *Stock assessment for oceanic whitetip shark in the Western and Central Pacific Ocean*. WCPFC-SC15-2019/SA-WP-06. Report to the Western and Central Pacific Fisheries Commission Scientific Committee. Fifteenth Regular Session, 12–20 August 2019, Pohnpei, Federated States of Micronesia.

Winker, H.; Carvalho, F., & Kapur, M. (2018). JABBA: just another Bayesian biomass assessment. *Fisheries Research*, *204*, 275–288.

Zhou, S.; Deng, R.; Hoyle, S., & Dunn, M. (2018). *Identifying appropriate reference points for elasmobranchs within the WCPFC*. WCPFC-SC14-2018/MI-WP-07. Report to the Western and Central Pacific Fisheries Commission Scientific Committee. Fourteenth Regular Session, 8–16 August 2018, Busan, Republic of Korea.

7. TABLES

Table 1: Proportion of effort (in terms of total hooks fished) imputed by flag and year, including effort where HBF was reported to be zero.

flag_id	1995	1996	1997	1998	1999	2000	2001	2002	2003	2004	2005	2006	2007	2008	2009	2010	2011	2012	2013	2014	2015	2016	2017	2018	2019	2020	2021	2022	2023
AU	0.13	0.11	0.06	0.07	0.05	0.07	0.12	0.11	0.16	0.15	0.01	0.07	0.04	0.05	0.04	0.01	0.01	0.02	0.03	0.02	0.02	0.01	0.00	0.00	0.01	0.00	0.03	0.04	0.01
BZ	0.02	0.01	0.01	0.83	1.00	0.80	0.50	0.81	0.93	0.83	0.56	0.55	1.00	0.00	0.00	0.00	0.70	0.00	0.00	0.00	0.00	0.00	0.00	0.00	0.00	0.00	0.00	0.00	0.00
CK	0.33	1.00	1.00	0.00	0.00	0.00	1.00	0.17	0.04	0.16	0.04	0.17	0.23	0.16	0.03	0.10	0.18	0.74	0.18	0.03	0.11	0.00	0.21	0.00	0.06	0.03	0.03	0.09	0.00
CN	0.28	0.38	0.84	0.69	0.79	0.76	0.76	0.76	0.89	0.91	0.90	0.92	0.88	0.98	0.19	0.95	1.00	1.00	1.00	0.00	0.00	0.00	0.00	0.00	0.00	0.00	0.00	0.00	0.00
ES	0.00	0.00	0.00	0.00	0.00	0.00	0.00	0.00	0.00	0.00	0.00	0.00	0.00	0.00	0.00	0.00	0.00	0.00	0.00	0.00	0.00	0.00	0.00	0.00	0.00	0.00	0.00	0.00	0.00
FJ	0.71	0.66	0.51	0.48	0.43	0.72	0.73	0.95	0.98	0.99	0.96	1.00	0.99	0.93	0.65	0.69	0.88	0.92	0.62	0.09	0.01	0.13	0.15	0.09	0.14	0.09	0.02	0.07	0.17
FM	0.66	0.49	0.61	0.72	0.65	0.78	0.66	0.76	0.59	0.36	0.48	0.64	0.95	0.79	0.58	0.53	0.76	0.54	0.39	0.54	0.05	0.44	0.41	0.35	0.55	0.00	0.00	0.07	0.01
GU	0.17	0.03	0.00	0.66	1.00	1.00	0.00	0.00	0.00	0.00	0.00	0.00	0.00	0.00	0.00	0.00	0.00	0.00	0.00	0.00	0.00	0.00	0.00	0.00	0.00	0.00	0.00	0.00	0.00
ID	1.00	1.00	1.00	1.00	1.00	1.00	1.00	1.00	1.00	1.00	0.99	0.99	1.00	1.00	1.00	1.00	1.00	1.00	1.00	0.99	1.00	1.00	1.00	1.00	1.00	1.00	1.00	1.00	1.00
JP	0.35	0.40	0.43	0.39	0.40	0.42	0.44	0.44	0.45	0.50	0.52	0.52	0.52	0.56	0.59	0.11	0.11	0.13	0.13	0.09	0.10	0.10	0.12	0.11	0.10	0.16	0.29	0.28	0.23
KI	0.60	0.00	0.00	0.00	0.00	0.00	0.00	0.00	0.00	0.00	0.00	0.00	0.00	0.32	0.00	0.00	0.86	0.46	0.35	0.48	0.65	0.00	0.05	0.49	0.35	0.30	0.05	0.28	0.02
KR	1.00	1.00	1.00	1.00	1.00	1.00	1.00	1.00	1.00	1.00	1.00	1.00	1.00	0.31	0.26	0.21	0.20	0.22	0.09	0.09	0.08	0.09	0.01	0.01	0.00	0.01	0.01	0.01	0.19
MH	1.00	0.00	0.00	0.00	0.00	0.00	0.00	0.00	0.00	1.00	0.00	0.00	0.68	0.94	0.86	0.80	0.72	0.41	0.00	0.00	0.00	0.28	0.44	0.00	0.12	0.06	0.00	0.07	0.02
NC	1.00	1.00	1.00	0.98	1.00	1.00	1.00	0.65	0.58	0.54	0.45	0.30	0.34	0.14	0.28	0.20	0.52	0.05	0.09	0.07	0.06	0.08	0.08	0.04	0.11	0.06	0.06	0.05	0.09
NU	0.00	0.00	0.00	0.00	0.00	0.00	0.00	0.00	0.00	0.00	0.08	0.28	0.11	0.05	0.84	0.19	0.00	0.00	0.00	0.00	0.00	0.00	0.00	0.00	0.00	0.00	0.00	0.00	0.00
NZ	1.00	1.00	1.00	1.00	1.00	1.00	1.00	1.00	1.00	1.00	0.27	0.25	0.16	0.38	0.16	0.18	0.32	0.22	0.20	0.35	0.41	0.08	0.05	0.19	0.03	0.21	0.00	0.05	0.00
PF	0.49	0.62	0.93	1.00	1.00	0.37	0.40	0.38	0.37	0.43	0.39	0.34	0.37	0.34	0.37	0.36	0.42	0.38	0.35	0.28	0.12	0.14	0.16	0.14	0.09	0.07	0.14	0.09	0.09
PG	0.86	0.77	0.90	0.89	0.93	0.87	0.81	0.67	0.51	0.58	0.67	0.73	0.86	0.85	0.87	0.87	0.99	1.00	0.41	0.51	0.08	0.29	0.07	0.23	0.84	0.00	0.00	0.09	0.09
PH	1.00	1.00	1.00	1.00	1.00	1.00	1.00	1.00	1.00	1.00	1.00	1.00	1.00	1.00	1.00	0.98	0.98	1.00	0.97	1.00	0.00	0.00	0.00	0.00	0.00	0.00	0.00	0.00	0.00
PT	0.00	0.00	0.00	0.00	0.00	0.00	0.00	0.00	0.00	0.00	0.00	0.00	0.00	0.00	0.00	0.00	0.00	0.00	0.00	0.00	0.89	0.61	0.00	0.00	0.00	0.00	0.00	0.00	0.00
PW	0.00	0.00	0.00	0.00	0.00	0.79	1.00	0.00	0.00	1.00	0.00	0.00	0.00	0.00	0.00	0.00	0.00	0.00	0.00	0.00	0.00	0.00	0.06	0.25	0.28	0.48	0.00	0.76	0.09
SB	0.00	0.00	0.00	0.00	0.00	0.00	0.00	0.00	0.00	0.00	0.00	0.00	0.00	0.00	0.00	0.89	0.87	0.41	0.11	0.84	0.58	0.37	0.00	0.20	0.13	0.00	0.03	0.28	0.47
SN	0.00	0.00	0.00	0.00	0.00	0.00	0.00	0.00	0.00	0.00	0.00	1.00	1.00	0.00	0.00	0.00	0.00	0.00	0.00	0.00	0.00	0.00	0.00	0.00	0.00	0.00	0.00	0.00	0.00
TO	0.00	0.87	1.00	0.91	0.86	0.49	0.56	0.28	0.15	0.15	0.31	0.20	0.17	0.09	0.27	0.74	0.67	0.63	0.54	0.31	0.11	0.12	0.00	0.09	0.01	0.00	0.02	0.01	0.05
TV	0.00	0.00	0.00	0.00	0.00	0.00	0.00	0.00	0.00	0.00	1.00	0.00	0.00	0.00	0.00	1.00	1.00	0.69	0.21	0.38	0.14	0.00	0.01	0.02	0.01	0.00	0.04	0.00	0.00
TW	0.95	0.96	0.97	0.98	0.98	0.97	0.99	0.66	0.54	0.98	0.68	0.78	0.82	0.84	0.85	0.80	0.83	0.00	0.00	0.00	0.00	0.00	0.11	0.12	0.10	0.09	0.07	0.07	0.09
US	0.62	0.20	0.17	0.25	0.17	0.07	0.02	0.02	0.02	0.02	0.01	0.01	0.01	0.00	0.02	0.01	0.00	0.00	0.00	0.02	0.10	0.09	0.03	0.02	0.01	0.02	0.01	0.02	0.01
VN	0.00	0.00	0.00	0.00	0.00	1.00	1.00	1.00	1.00	1.00	1.00	1.00	1.00	1.00	1.00	1.00	1.00	1.00	1.00	1.00	1.00	1.00	1.00	1.00	1.00	1.00	1.00	1.00	1.00
VU	0.03	0.13	0.07	0.00	0.00	0.88	0.91	0.85	0.93	0.95	0.88	0.89	0.33	0.68	0.78	0.08	0.53	0.83	0.50	0.20	0.27	0.01	0.30	0.16	0.32	0.03	0.09	0.01	0.10
WS	1.00	1.00	1.00	1.00	1.00	1.00	1.00	1.00	1.00	1.00	1.00	1.00	1.00	1.00	1.00	1.00	0.80	0.19	0.29	0.05	0.02	0.00	0.20	0.07	0.13	0.35	0.42	0.09	0.03

7.1 Stock synthesis assessment

Table 2: Estimates and associated uncertainty estimated using MCMC for model parameters and derived quantities for the 2025 diagnostic model for oceanic whitetip shark. SD: Standard deviation, MAD: median absolute deviation, credible intervals (5% and 95%).

Variable	Mean	Median	SD	MAD	5%	95%
SB_{recent}/SB_0	0.06	0.06	0.01	0.01	0.04	0.08
$F_{recent}/F_{\text{MSY}}$	1.07	1.19	0.25	0.28	0.73	1.39
F_{Init}	0.21	0.21	0.03	0.04	0.16	0.27
$\ln(R_0)$	5.29	5.29	0.13	0.14	5.08	5.52
M	0.15	0.15	0.01	0.01	0.13	0.17
z_{frac}	0.93	0.93	0.03	0.03	0.87	0.97

7.2 Dynamic surplus production model

Table 3: Parameter estimates and derived quantities for different model runs with alternative prior assumptions about discards (Disc.) and initial depletion (start_N - halved or doubled). SD: Standard deviation, MAD: median absolute deviation, credible intervals (5% and 95%), the $\hat{R}$ convergence diagnostic (should be as close as possible to 1.00) and the Effective Sample Size (ESS).

Model	Variable	Mean	Median	SD	MAD	5%	95%	$\hat{R}$	ESS
High Disc. (Post exp.) start_N /0.5	N_{recent}/N_0	0.12	0.11	0.05	0.05	0.05	0.23	1.00	8133.86
High Disc. (Post exp.) start_N /1	N_{recent}/N_0	0.07	0.06	0.03	0.03	0.03	0.13	1.00	7452.45
High Disc. (Post exp.) start_N /2	N_{recent}/N_0	0.02	0.02	0.01	0.01	0.01	0.04	1.00	8139.45
Mean Disc. (Post exp.) start_N /0.5	N_{recent}/N_0	0.12	0.11	0.05	0.05	0.05	0.22	1.00	8115.29
Mean Disc. (Post exp.) start_N /1	N_{recent}/N_0	0.07	0.06	0.03	0.03	0.03	0.13	1.00	7913.28
Mean Disc. (Post exp.) start_N /2	N_{recent}/N_0	0.02	0.02	0.01	0.01	0.01	0.04	1.00	8071.53
High Disc. (Post exp.) start_N /0.5	U_{recent}	0.04	0.04	0.02	0.02	0.02	0.08	1.00	7775.18
High Disc. (Post exp.) start_N /1	U_{recent}	0.04	0.04	0.02	0.02	0.02	0.08	1.00	7259.00
High Disc. (Post exp.) start_N /2	U_{recent}	0.04	0.04	0.02	0.02	0.02	0.09	1.00	7832.71
Mean Disc. (Post exp.) start_N /0.5	U_{recent}	0.06	0.06	0.02	0.02	0.03	0.10	1.00	7201.38
Mean Disc. (Post exp.) start_N /1	U_{recent}	0.06	0.06	0.02	0.02	0.03	0.11	1.00	8011.79
Mean Disc. (Post exp.) start_N /2	U_{recent}	0.07	0.06	0.03	0.02	0.03	0.11	1.00	7721.54
High Disc. (Post exp.) start_N /0.5	$\log(K)$	14.45	14.42	0.38	0.38	13.90	15.12	1.00	8009.33
High Disc. (Post exp.) start_N /1	$\log(K)$	14.99	14.98	0.43	0.44	14.29	15.72	1.00	7660.02
High Disc. (Post exp.) start_N /2	$\log(K)$	16.20	16.19	0.45	0.47	15.46	16.94	1.00	8030.00
Mean Disc. (Post exp.) start_N /0.5	$\log(K)$	14.42	14.37	0.37	0.37	13.87	15.10	1.00	7969.99
Mean Disc. (Post exp.) start_N /1	$\log(K)$	14.98	14.97	0.45	0.46	14.25	15.76	1.00	7674.94
Mean Disc. (Post exp.) start_N /2	$\log(K)$	16.19	16.19	0.46	0.47	15.42	16.95	1.00	7315.28
High Disc. (Post exp.) start_N /0.5	q	6.85	6.26	2.91	2.40	3.44	12.39	1.00	8028.26
High Disc. (Post exp.) start_N /1	q	12.58	11.43	5.61	4.68	5.88	23.02	1.00	7451.12
High Disc. (Post exp.) start_N /2	q	43.55	39.88	19.10	16.54	19.88	78.76	1.00	8055.99
Mean Disc. (Post exp.) start_N /0.5	q	6.52	5.94	2.67	2.20	3.38	11.74	1.00	8139.16
Mean Disc. (Post exp.) start_N /1	q	12.20	11.05	5.52	4.55	5.67	22.65	1.00	8000.43
Mean Disc. (Post exp.) start_N /2	q	42.74	39.11	19.07	16.19	19.37	78.59	1.00	7827.92
High Disc. (Post exp.) start_N /0.5	r	0.12	0.12	0.04	0.04	0.07	0.19	1.00	8245.45
High Disc. (Post exp.) start_N /1	r	0.12	0.11	0.04	0.04	0.06	0.19	1.00	8025.44
High Disc. (Post exp.) start_N /2	r	0.11	0.11	0.04	0.04	0.06	0.18	1.00	7381.91
Mean Disc. (Post exp.) start_N /0.5	r	0.13	0.13	0.04	0.04	0.07	0.21	1.00	7944.50
Mean Disc. (Post exp.) start_N /1	r	0.13	0.12	0.04	0.04	0.07	0.21	1.00	7463.03
Mean Disc. (Post exp.) start_N /2	r	0.12	0.12	0.04	0.04	0.07	0.20	1.00	8229.89

Table 4: Predictive coverage: proportion of the posterior distribution for year $y + 1$ covered by the predictive distribution from a model fitted up to year y.

Year	Coverage	
	Harvest rate	Depletion
2014	1.00	1.00
2015	0.96	0.95
2016	0.96	0.97
2017	0.96	0.96
2018	0.95	0.94
2019	0.97	0.97
2020	0.95	0.94
2021	0.96	0.98
2022	0.94	0.94

7.3 Model Comparison

Table 5: Estimates of management quantities (stock status as SB_{recent}/SB_0, and fishing mortality (F) relative to indicators (F_{MSY}) and possible limit reference points F_{lim}, F_{crash}) across models ensembles (number of models in parentheses), arranged by model type. P(>RP) refers to the probability that the metric (status, fishing mortality) is above the respective indicator (B_0, F_{MSY}, F_{lim}, F_{crash}). SS3: Stock Synthesis 3, DSPM: Dynamic surplus production model.

Model	Subset	Metric	Mean	SD	Median	2.5%	25%	75%	97.5%	P(>RP)
SS3	Ensemble (36)	SB_{recent}/SB_0	0.06	0.01	0.06	0.04	0.05	0.07	0.08	0.00
SS3	Ensemble (36)	$F_{recent}/F_{\text{MSY}}$	1.03	0.26	1.02	0.71	0.75	1.33	1.42	0.50
SS3	Ensemble (36)	F_{recent}/F_{lim}	0.69	0.17	0.68	0.48	0.51	0.89	0.95	0.00
SS3	Ensemble (36)	F_{recent}/F_{crash}	0.54	0.13	0.53	0.37	0.39	0.69	0.74	0.00
DSPM	Ensemble (2)	N_{recent}/N_0	0.07	0.03	0.06	0.02	0.04	0.11	0.16	0.00
DSPM	Ensemble (2)	$U_{recent}/U_{\text{MSY}}$	0.62	0.26	0.56	0.27	0.36	0.90	1.25	0.08
DSPM	Ensemble (2)	U_{recent}/U_{lim}	0.41	0.17	0.38	0.18	0.24	0.60	0.83	0.01
DSPM	Ensemble (2)	U_{recent}/U_{crash}	0.31	0.13	0.28	0.13	0.18	0.45	0.62	0.00

8. FIGURES

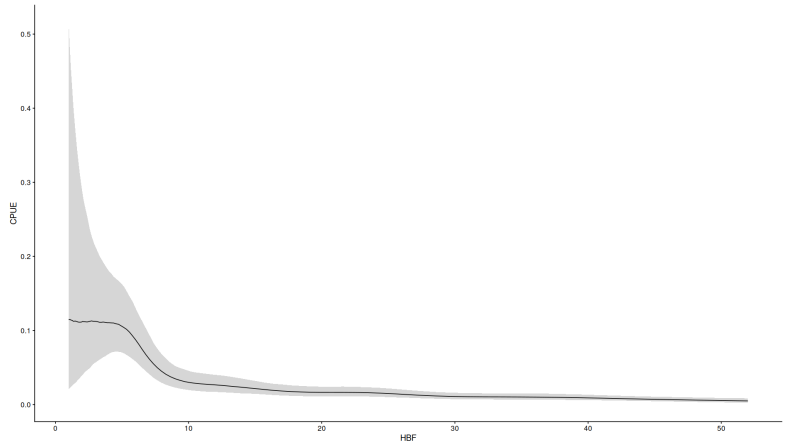

Figure 1: Estimated effect of hooks - between - floats (HBF) on CPUE (catch per thousand hooks) for oceanic whitetip shark from the final index model presented in Hill - Moana et al. (2024).

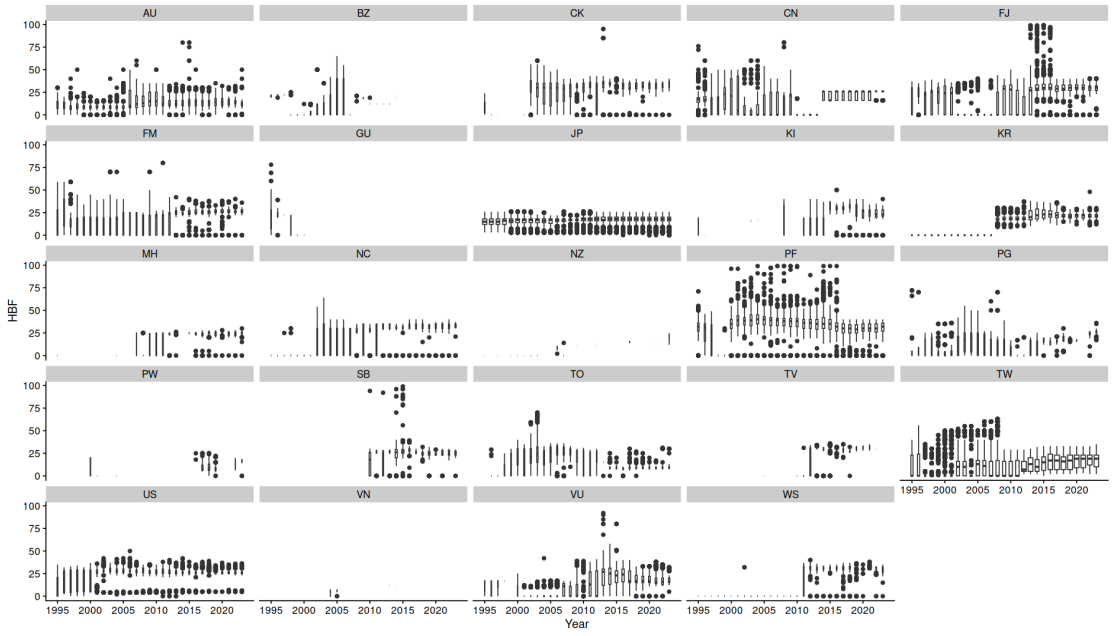

Figure 2: Distribution of reported hooks - between - floats (HBF) by flag and year.

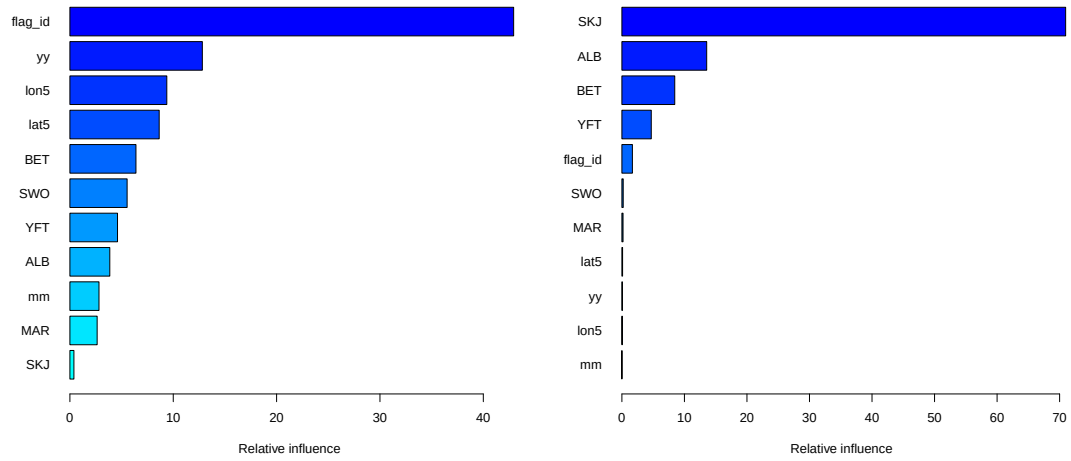

Figure 3: Relative importance of predictors in boosted regression trees for imputing HBF, for models using target species catch rates (left) and catch proportions (right; used for subsequent analyses).

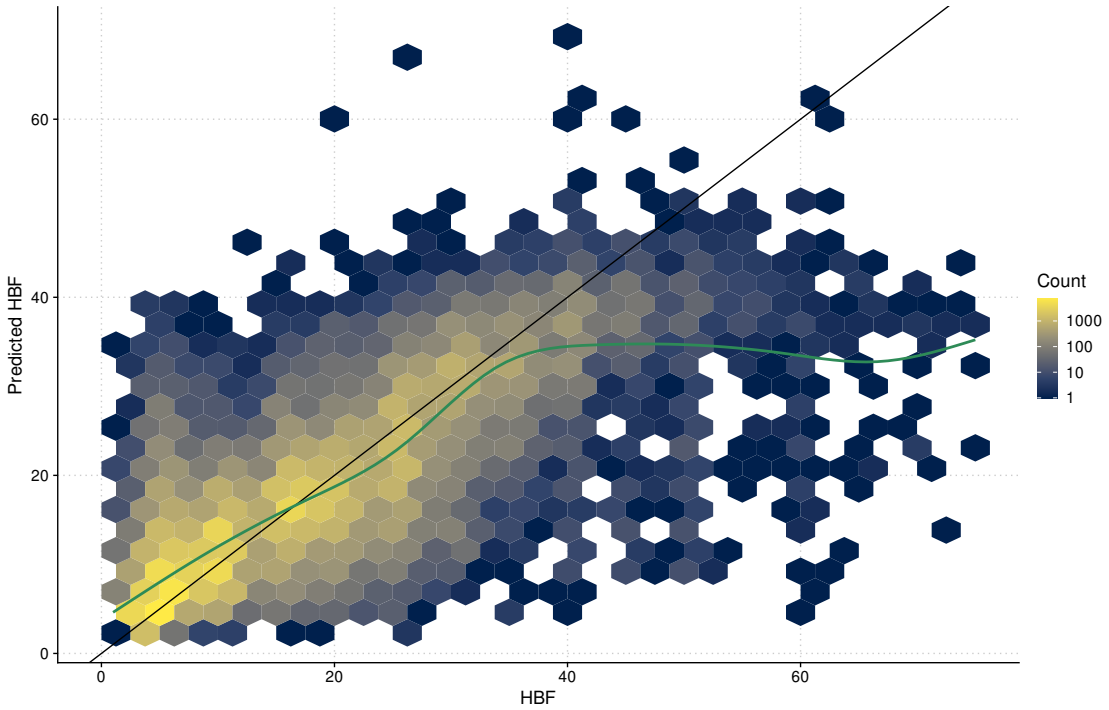

Figure 4: Observed vs. predicted hooks-between-floats (HBF) in the training dataset for HBF imputation; black line is the 1 to 1, green line is a loess smoother showing deviations from the 1 to 1 line.

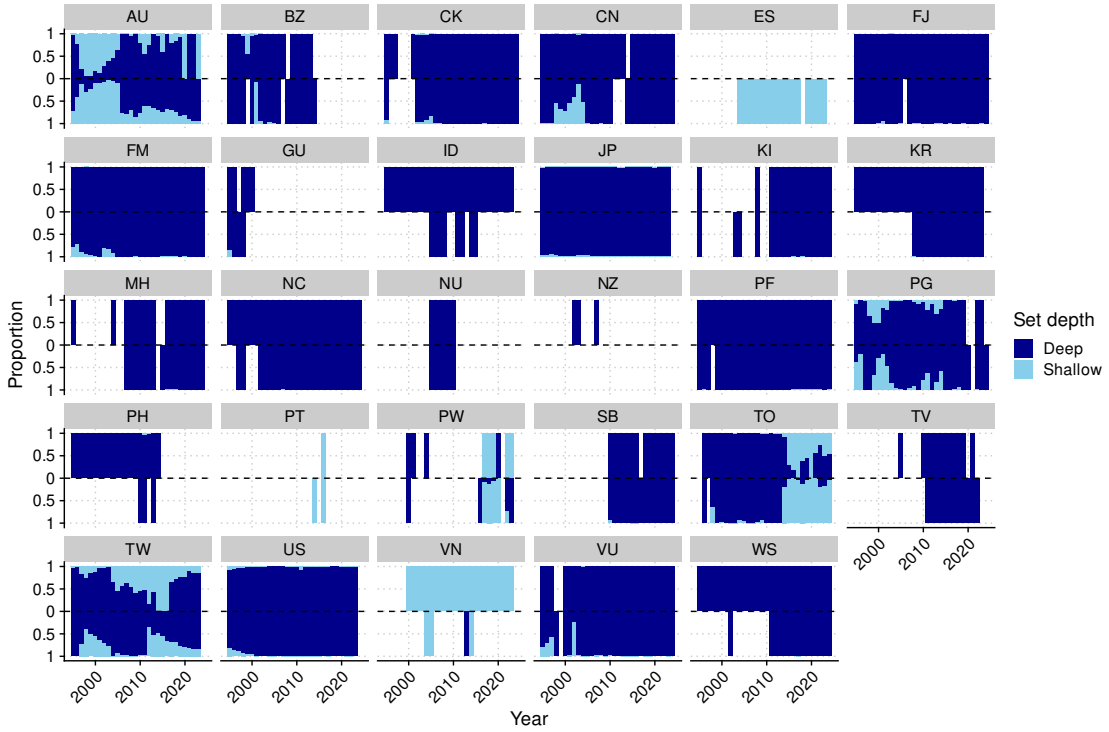

Figure 5: Observed (below zero line) vs. predicted (above zero) proportions of effort by hooks-between-floats (HBF) category and flag for shallow (<10 HBF) and deep (>=10 HBF) effort.

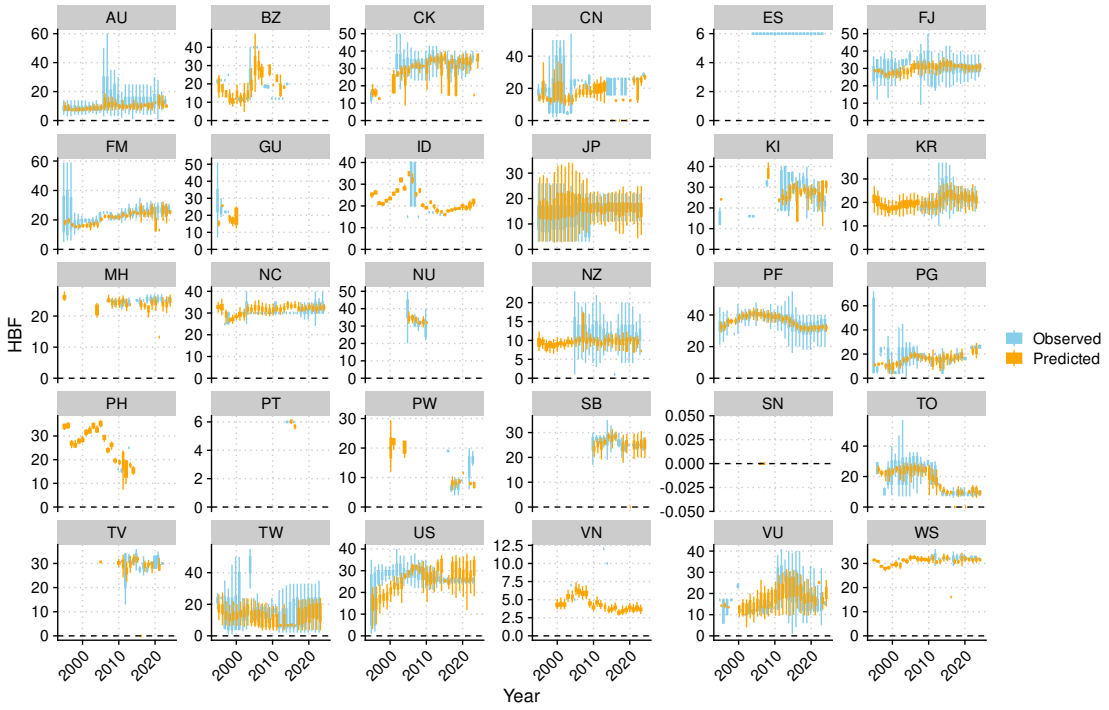

Figure 6: Observed (blue) vs. predicted (orange) hooks-between-floats (HBF) by flag. Note that outliers were not plotted, and some effort is therefore missing.

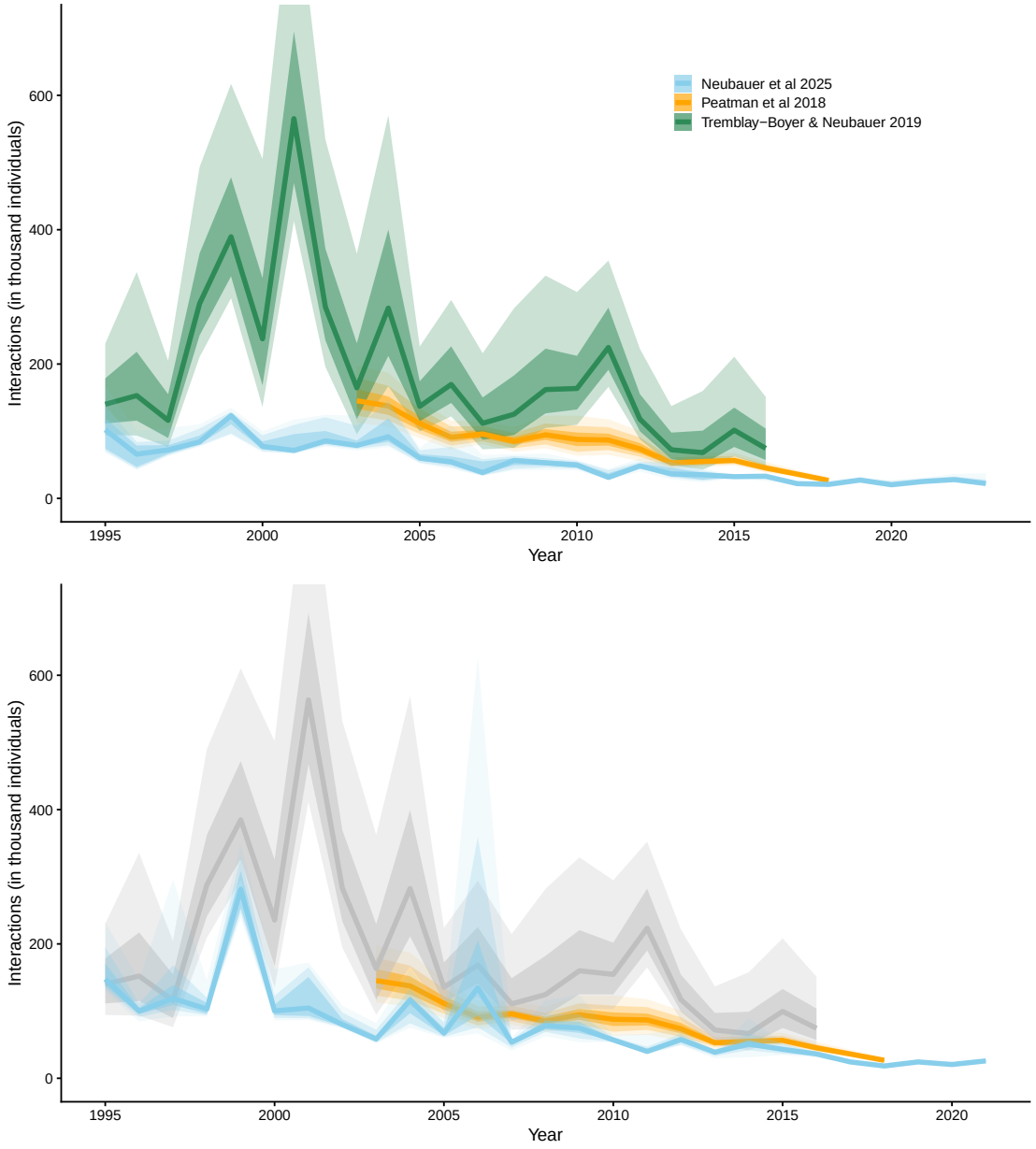

Figure 7: Comparison of updated predicted catches for the present assessment (blue) using imputed HBF (top panel), with initial 2024 OCS catch estimates based on models using proxies for HBF (bottom panel; based on Hill-Moana et al. (2024)) and previous catch reconstructions for OCS from Tremblay-Boyer et al. (2019) and Peatman et al. (2018a).

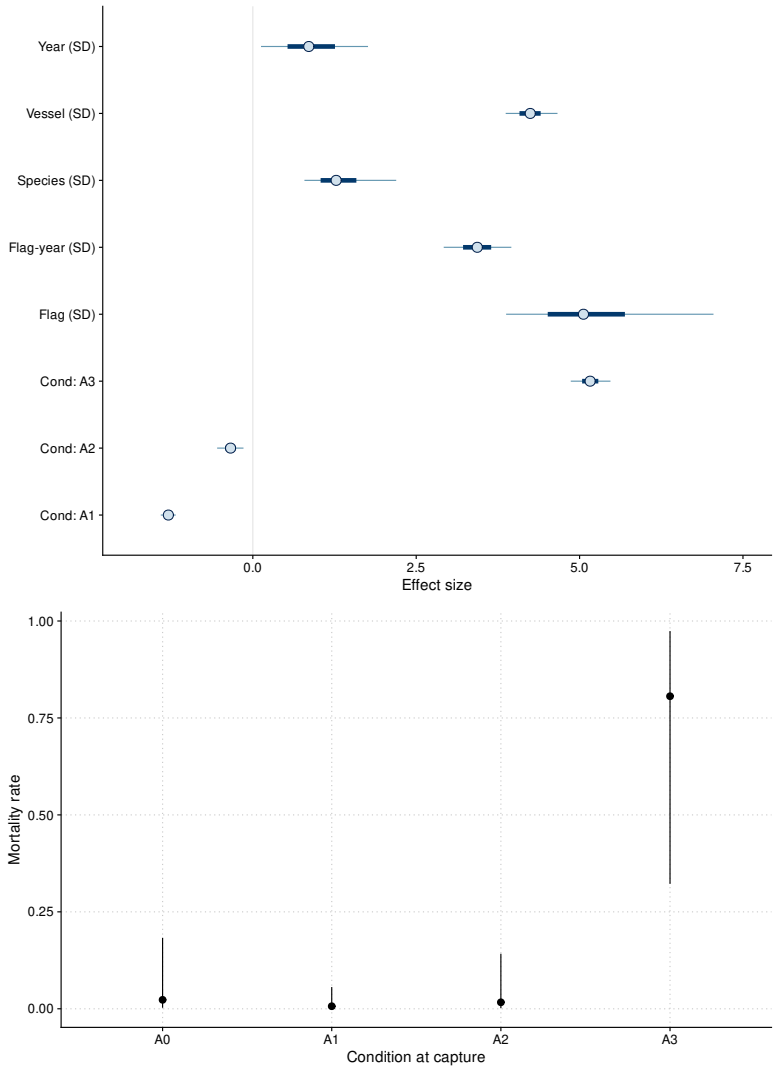

Figure 8: Estimated effect size of effects in the condition model to predict the condition at discard (top panel) and estimated effect of condition at capture on mortality for OCS.

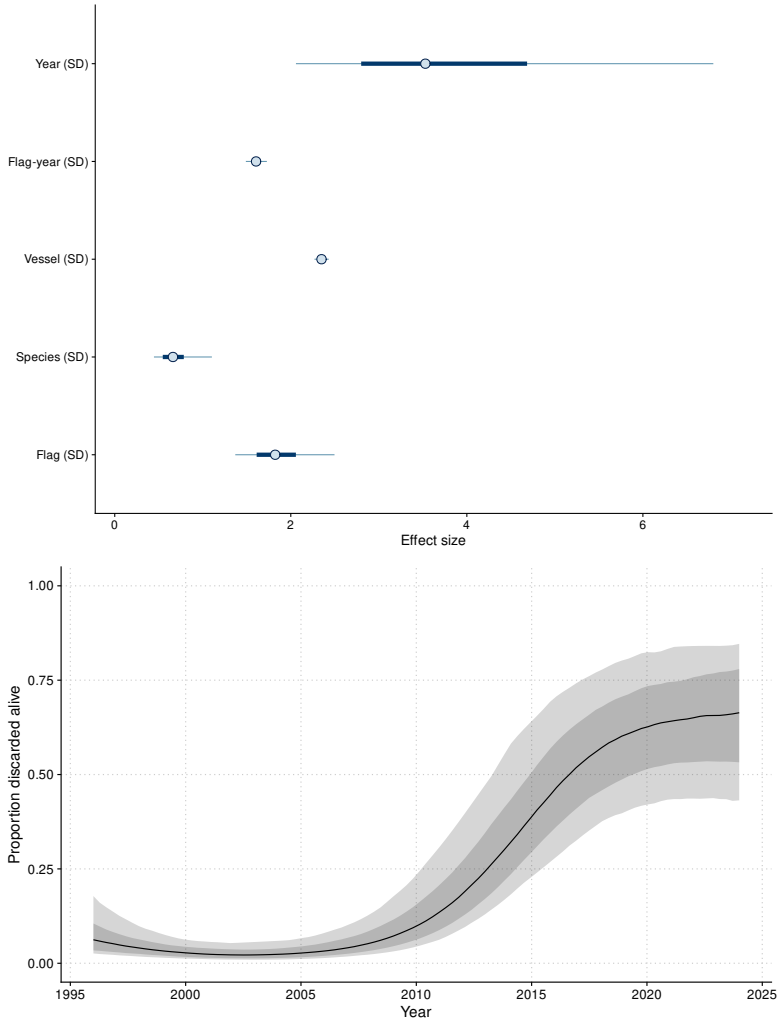

Figure 9: Estimated mean proportion of OCS discarded alive by year, including inter-quartile (dark shading) and 95% credible intervals for the posterior distribution.

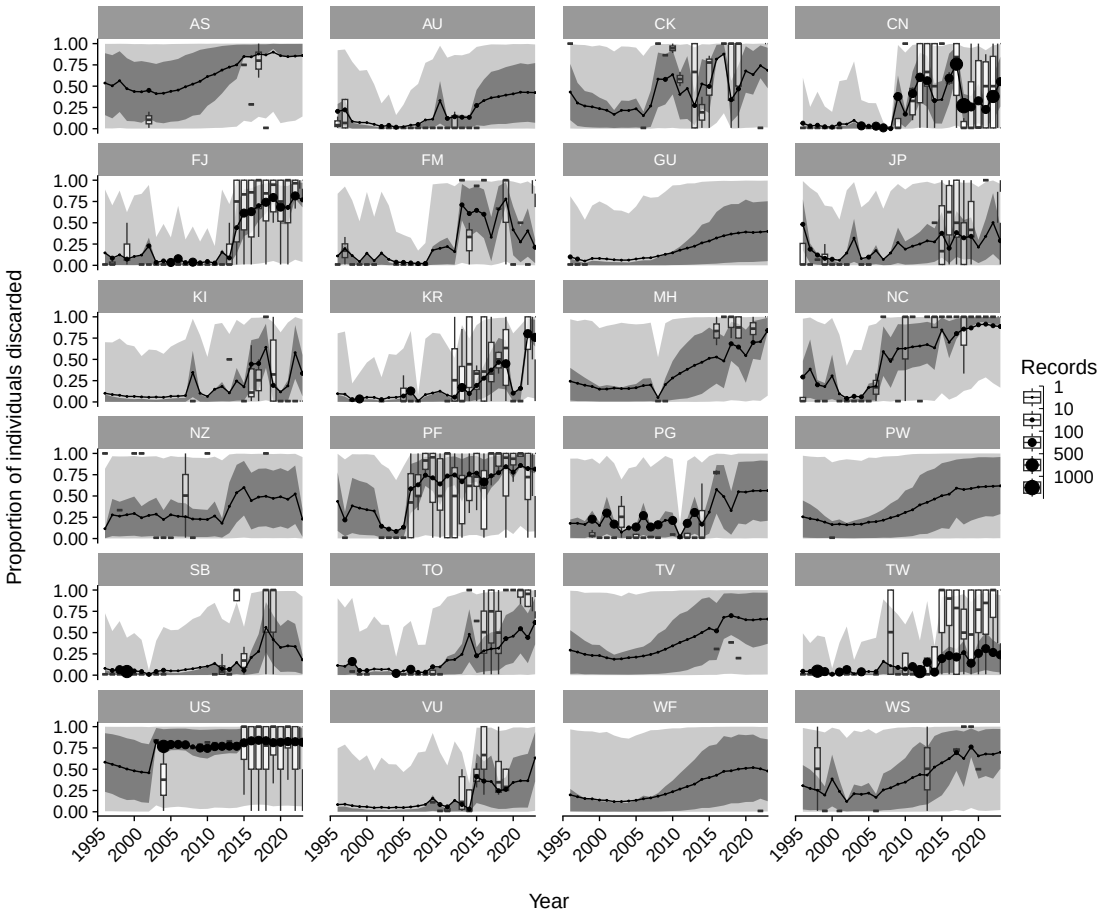

Figure 10: Observed (boxplots for within-flag variability within year) and predicted (posterior mean line and 75% (dark shade) and 95% (light shade) credible intervals) discard rates by flag for longline interactions with oceanic whitetip shark. The size of the points on the line indicates the number of records, with lines without points representing model predictions.

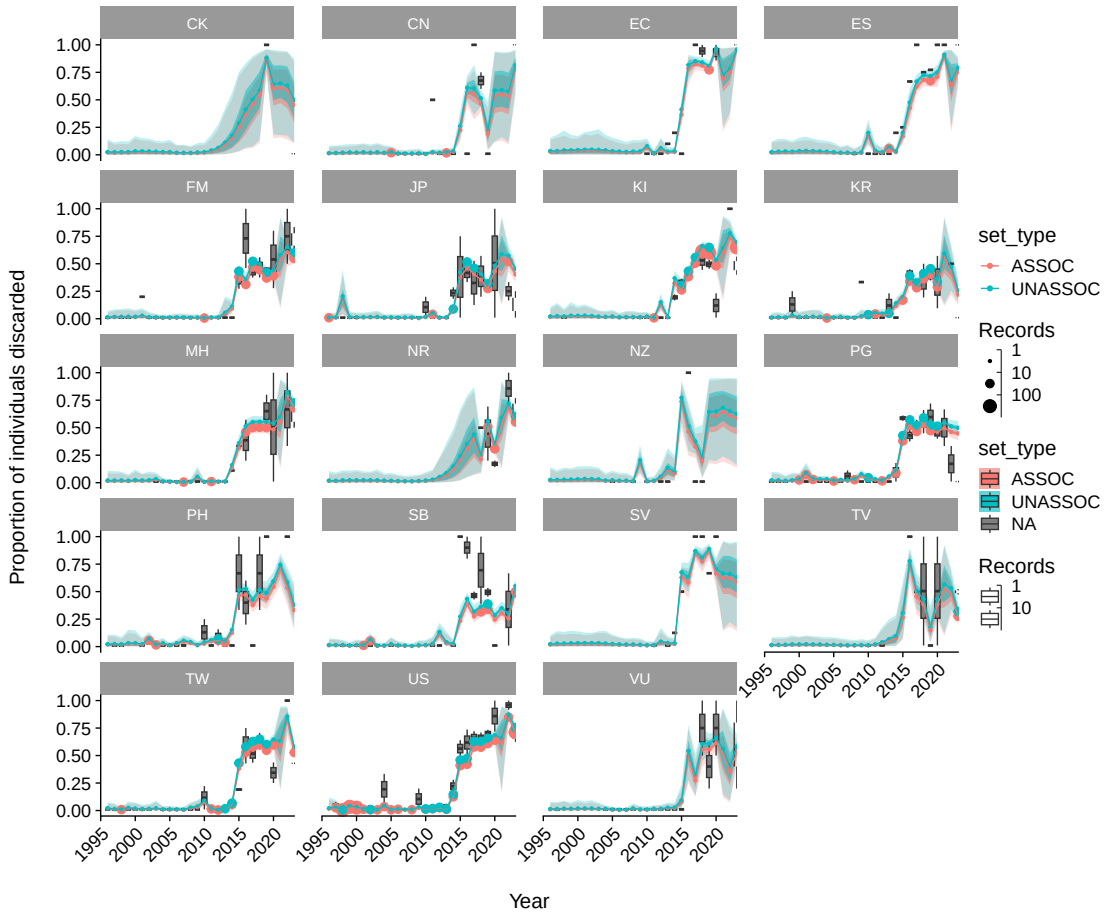

Figure 11: Observed (boxplots for within-flag variability within year) and predicted (posterior mean line and 75% (dark shade) and 95% (light shade) credible intervals) discard rates by flag and set-type for purse-seine interactions with oceanic whitetip shark. The size of the points on the line indicates the number of records, with lines without points representing model predictions.

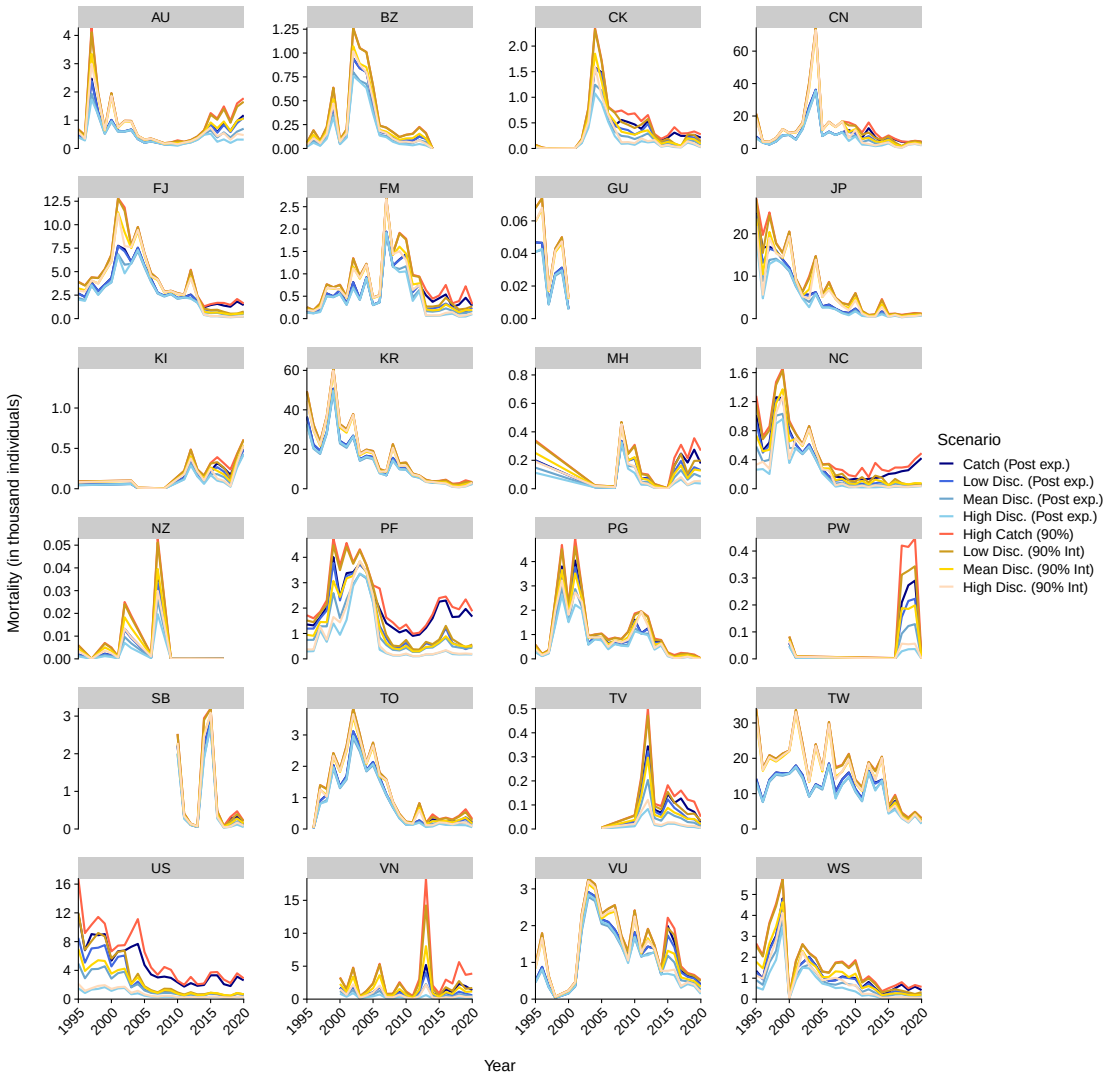

Figure 12: Predicted total fishing related mortality from longline fisheries by flag, including 15% post release mortality for live-discarded oceanic whitetip shark. Interactions refer to the posterior median (50%) and 90^{th} percentile (90%) of the predicted catch from the observer catch rate model. Low, median and high discard scenarios refer to the 25%, 50% (median) and 75% discard estimates.

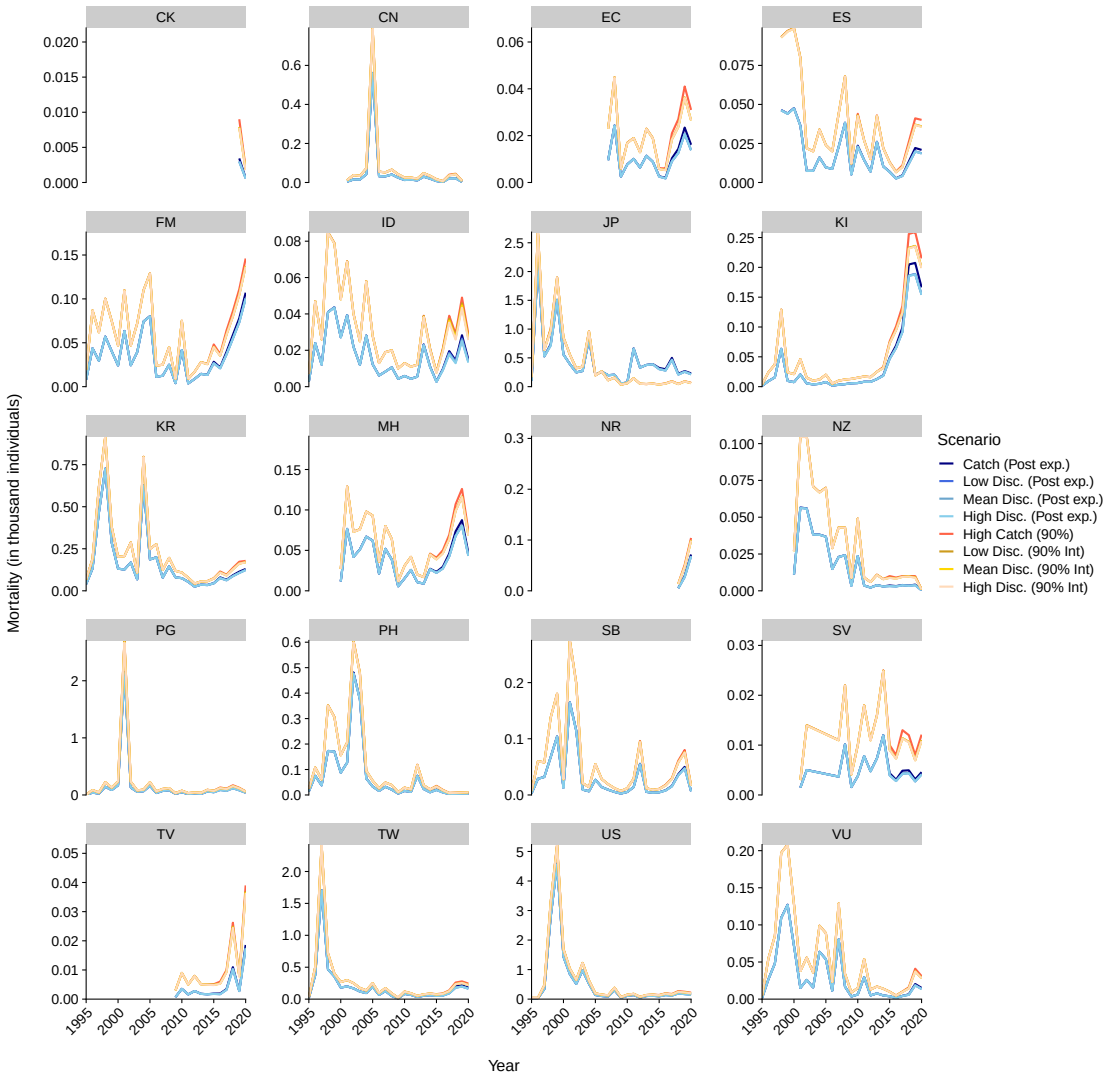

Figure 13: Predicted total fishing related mortality from purse-seine fisheries by flag, including 85% post release mortality for live-discarded oceanic whitetip shark. Interactions refer to the posterior median (50%) and 90^{th} percentile (90%) of the predicted catch from the observer catch rate model. Low, median and high discard scenarios refer to the 25%, 50% (median) and 75% discard estimates.

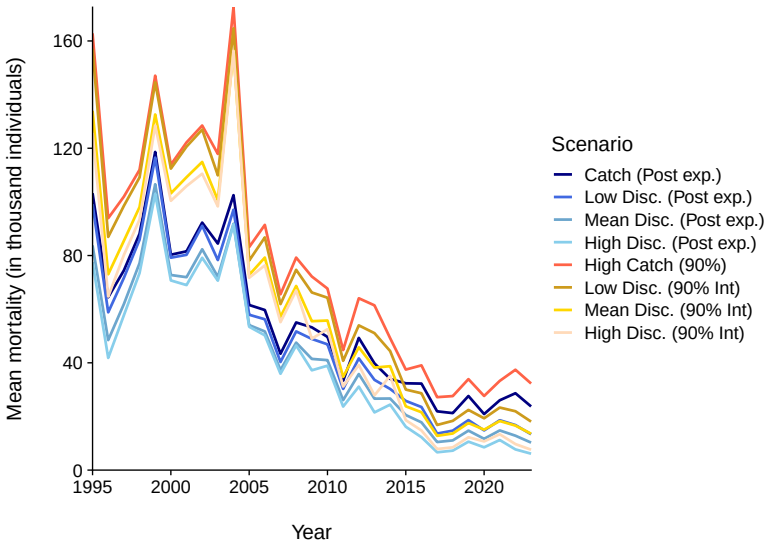

Figure 14: Predicted total fishing related mortality from longline, including 15% post release mortality for live-discarded oceanic whitetip sharks. Interactions refer to the posterior median (50%) and 90^{th} percentile (90%) of the predicted catch from the observer catch rate model. Low, median and high discard scenarios refer to the 25%, 50% (median) and 75% discard estimates. All discard estimates were applied at flag and latitudinal stratum level to overall interactions.

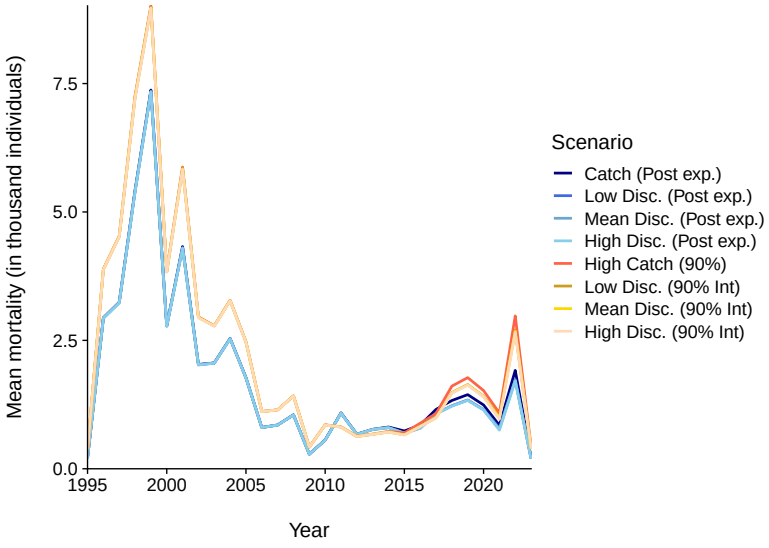

Figure 15: Predicted total fishing related mortality from purse-seine, including 15% post release mortality for live-discarded oceanic whitetip sharks. Interactions refer to the posterior median (50%) and 90^{th} percentile (90%) of the predicted catch from the observer catch rate model. Low, median and high discard scenarios refer to the 25%, 50% (median) and 75% discard estimates. All discard estimates were applied at flag and latitudinal stratum level to overall interactions.

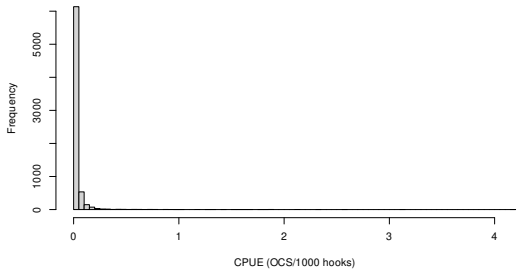

Figure 16: Histogram of nominal catch-rates for all non-zero catches used in CPUE models in Hill-Moana et al. (2024).

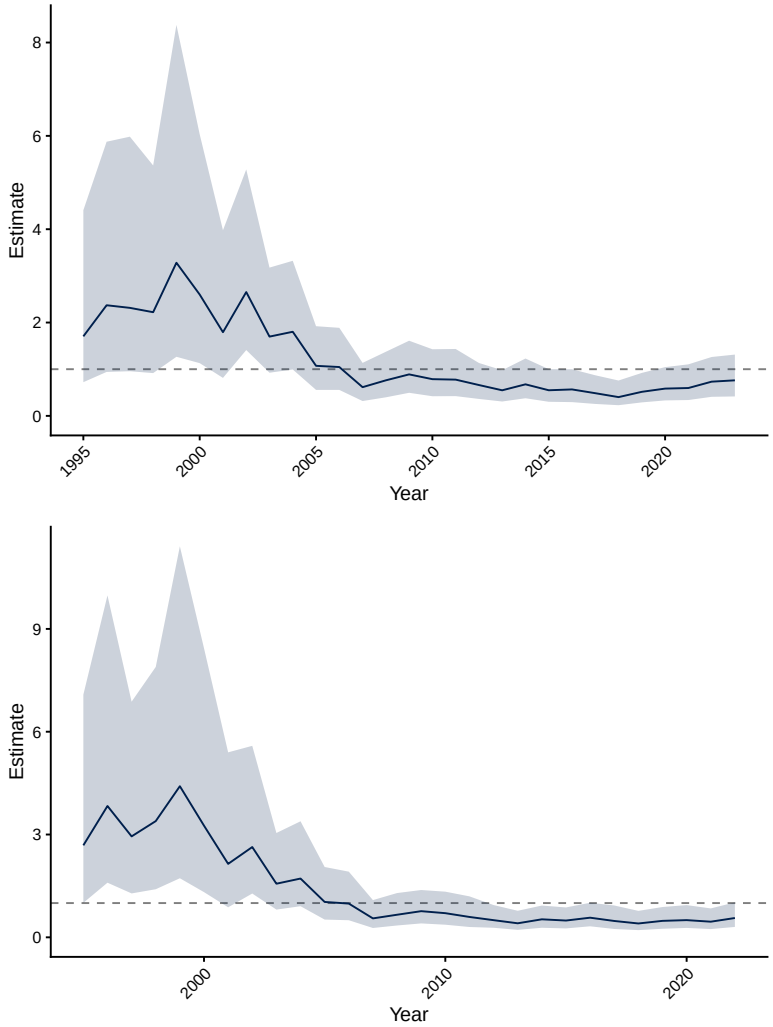

Figure 17: Longline CPUE index using long-running observer indices and excluding high CPUE values (top panel; see text). For comparison, the original index without filtering of high CPUE values is shown in the bottom panel. Shown is the posterior median and 95% credible interval for the year effect, standardised for regional trends and environmental variables.

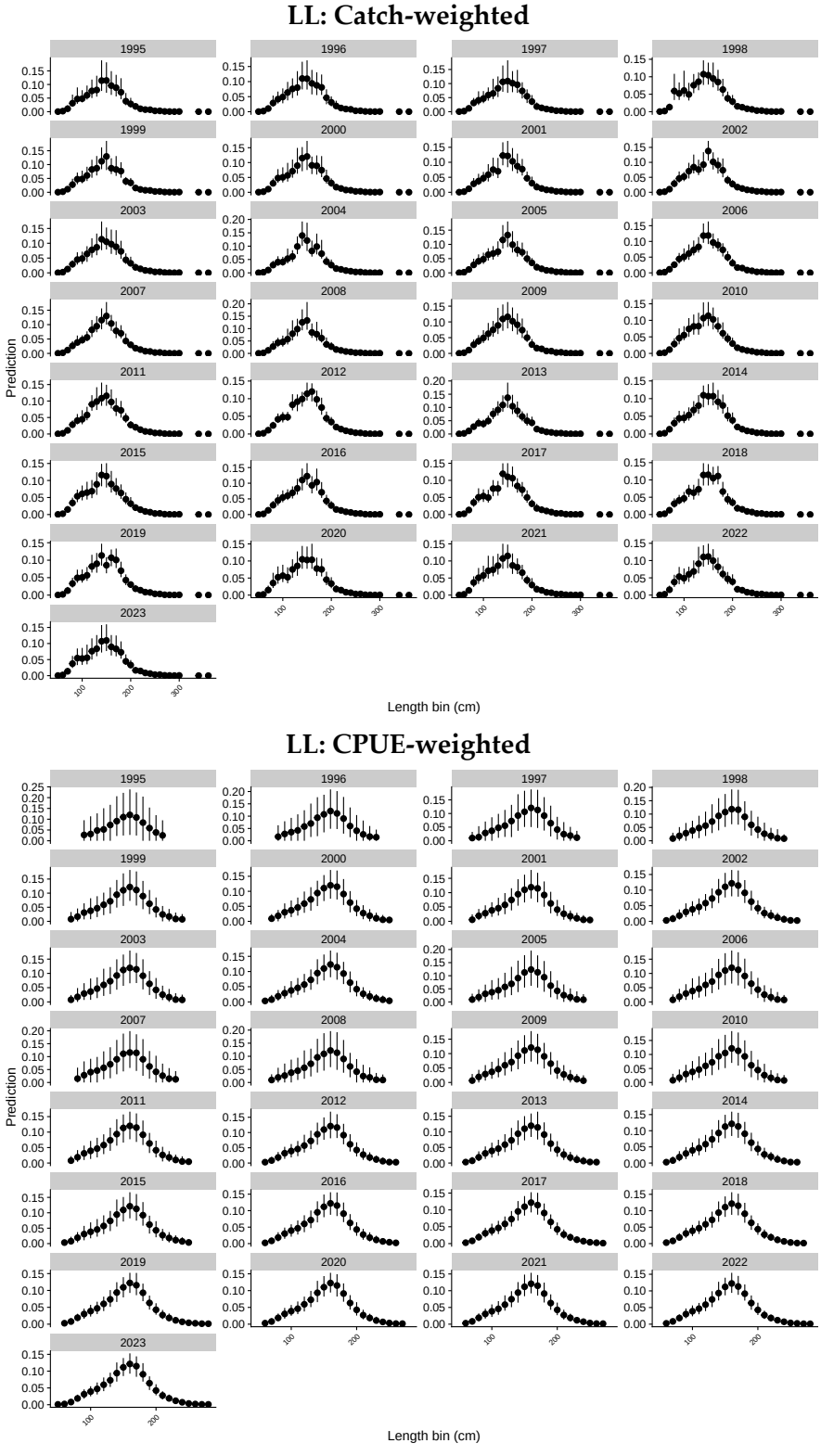

Figure 18: Comparing catch-weighted (top) and CPUE-weighted (bottom) length frequencies (LFs) for OCS in longline fisheries.

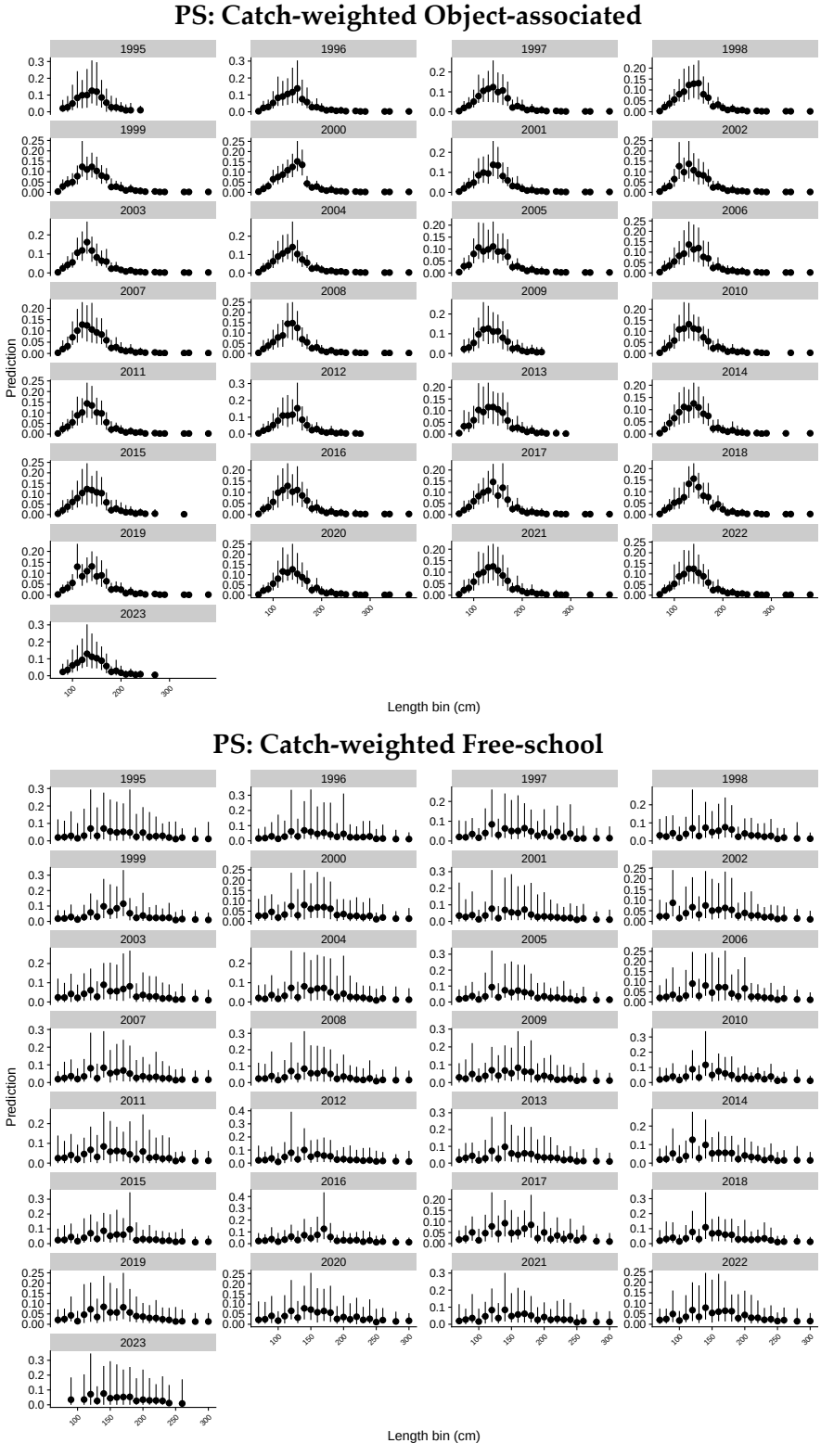

Figure 19: Comparing length frequencies (LFs) for OCS catch for object associated purse-seine (top) and free-school purse-seine (bottom) fisheries.

Figure 20: Western and Central Pacific Fisheries Commission convention area (light grey), including the stock assessment area for oceanic whitetip shark (dark grey), bounded by the 30°N and 30°S parallels.

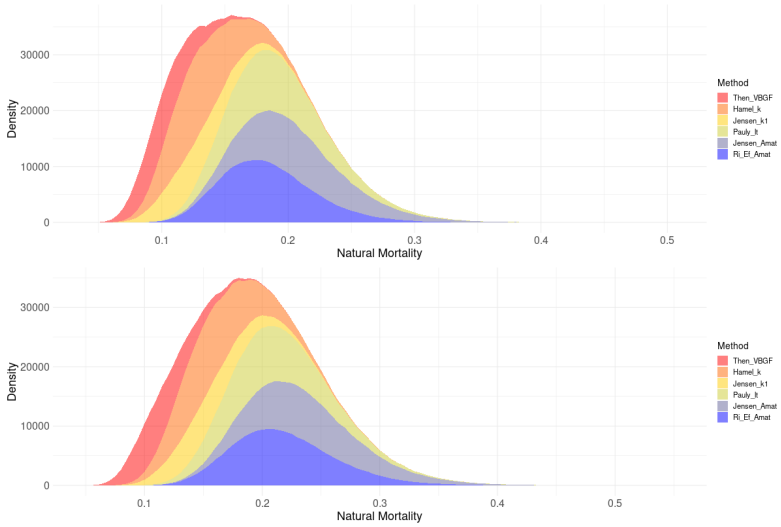

Figure 21: Meta-analytic priors for M using an assumed input CV of 30%, with colours representing individual life-history based estimators of natural mortality (Cope and Hamel 2022). The top panel shows the M prior derived under the growth parameters from Joung et al. (2016), the bottom panel reflects Seki et al. (1998) growth parameters.

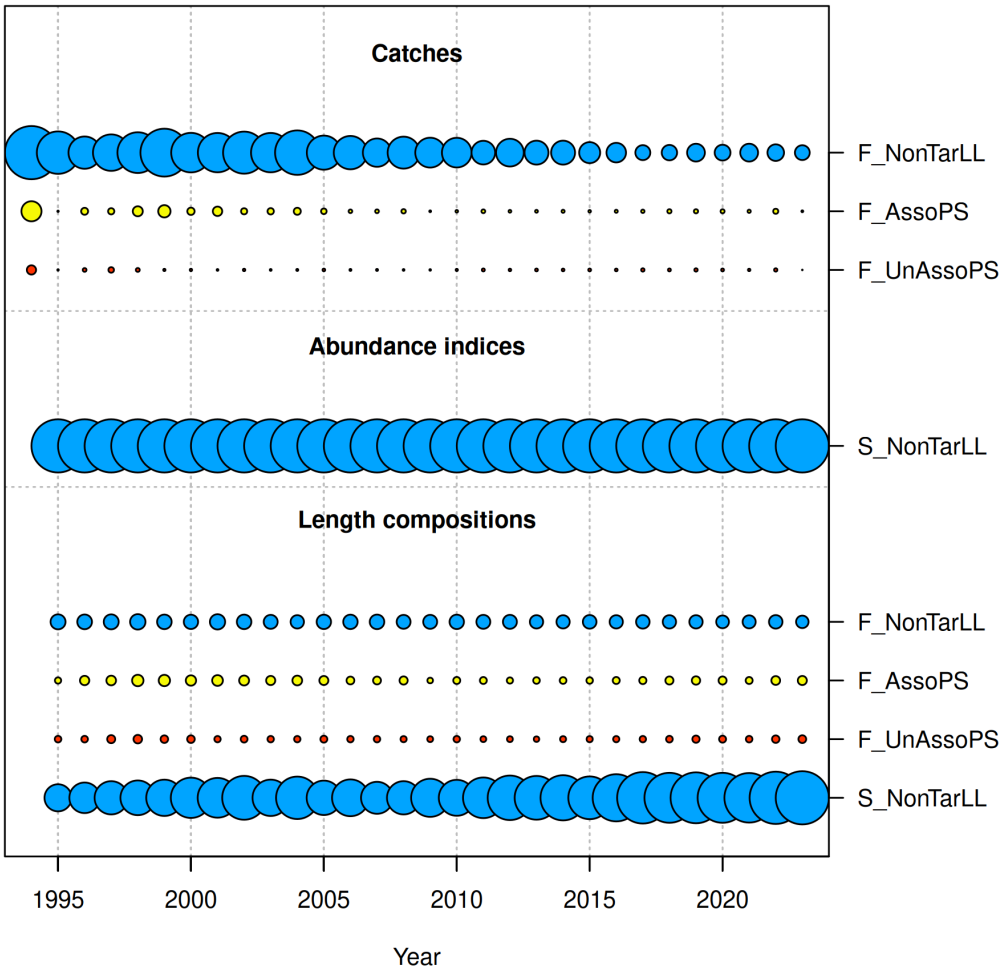

Figure 22: Data presence by year for each fleet, where circle area is relative within a data type. Circles are proportional to total catch for catches; to precision for indices, discards, and mean body weight observations; and to total sample size for compositions and mean weight- or length-at-age observations. Observations excluded from the likelihood have equal size for all years. Note, that since the circles are scaled relative to maximum within each type, the scaling within separate plots should not be compared.

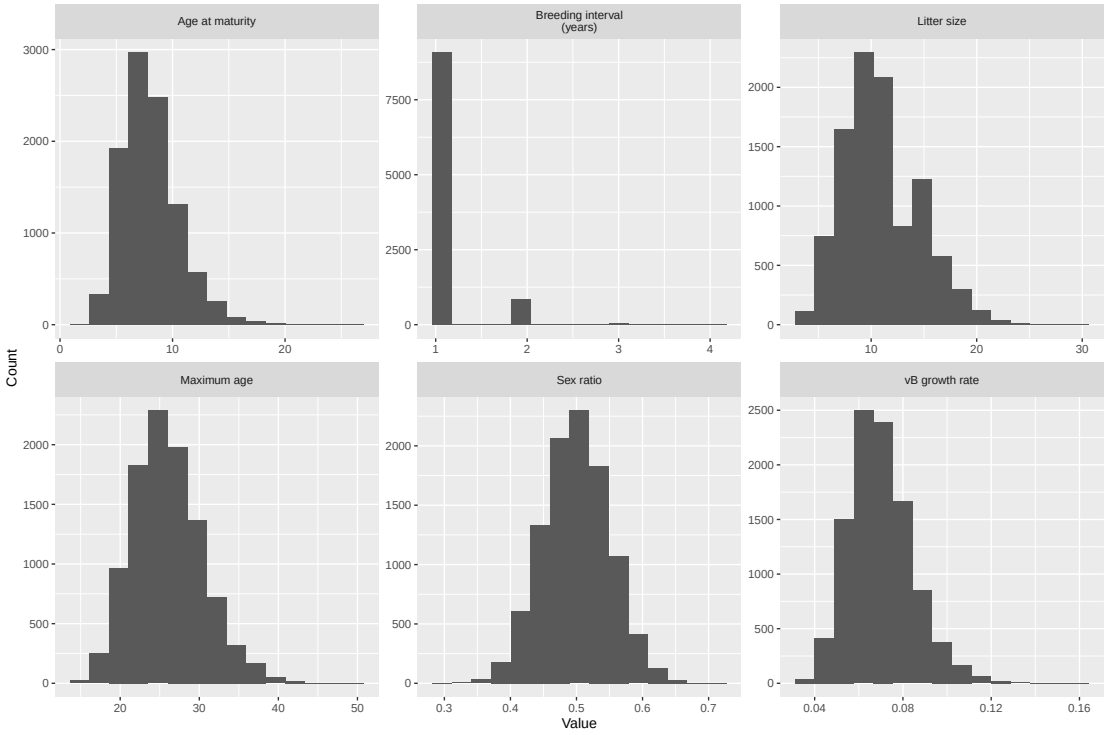

Figure 23: Input values for R_{max} simulations for oceanic whitetip shark, based on parameter values reported in the literature (vB, von Bertalanffy).

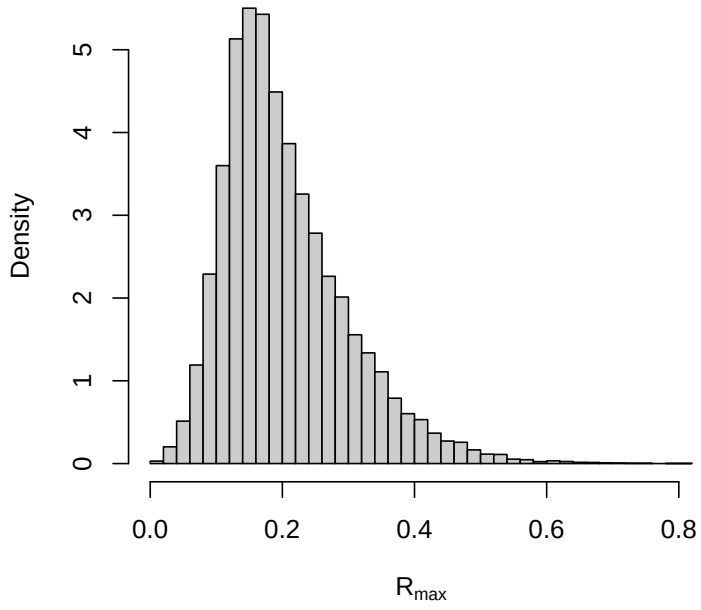

Figure 24: Simulated distribution over R_{max} for oceanic whitetip shark using distributions over input parameters shown in Figure 23.

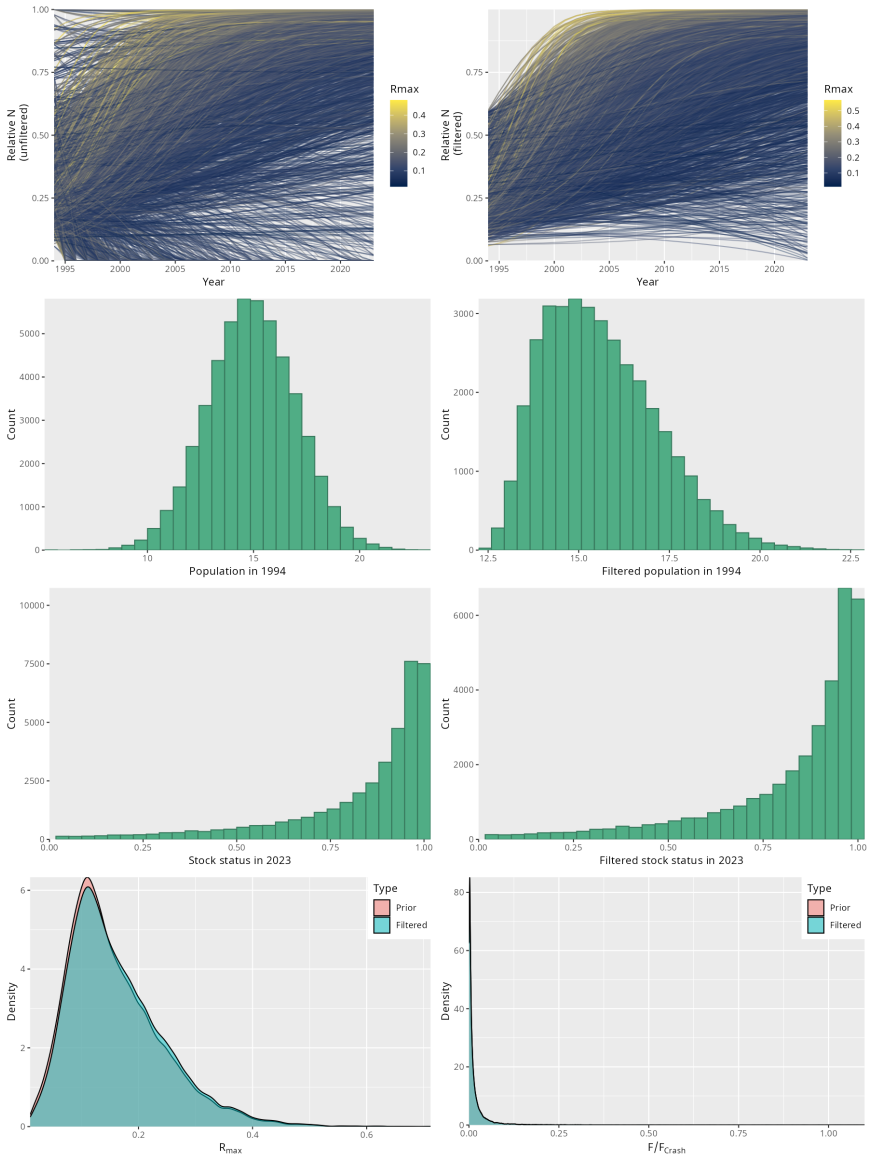

Figure 25: Summary of prior predictive simulations for oceanic whitetip shark shark. Top row: Simulated population trajectories (in terms of relative abundance N_t/K) coloured by the value of the draw from the prior distribution of R_{max}. For each simulation trajectory, a set of values for carrying capacity, initial depletion, and R_{max} were drawn from their prior distribution, and the median estimated catch from the catch reconstruction was applied. A subset of 1000 trajectories is shown on the left hand side, and a subset of 1000 trajectories from the filtered set (after applying constraints on current depletion relative to 1994). The corresponding draws from the prior distribution of stock size in 1994 are shown (2nd row) for the original prior and the constrained (filtered) prior. The prior distribution over stock status corresponding to the unconstrained prior (left) and the constrained prior (right) is shown in the third row. The constrained prior can be thought of as a joint Bayesian prior over parameters and current stock status in the simple surplus production model, and therefore implies a constrained prior for R_{max} and overfishing risk (last row; overfishing risk in terms of $F_{curr}/F_{crash} = F_{curr}/R_{max}$).

8.1 Stock synthesis assessment

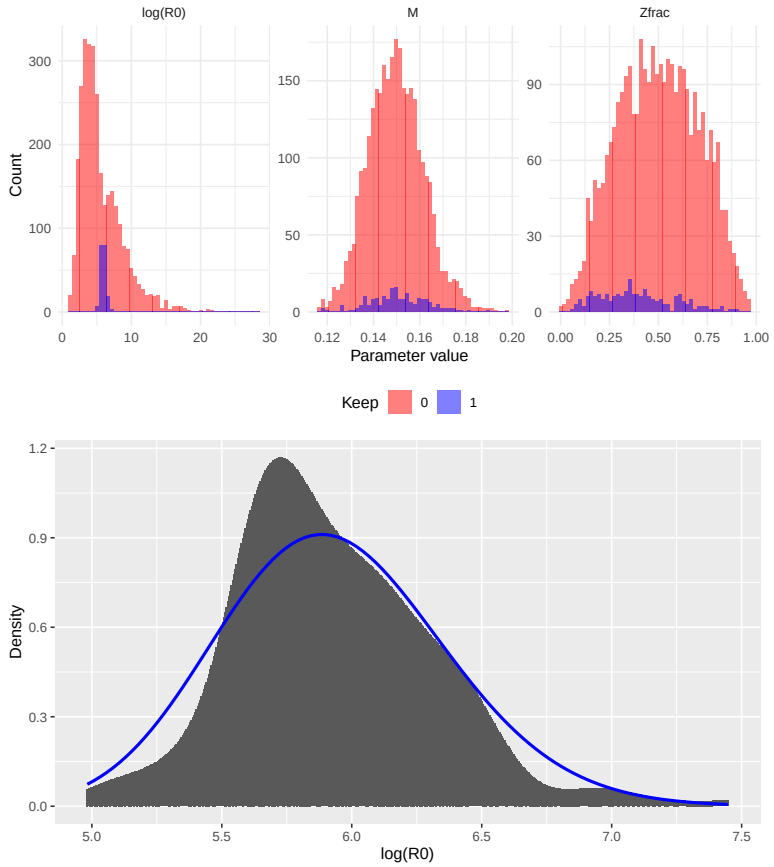

Figure 26: Prior predictive draws (red) and retained draws (purple) from 2000 simulations of the stock assessment model under priors and catches only (left panel). The updated prior for $logR_0$ was derived by fitting a log-normal distribution to the retained $logR_0$ draws after filtering.

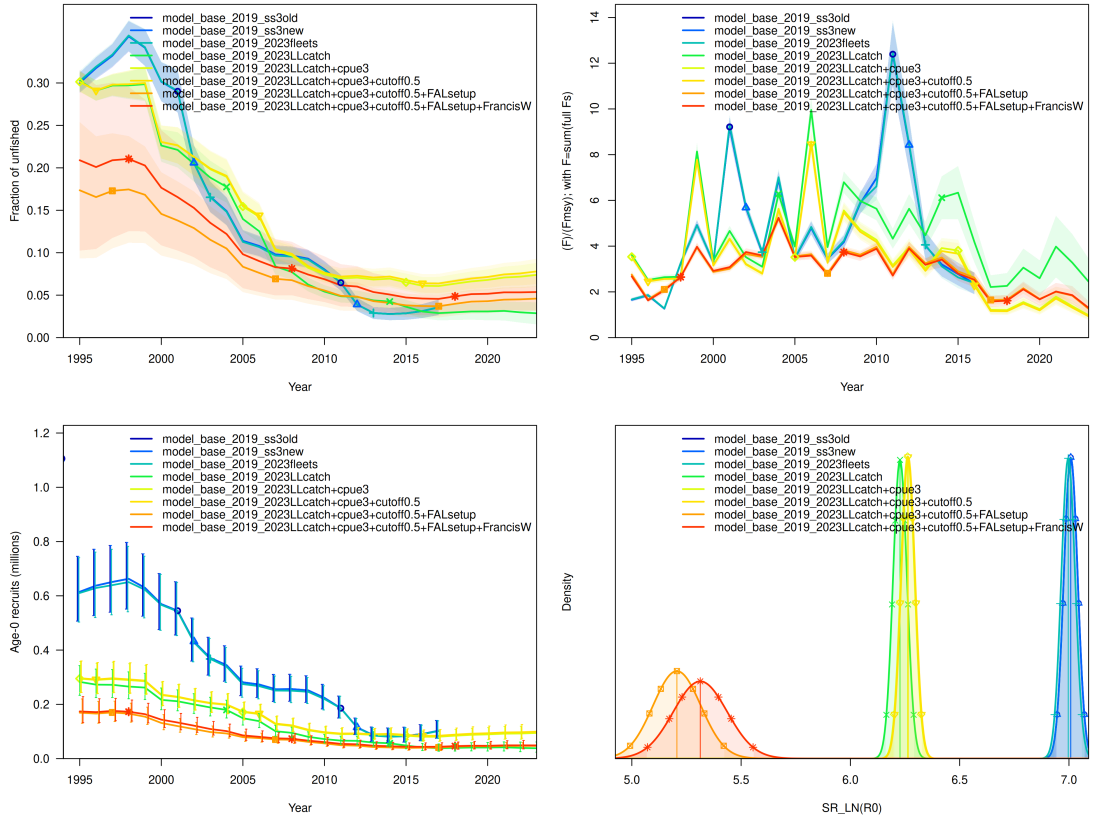

Figure 27: Stepwise model development from the 2019 diagnostic model to the 2025 diagnostic model. Shown are fraction of unfished spawning biomass (relative to equilibrium), fishing mortality, recruitment and unfished biomass size for the 2025 diagnostic, with estimated uncertainty levels from stock synthesis.

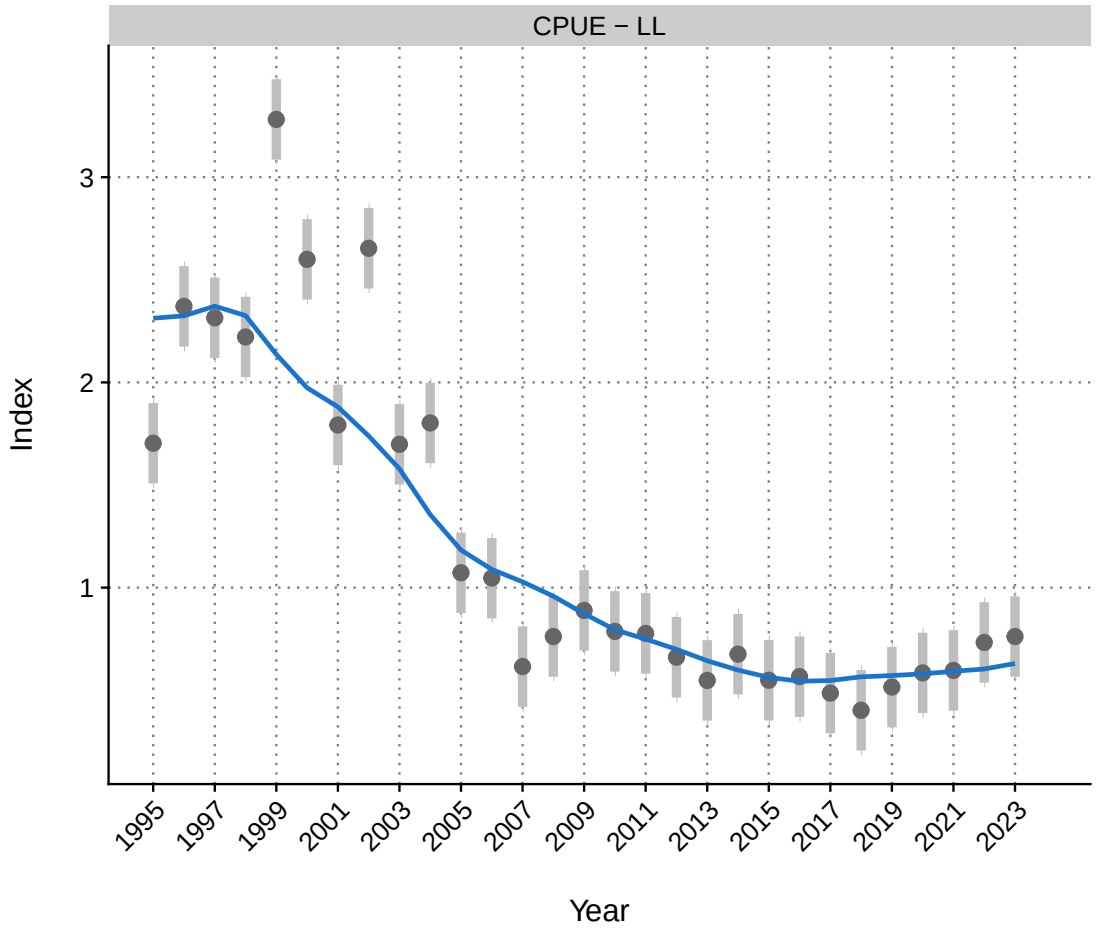

Figure 28: Observed (grey dots) vs. predicted (blue line) CPUE on the log-scale for index longline fleets under the diagnostic case, with vertical light grey bands showing the 95% credible interval for each year index.

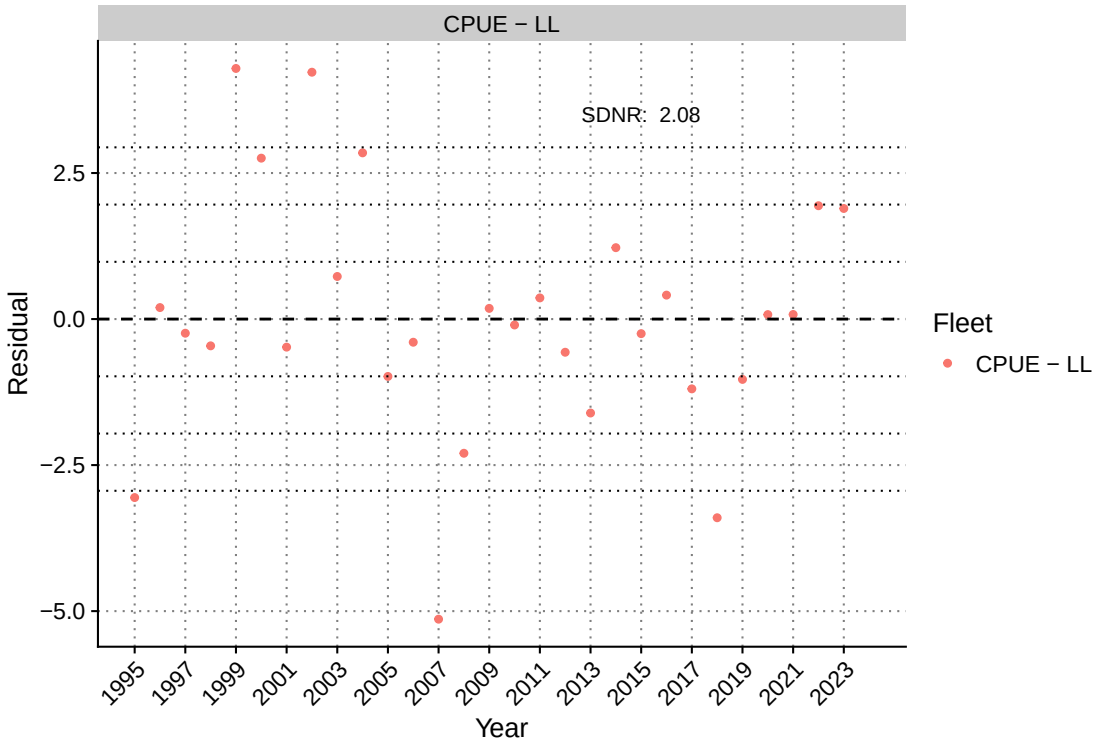

Figure 29: Residuals for CPUE indices from two longline fleets under the diagnostic case.

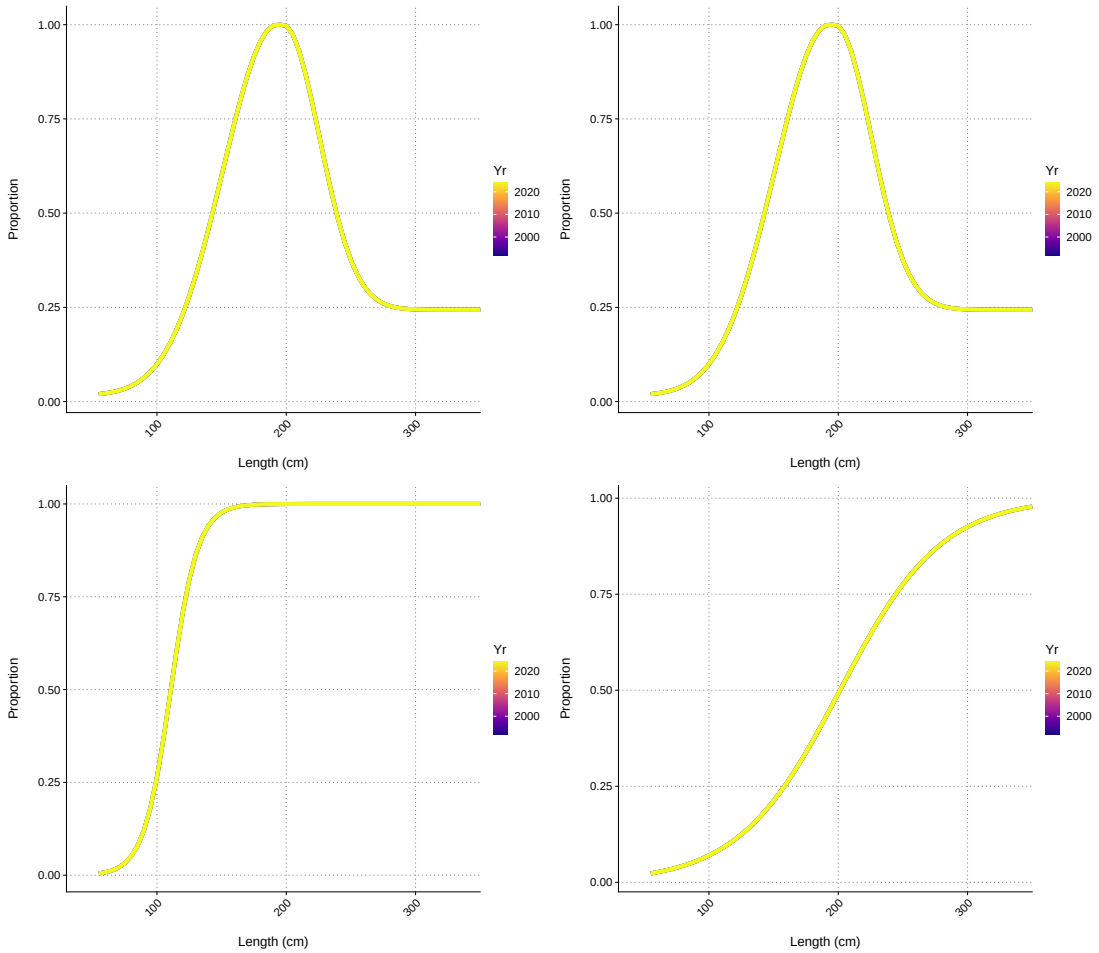

Figure 30: Mean estimated selectivity (yellow) for the longline capture fleet (top-left), longline CPUE index fleet (shared selectivity for capture and index fleets; top right), free-school purse-seine CPUE index fleet object-associated purse-seine (bottom-left) and free-school purse-seine capture fleets (bottom-right).

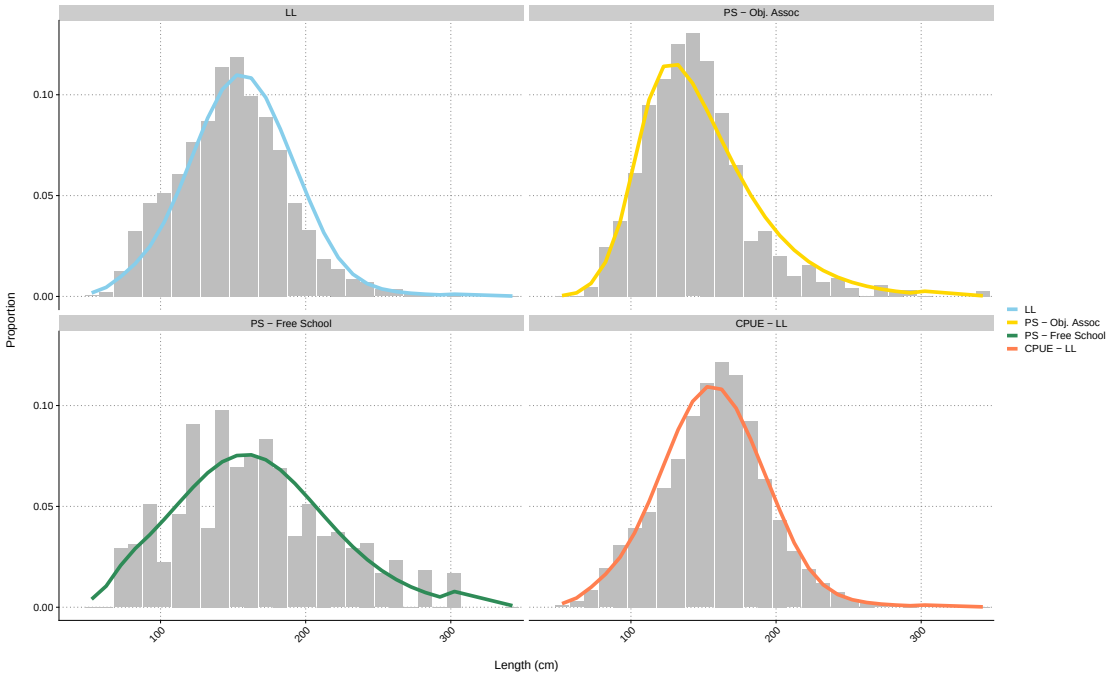

Figure 31: Observed (grey bars) vs. predicted (coloured line) catch-at-length for each fleet aggregated over all years for the diagnostic case.

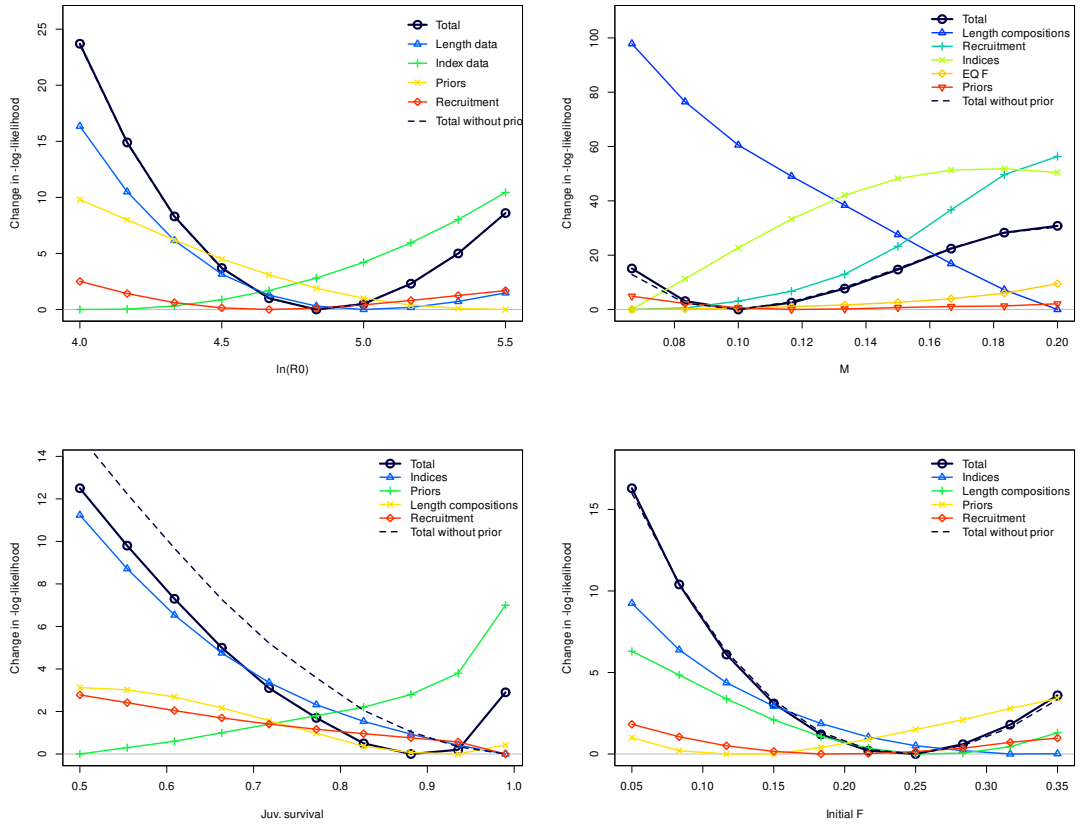

Figure 32: Relative change in log-likelihood for different values of $LN(R_0)$, M, z_{frac}, and initial F for the total likelihood and contribution by each component.

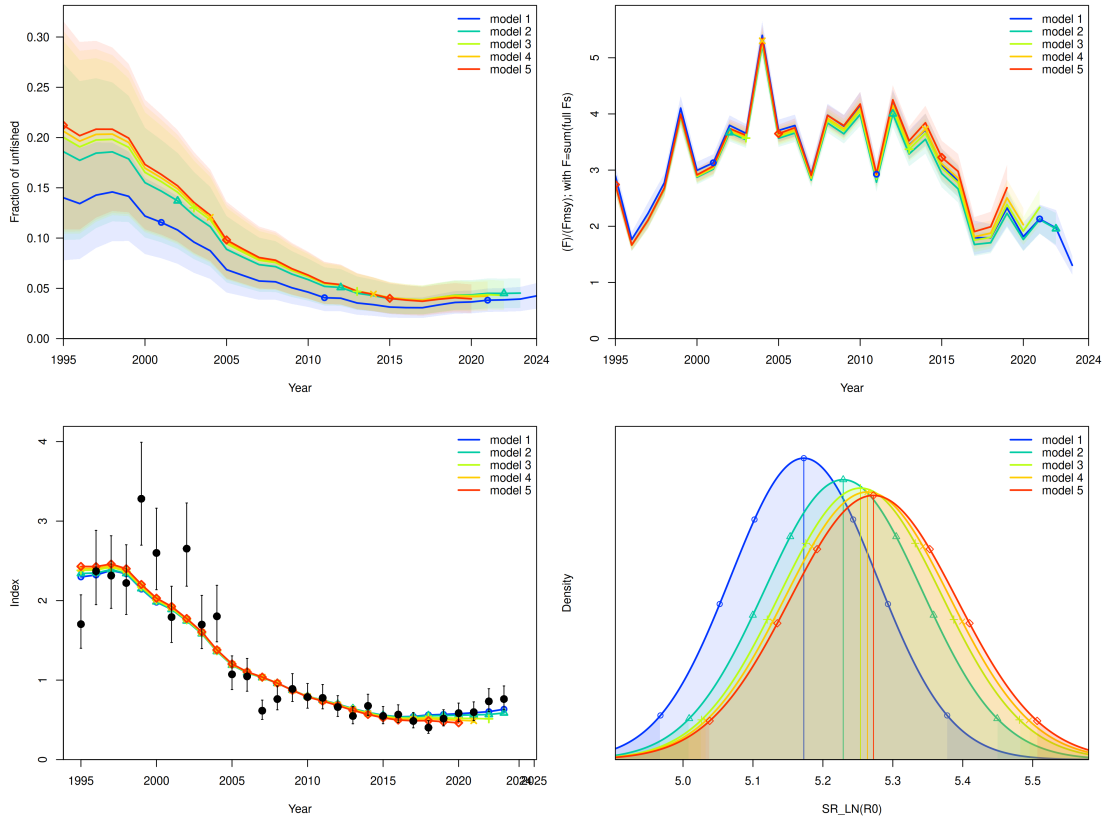

Figure 33: Retrospective patterns of fraction of unfished spawning biomass (relative to equilibrium), fishing mortality, CPUE fits and unfished biomass with estimated uncertainty levels.

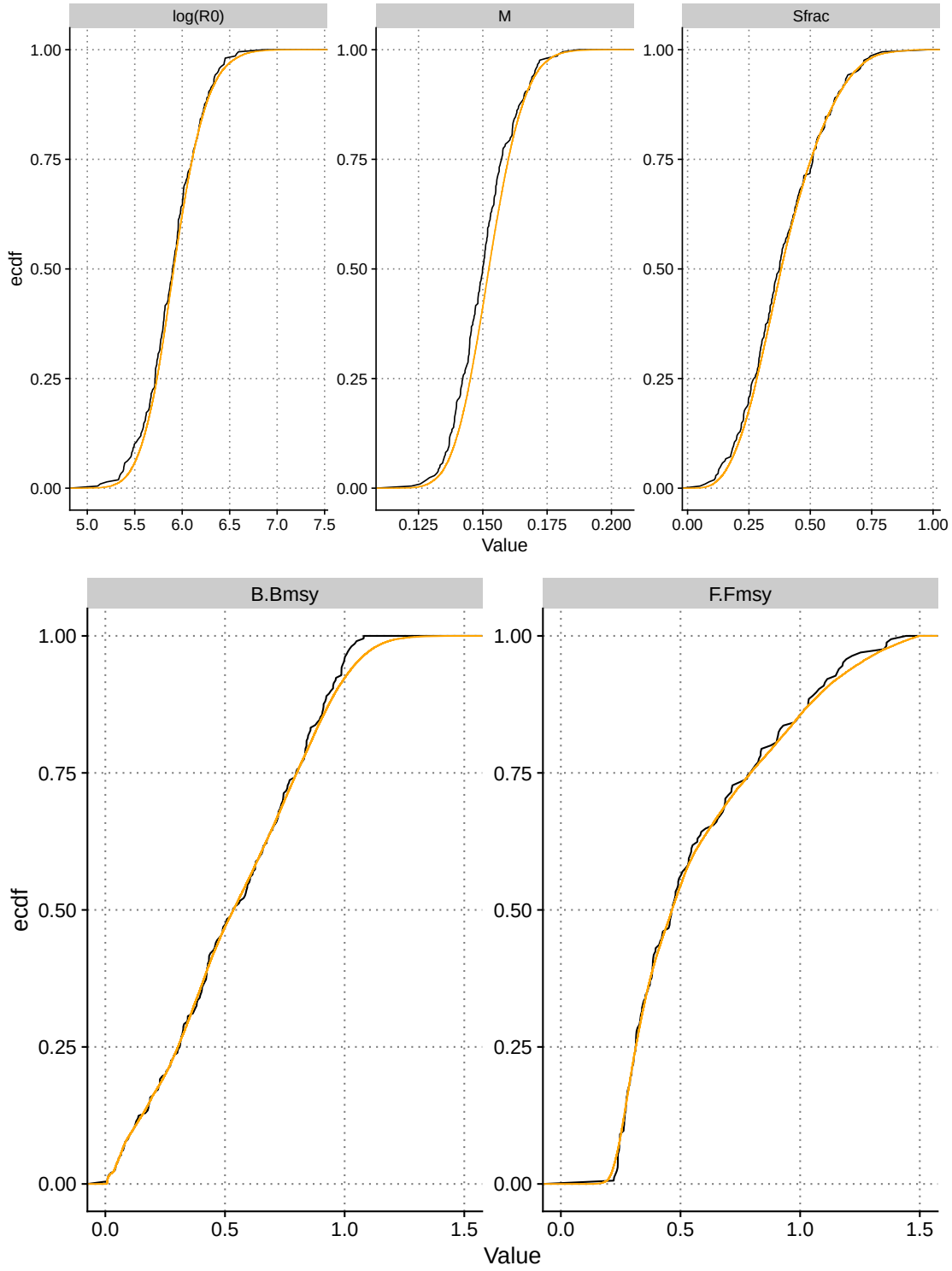

Figure 34: Comparison of the joint simulation - based calibration posterior (orange) to the cumulative distribution of prior draws that were used to simulate the SBC datasets, for model parameters (top panel) and derived management quantities (bottom panel).

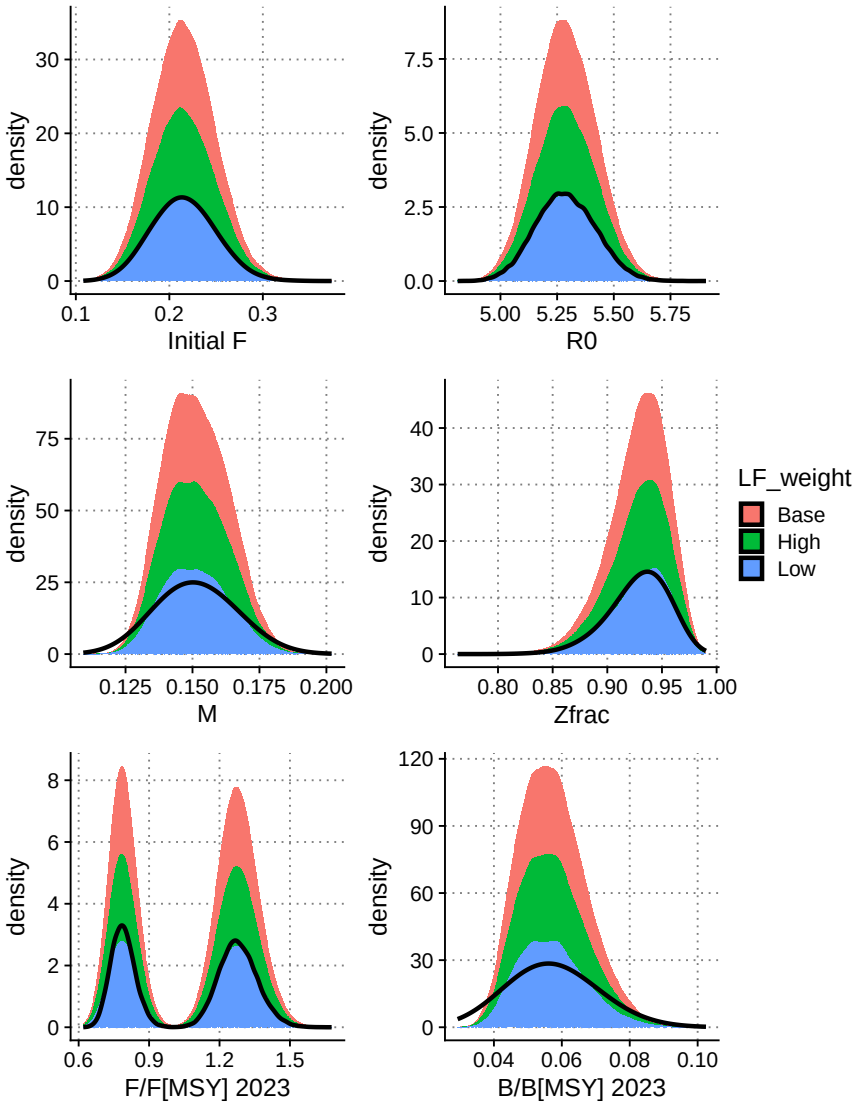

Figure 35: Posterior densities of R_O and natural mortality (M), the stock-recruit parameter z_{frac}, initial fishing mortality F, stock status and fishing mortality derived from a model ensemble length-frequency weights. The thick black lines shows the joint posterior density across parameters.

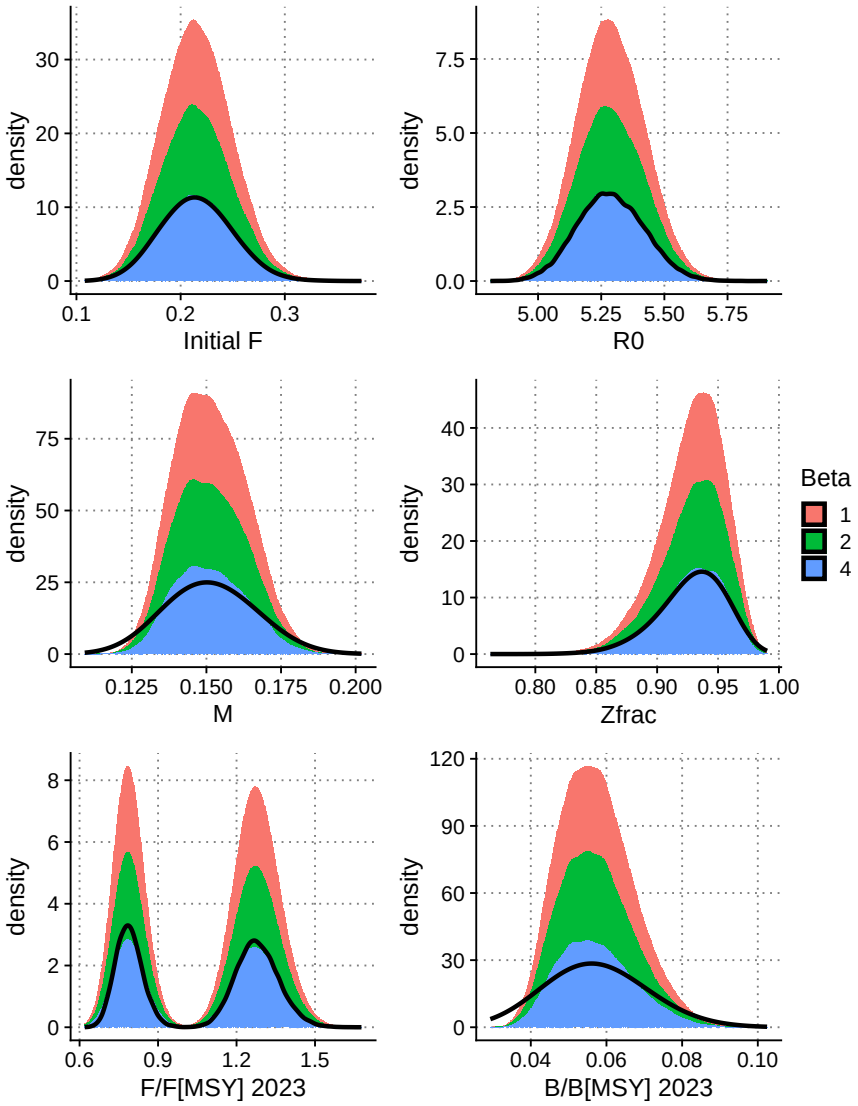

Figure 36: Posterior densities of R_O and natural mortality (M), the stock-recruit parameter z_{frac}, initial fishing mortality F, stock status and fishing mortality derived from a model ensemble across stock-recruit assumptions. The thick black lines shows the joint posterior density across parameters.

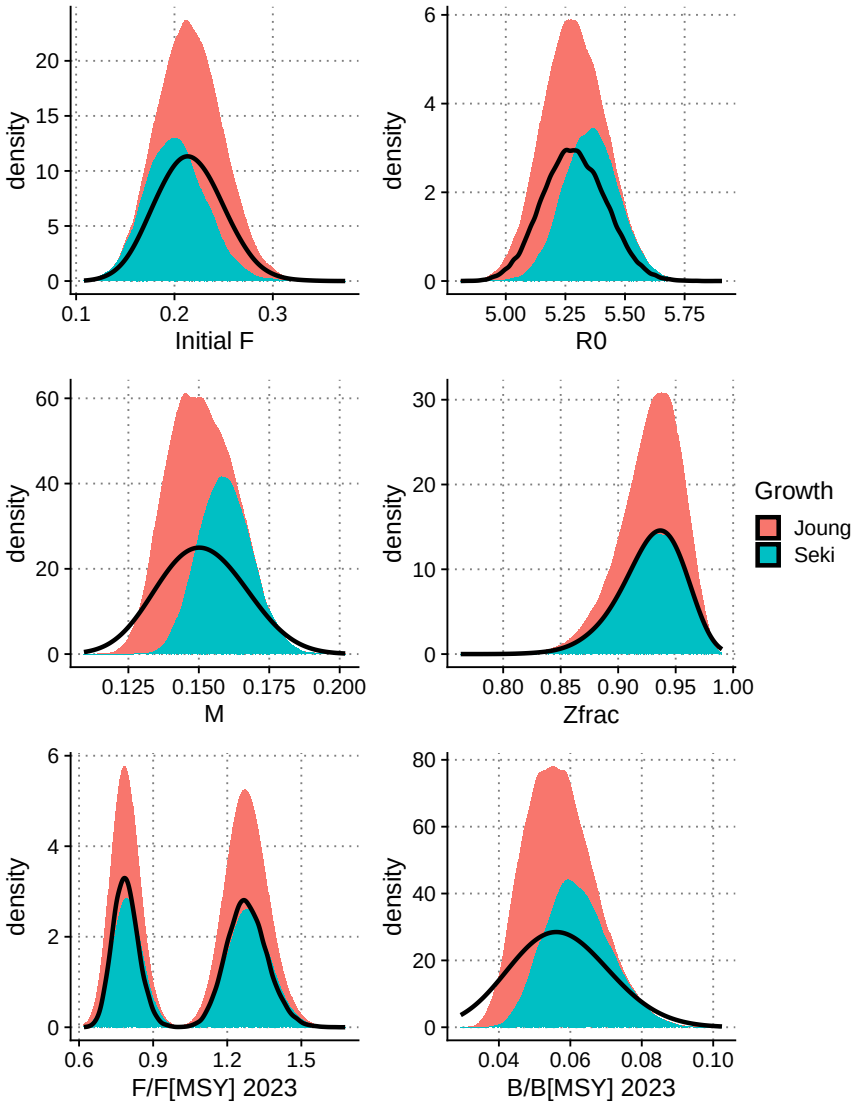

Figure 37: Posterior densities of R_O and natural mortality (M), the stock-recruit parameter z_{frac}, initial fishing mortality F, stock status and fishing mortality derived from a model ensemble across growth assumptions. The thick black lines shows the joint posterior density across parameters.

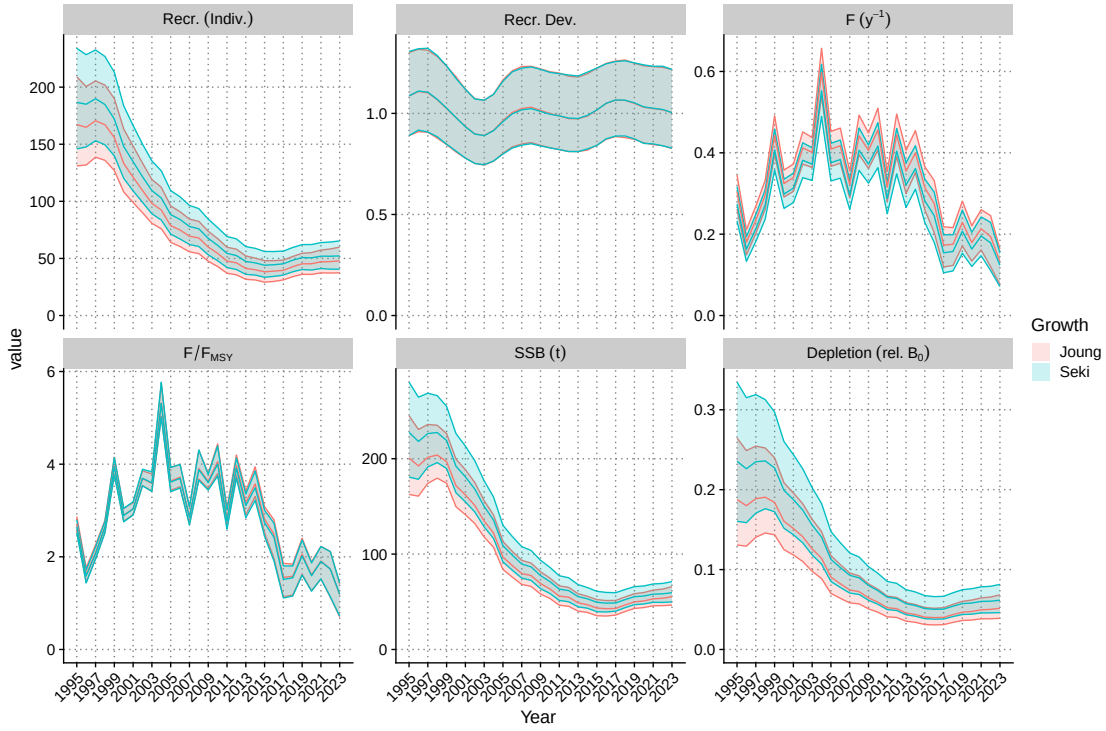

Figure 38: Catch, fishing mortality, recruitment, spawning biomass and depletion trajectories plotted by growth assumption for the ensemble formed by models over the (weighted) grid, estimated using MCMC.

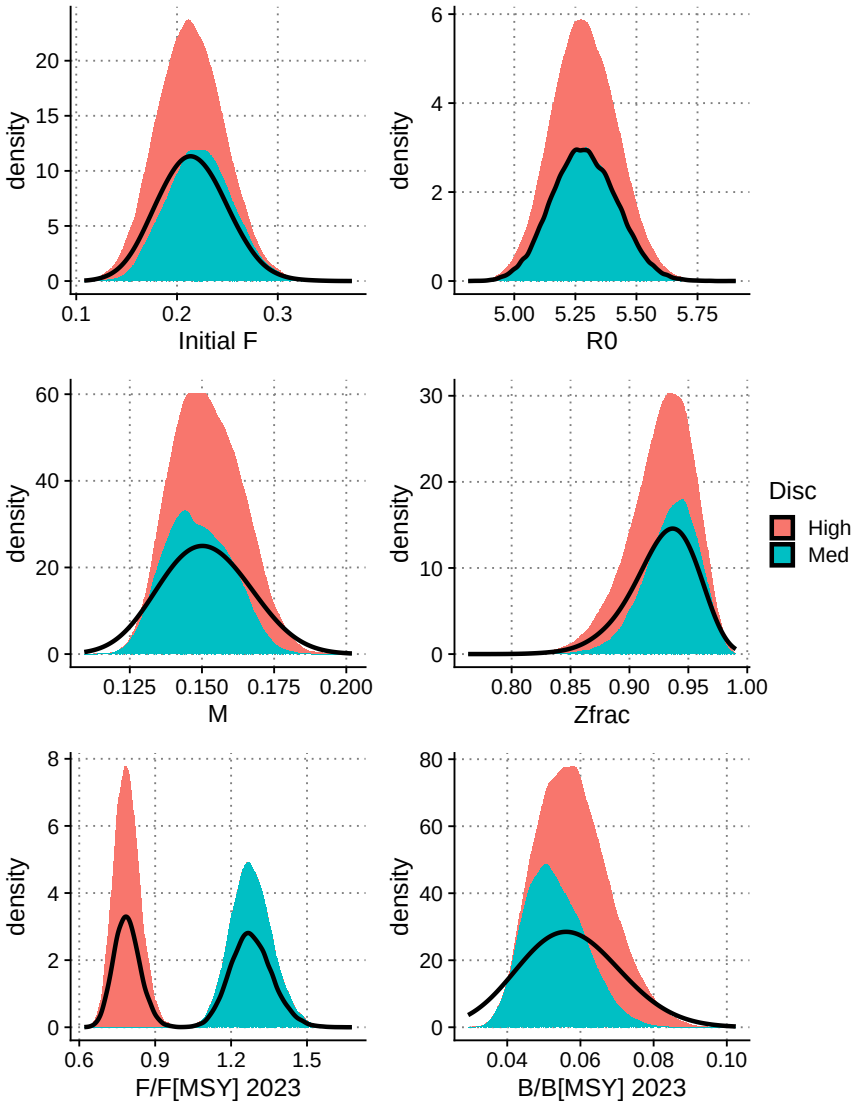

Figure 39: Posterior densities of R_O and natural mortality (M), the stock-recruit parameter z_{frac}, initial fishing mortality F, stock status and fishing mortality derived from a model ensemble across discard assumptions. The thick black lines shows the joint posterior density across parameters.

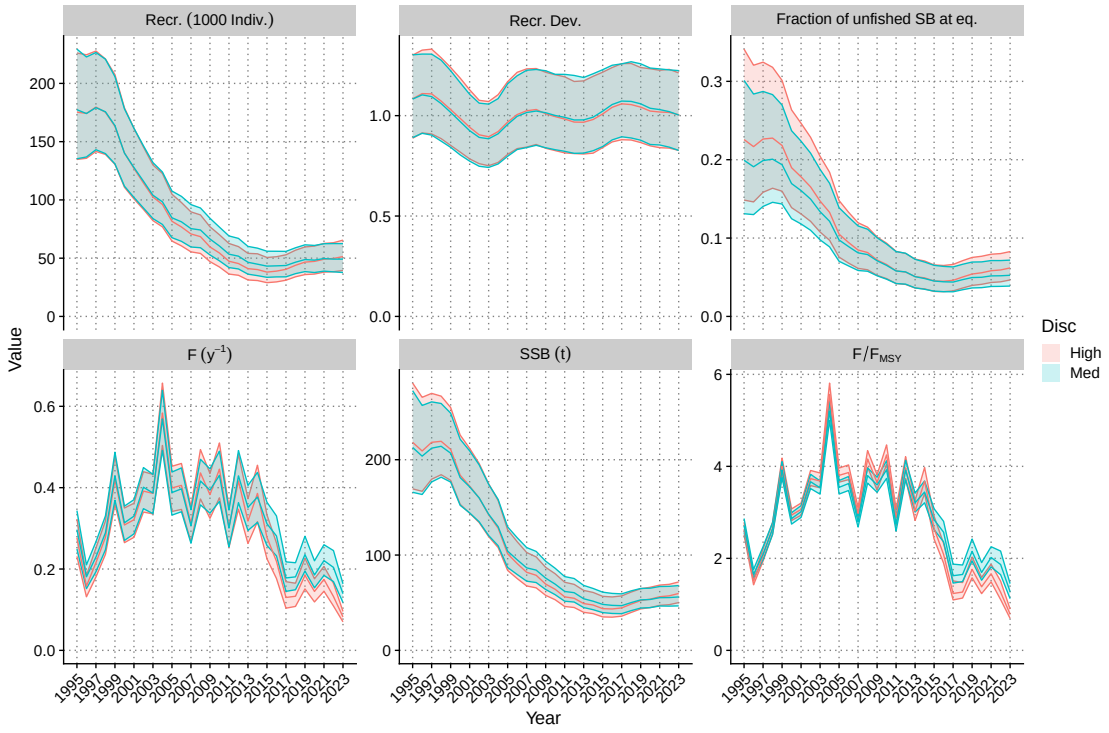

Figure 40: Catch, fishing mortality, recruitment, spawning biomass and depletion trajectories plotted by discard assumption for an ensemble formed by models over the (weighted) grid, estimated using MCMC.

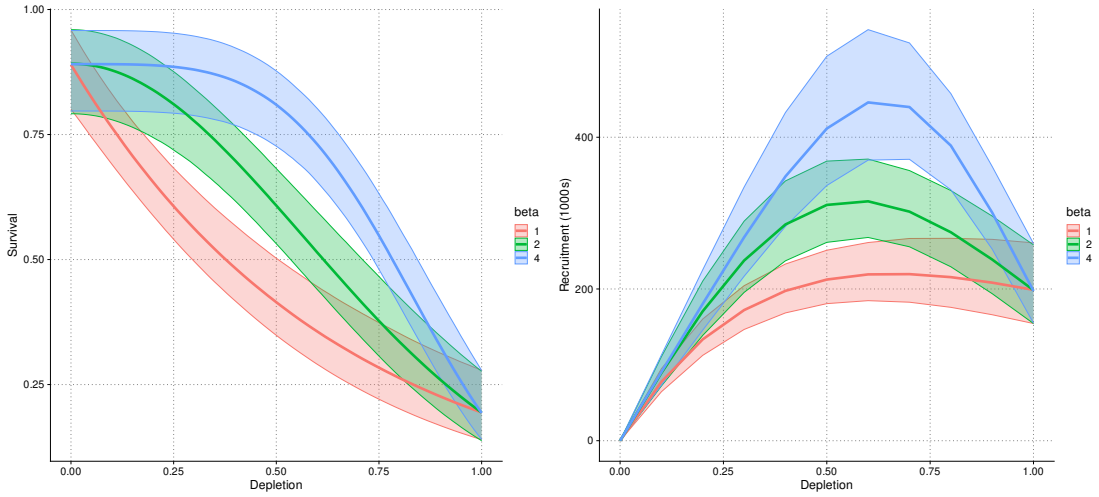

Figure 41: Estimated stock recruit relationship across the MCMC model ensemble at different levels of fixed $beta$: Expected pre-recruit-survival (left) and expected recruitment (right) with associated 95% credible intervals estimated by MCMC.

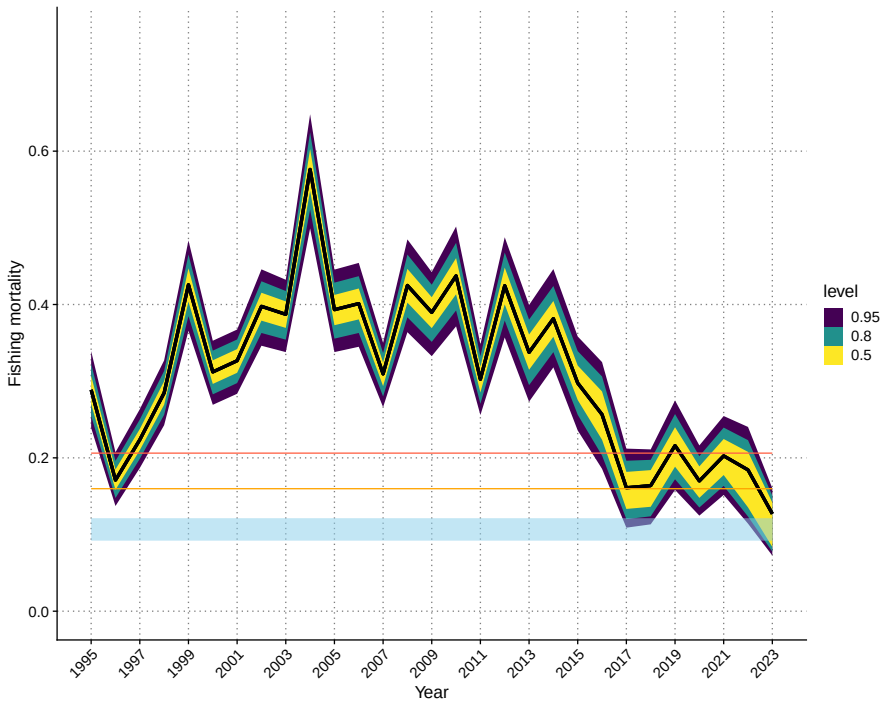

Figure 42: Posterior densities of Fishing mortality F, with posterior percentiles indicated by the colour fill. The posterior distribution of fishing mortality at MSY (F_{MSY}) is shown in green, point estimates of F_{lim} and F_{crash} are given in orange and red, respectively.

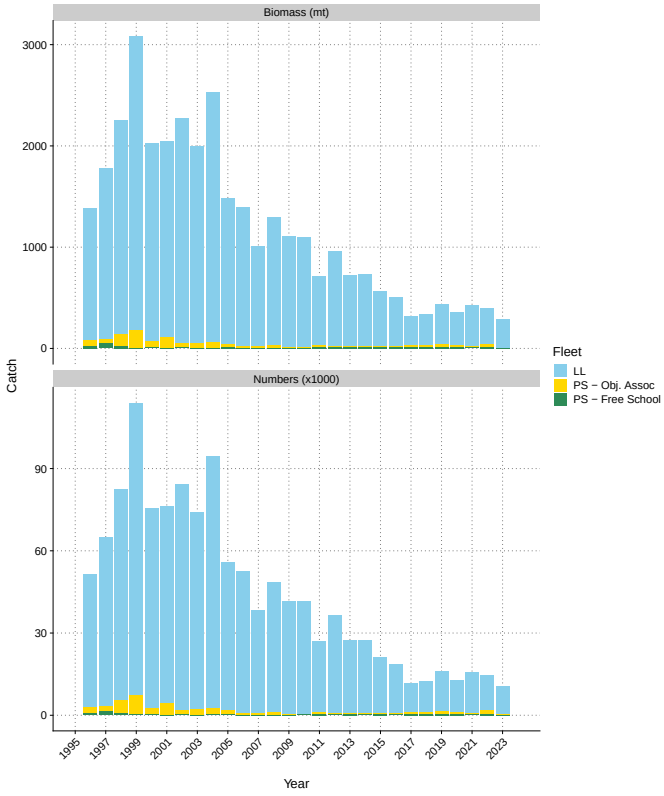

Figure 43: Retained catch by fleet in biomass and numbers.

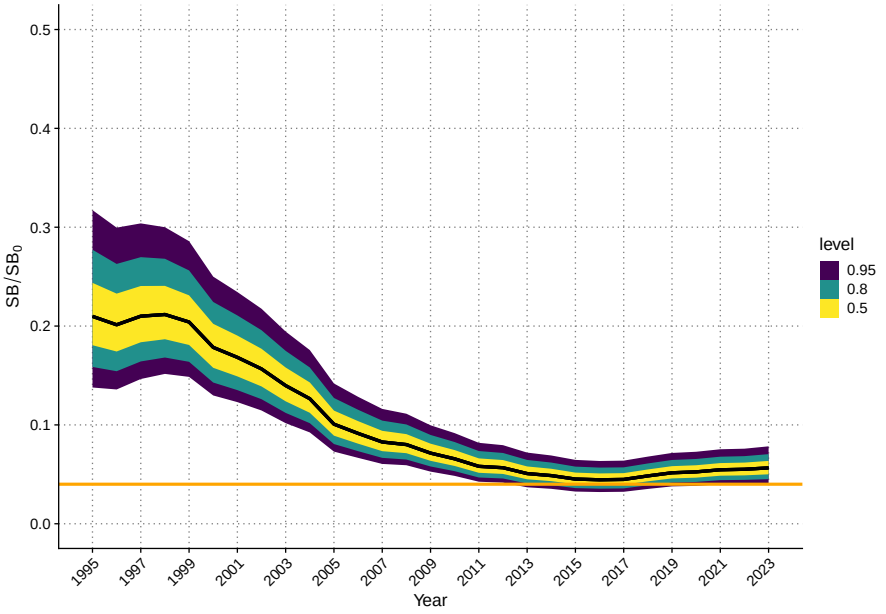

Figure 44: Posterior densities of stock status (SB/SB_0, with SB_0 the unfished spawning biomass at equilibrium), with posterior percentiles (90%, 95% and 99%) indicated by the colour fill.

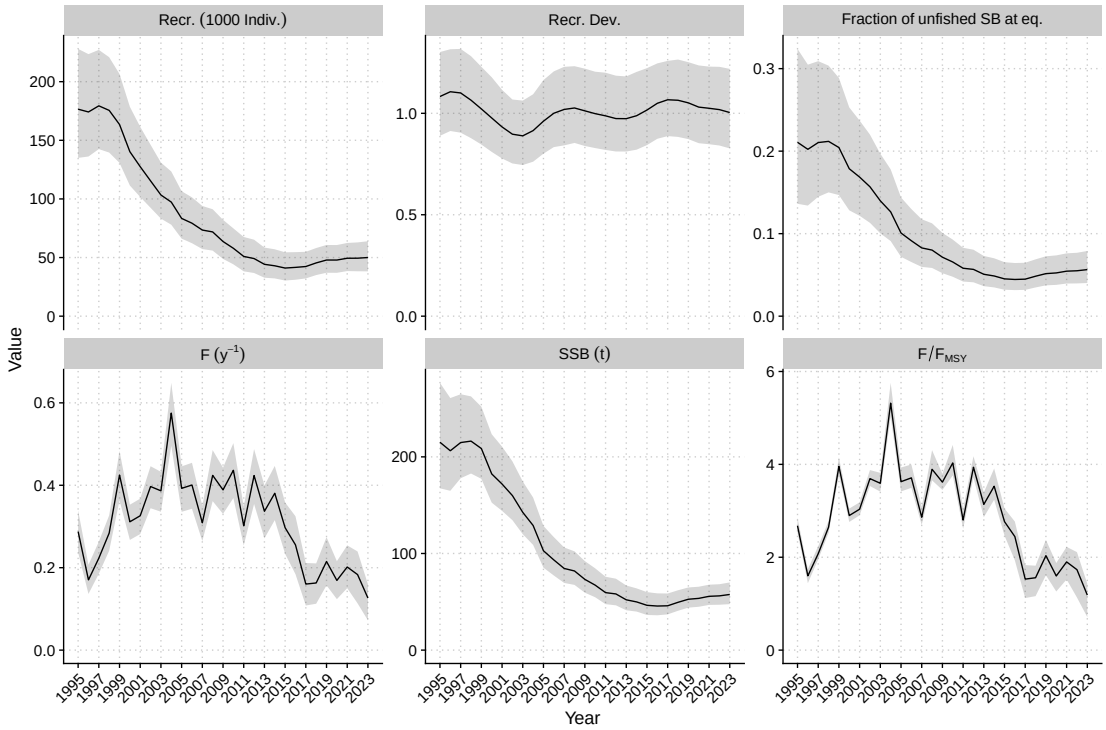

Figure 45: Catch, fishing mortality, recruitment, spawning biomass and depletion trajectories for an ensemble formed by models over the (weighted) grid, estimated using MCMC.

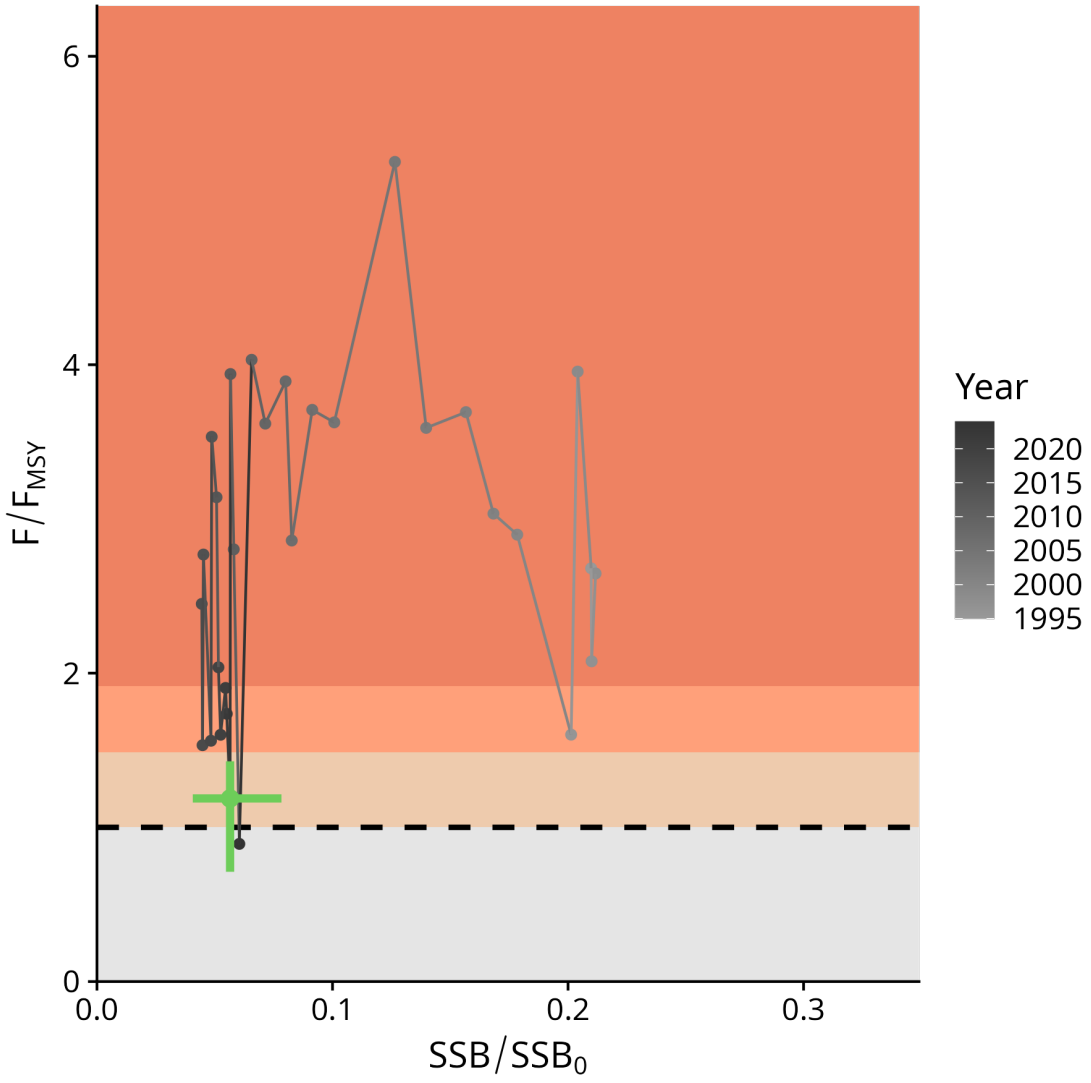

Figure 46: Majuro plots for recent stock status based on an ensemble formed by SS3 models for oceanic whitetip shark over an weighted grid of model options. The plot shows the stock trajectory, with uncertainty shown for the most recent year in the analysis (2023).

8.2 Dynamic surplus production model

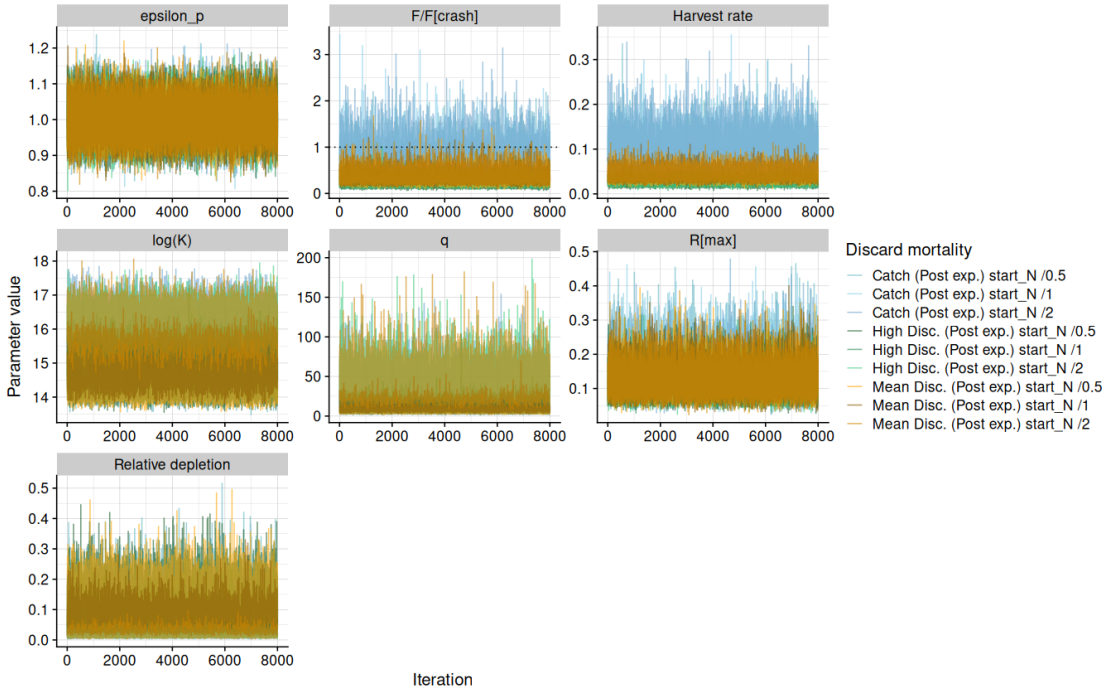

Figure 47: MCMC traces for derived parameters (harvest rate, risk of population collapse F/F_{Crash}) and selected estimated parameters (initial depletion, carrying capacity K, intrinsic population growth R_{max} and relative depletion) for different model runs with alternative prior assumptions about initial depletion.

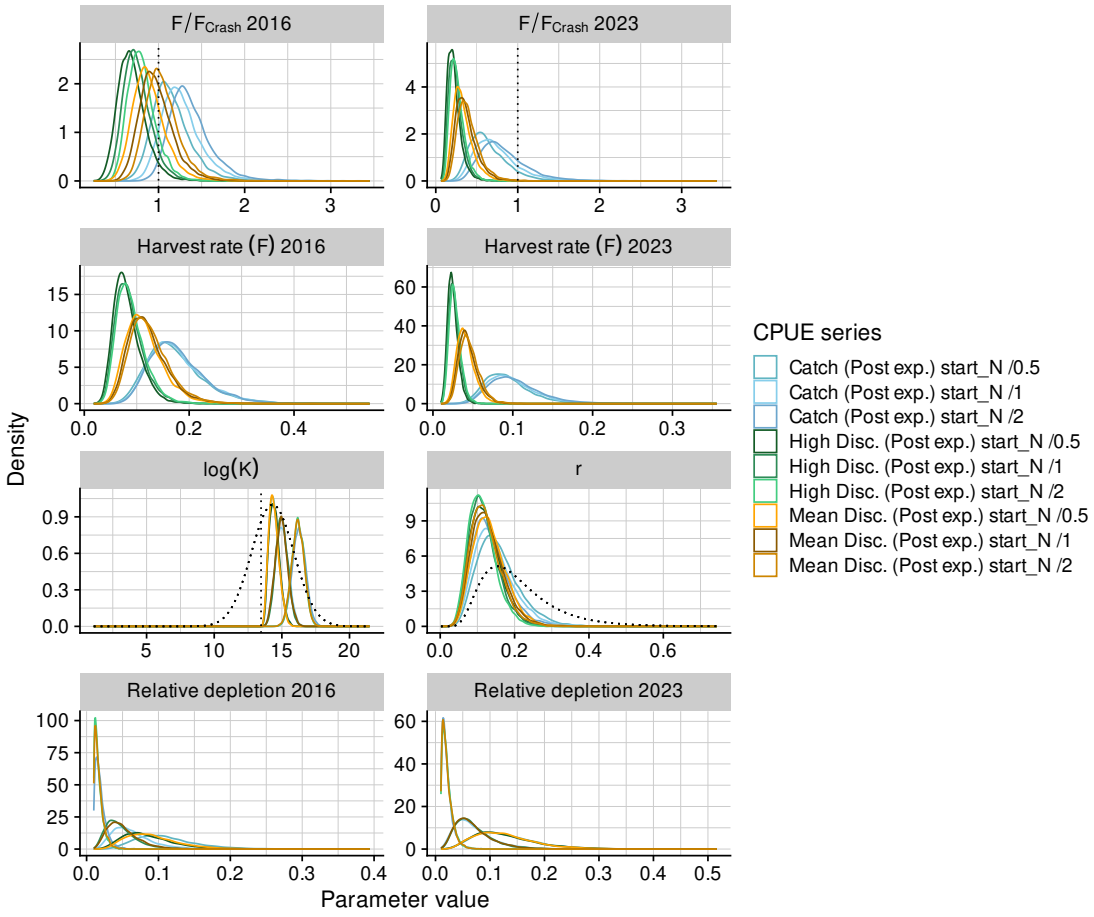

Figure 48: Marginal posterior densities for derived parameters (harvest rate, risk of population collapse F/F_{Crash}) and selected estimated parameters (initial depletion, carrying capacity K, intrinsic population growth R_{max} and relative depletion) for different model runs with alternative prior assumptions about initial depletion.

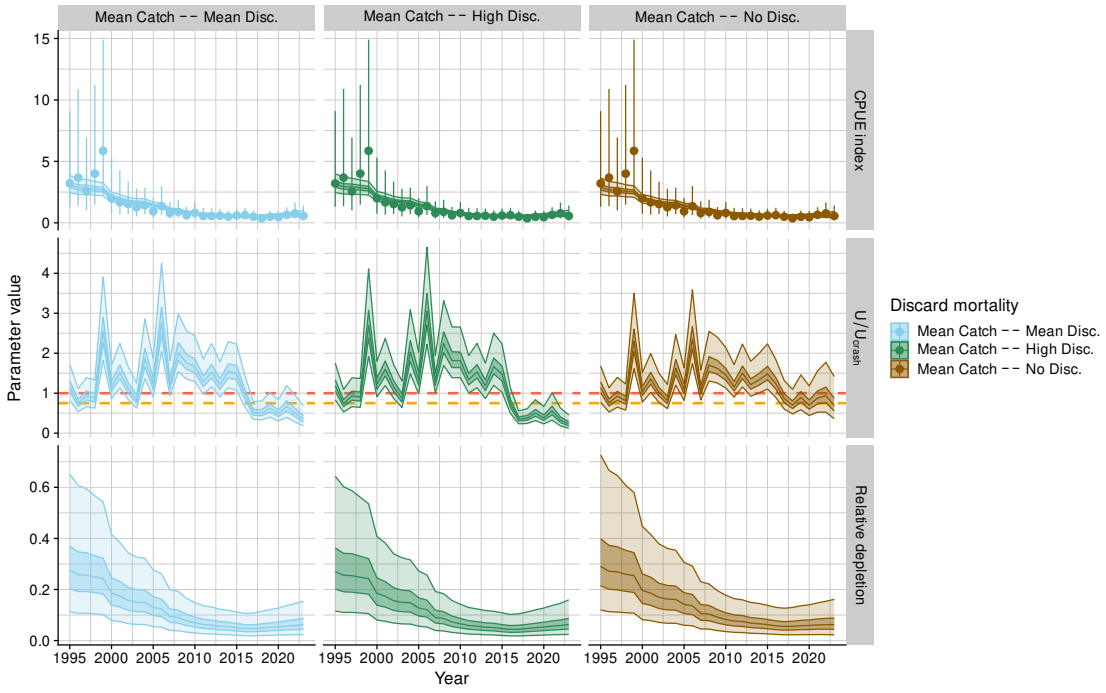

Figure 49: Dynamic surplus production model across assumptions for discard mortality (dark shading, inter-quartile; light shading, 95% credible interval). Top row: Predicted CPUE with input CPUE (points) and observation error (inter-quartile range). Middle row: Time series of fishing mortality relative to the F_{Crash} (red) and $F_{lim} = 0.75 \cdot F_{Crash}$ (orange) as estimated in the dynamic surplus production model. Bottom row: Estimated relative depletion (relative to unfished abundance K). The stock was not unfished in the first year of the time-series, and each column shows an alternative prior assumption about initial depletion.

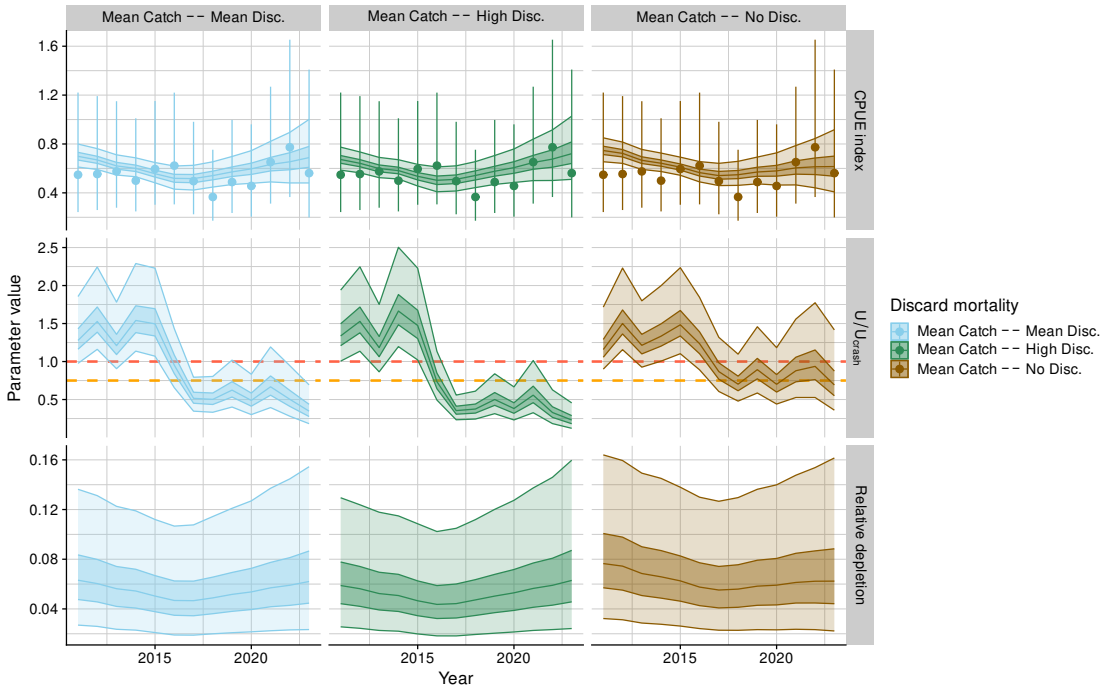

Figure 50: Focus on model fit in recent years for the dynamic surplus production model across assumptions for discard mortality (dark shading, inter-quartile; light shading, 95% credible interval). Top row: Predicted CPUE with input CPUE (points) and observation error (inter-quartile range). Middle row: Time series of fishing mortality relative to the F_{Crash} (red) and $F_{lim} = 0.75 \cdot F_{Crash}$ (orange) as estimated in the dynamic surplus production model. Bottom row: Estimated relative depletion (relative to unfished abundance K). The stock was not unfished in the first year of the time-series, and each column shows an alternative prior assumption about initial depletion.

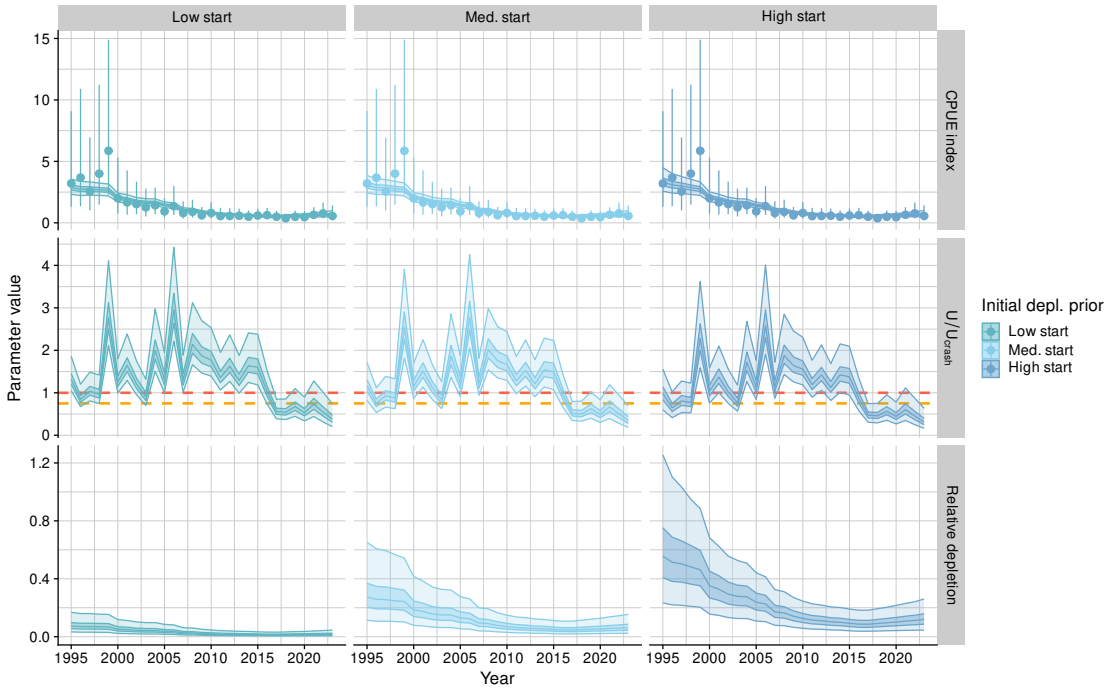

Figure 51: Dynamic surplus production model across assumptions for starting depletion levels in 1995 (dark shading, inter-quartile; light shading, 95% credible interval). Top row: Predicted CPUE with input CPUE (points) and observation error (inter-quartile range). Middle row: Time series of fishing mortality relative to the F_{Crash} (red) and $F_{lim} = 0.75 \cdot F_{Crash}$ (orange) as estimated in the dynamic surplus production model. Bottom row: Estimated relative depletion (relative to unfished abundance K). The stock was not unfished in the first year of the time-series, and each column shows an alternative prior assumption about initial depletion.

Figure 52: Focus on model fit in recent years for the dynamic surplus production model across assumptions for starting depletion levels in 1995 (dark shading, inter-quartile; light shading, 95% credible interval). Top row: Predicted CPUE with input CPUE (points) and observation error (inter-quartile range). Middle row: Time series of fishing mortality relative to the F_{Crash} (red) and $F_{lim} = 0.75 \cdot F_{Crash}$ (orange) as estimated in the dynamic surplus production model. Bottom row: Estimated relative depletion (relative to unfished abundance K). The stock was not unfished in the first year of the time-series, and each column shows an alternative prior assumption about initial depletion.

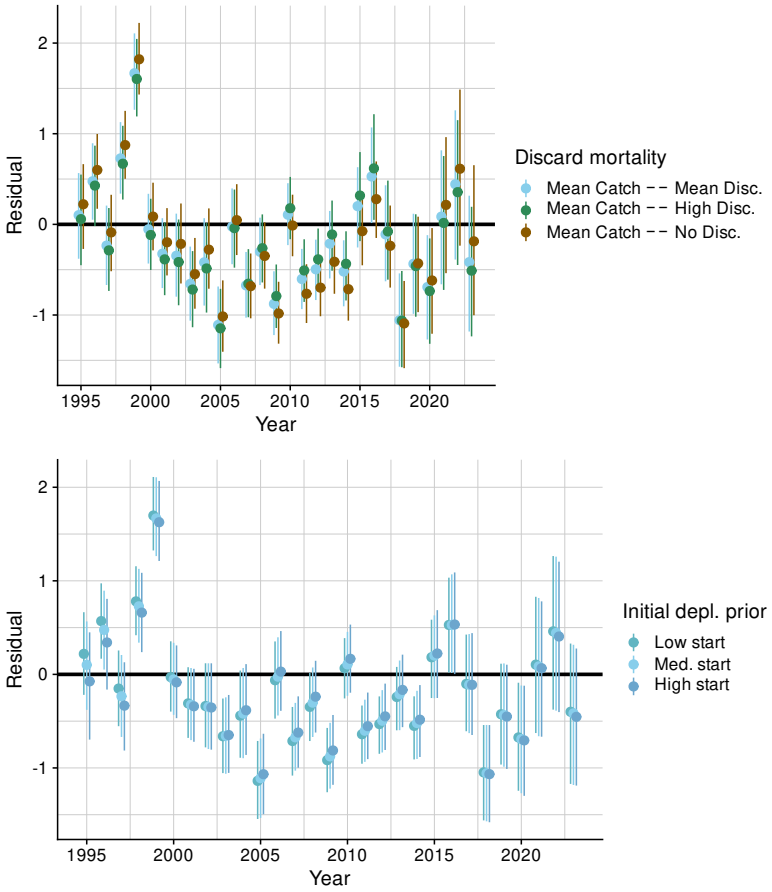

Figure 53: Standardised residuals for CPUE fits by discard and initial depletion assumption.

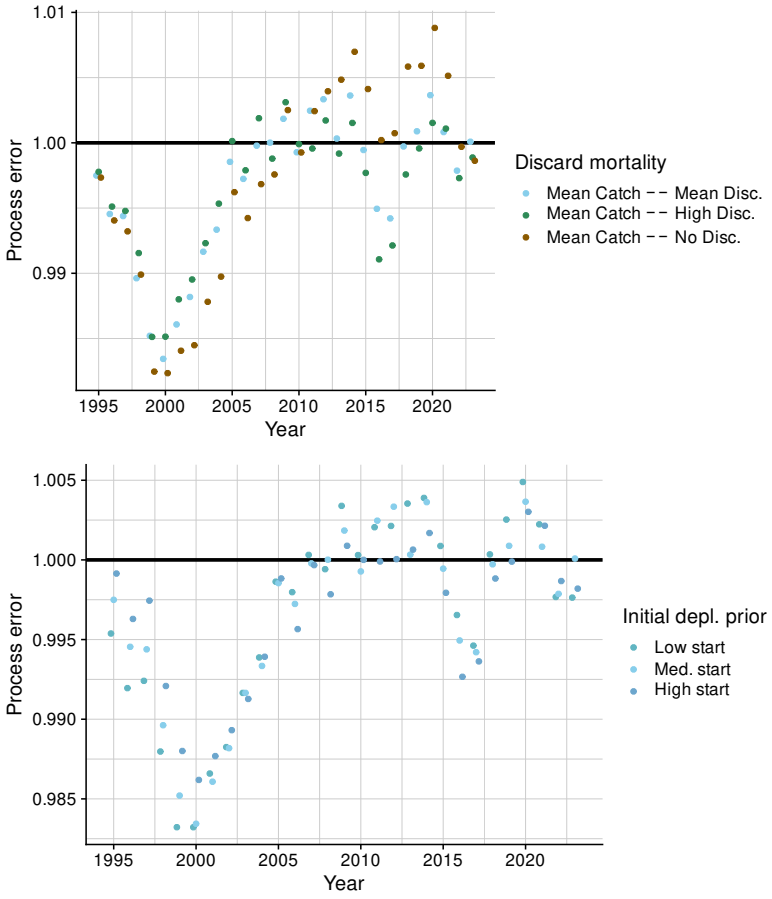

Figure 54: Estimated process error by discard and initial depletion assumption.

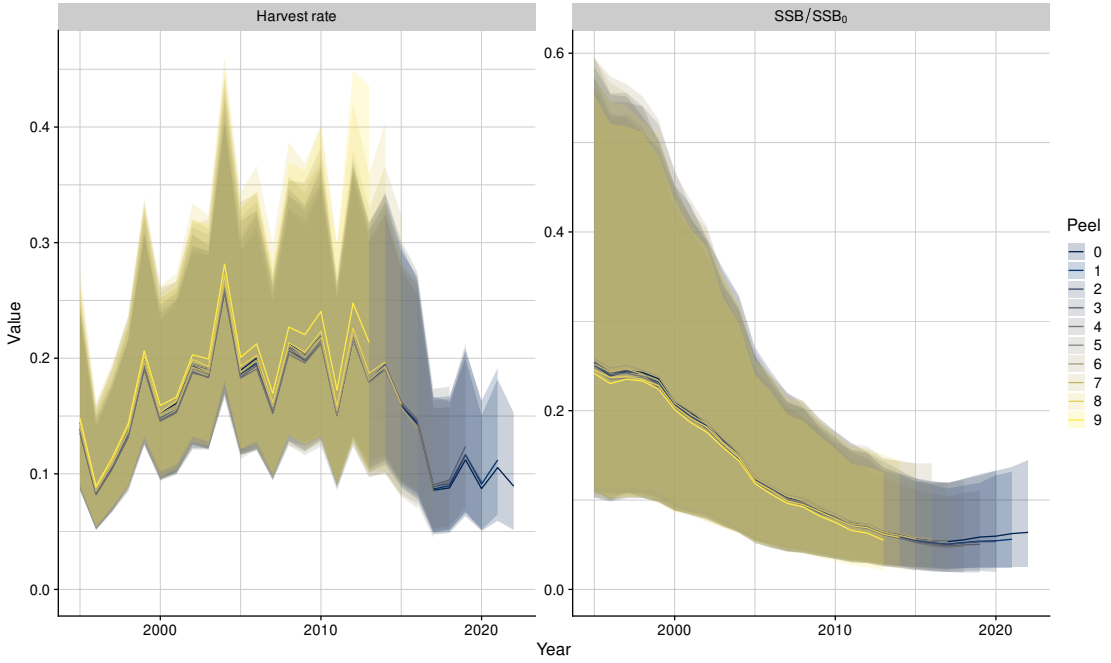

Figure 55: Retrospectives for harvest rate and biomass depletion for the base initial depletion assumption used for the dynamic surplus production model for oceanic whitetip shark.

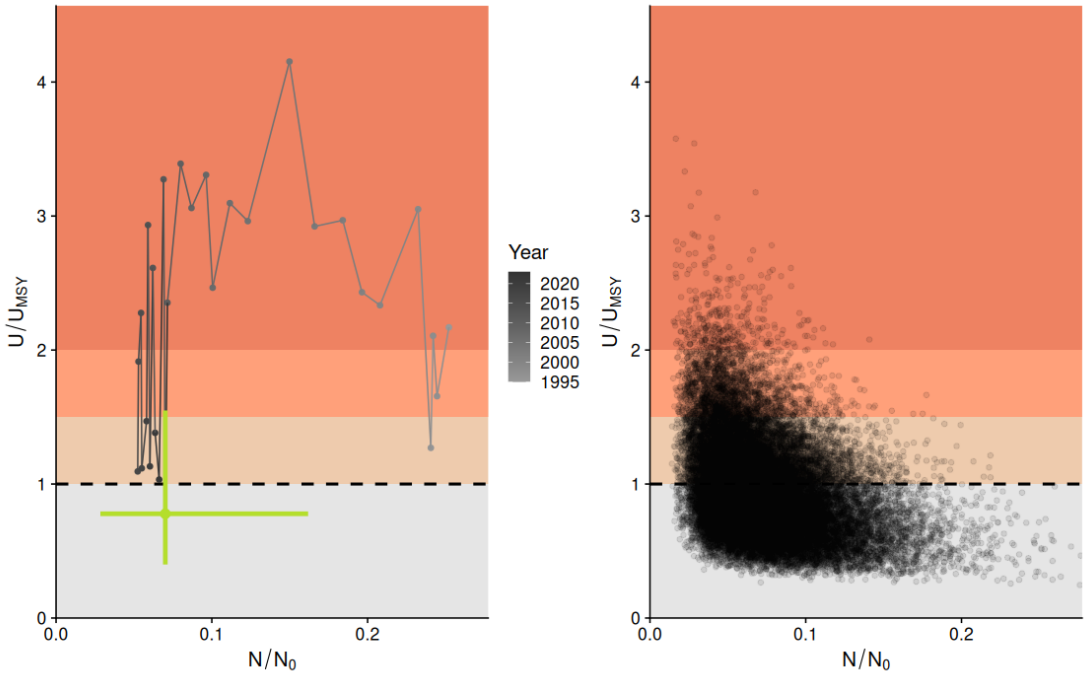

Figure 56: Majuro plots for recent stock status based on the dynamic surplus production model for oceanic whitetip shark in the WCPFC. The plot shows the stock trajectory, with uncertainty shown for the most recent year in the analysis (2023), whereas the plot on the right-hand side show individual draws from the posterior distribution(s) for recent (2022–2023) years.

8.3 Model Comparison

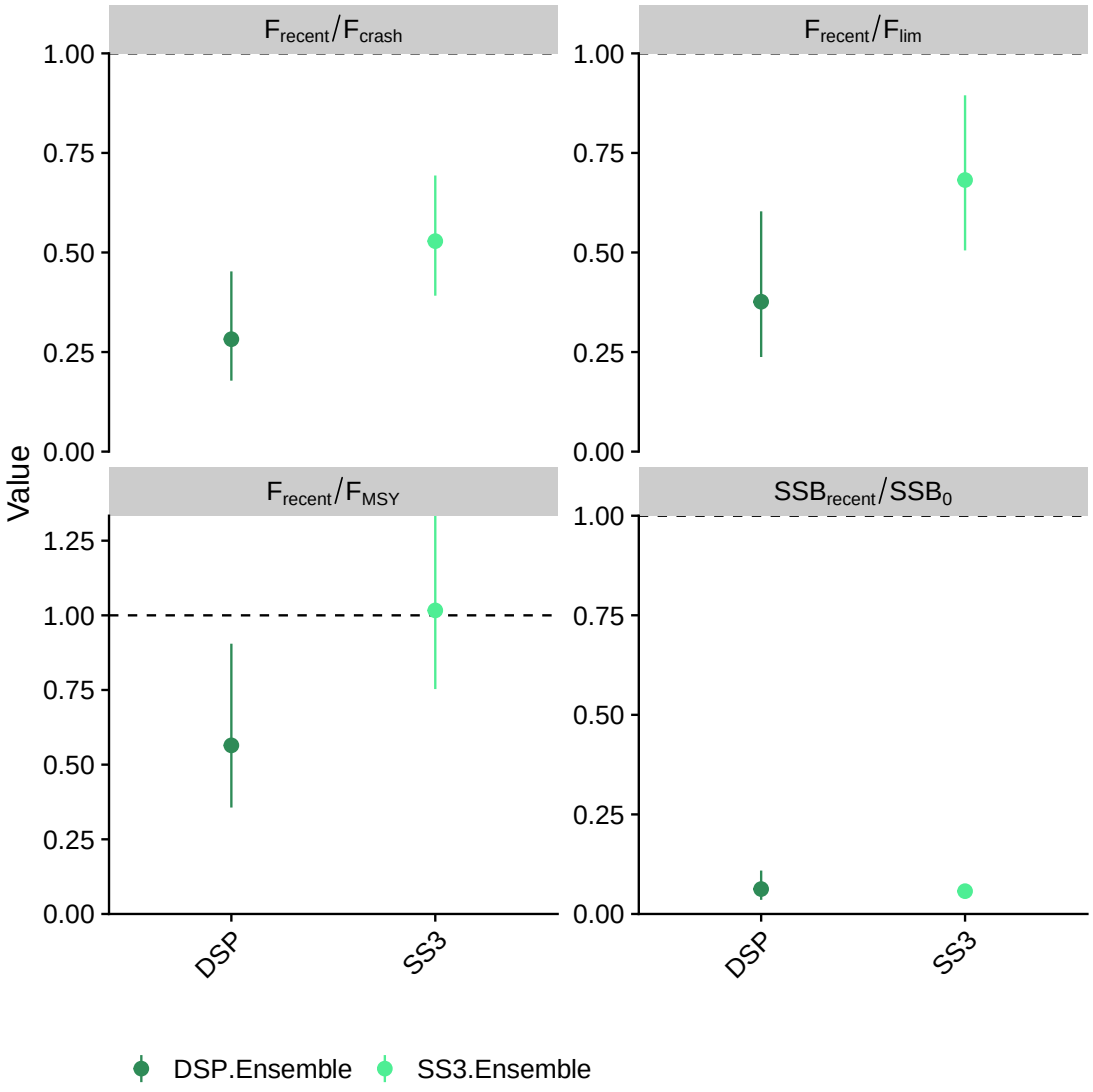

Figure 57: Estimates of management quantities (stock status as SSB_{recent}/SSB_0, and fishing mortality (F) relative to indicators (F_{MSY}) and possible limit reference points F_{lim}, F_{crash} (note, these should be read as harvest rates for the dynamic surplus production model); across model ensembles. P(>RP) refers to the probability that the metric (status, fishing mortality) is above the respective indicator (B_0, F_{MSY}, F_{lim}, F_{crash}). SS3: Stock Synthesis 3, DSP: Dynamic surplus production.

APPENDIX A ADDITIONAL FIGURES

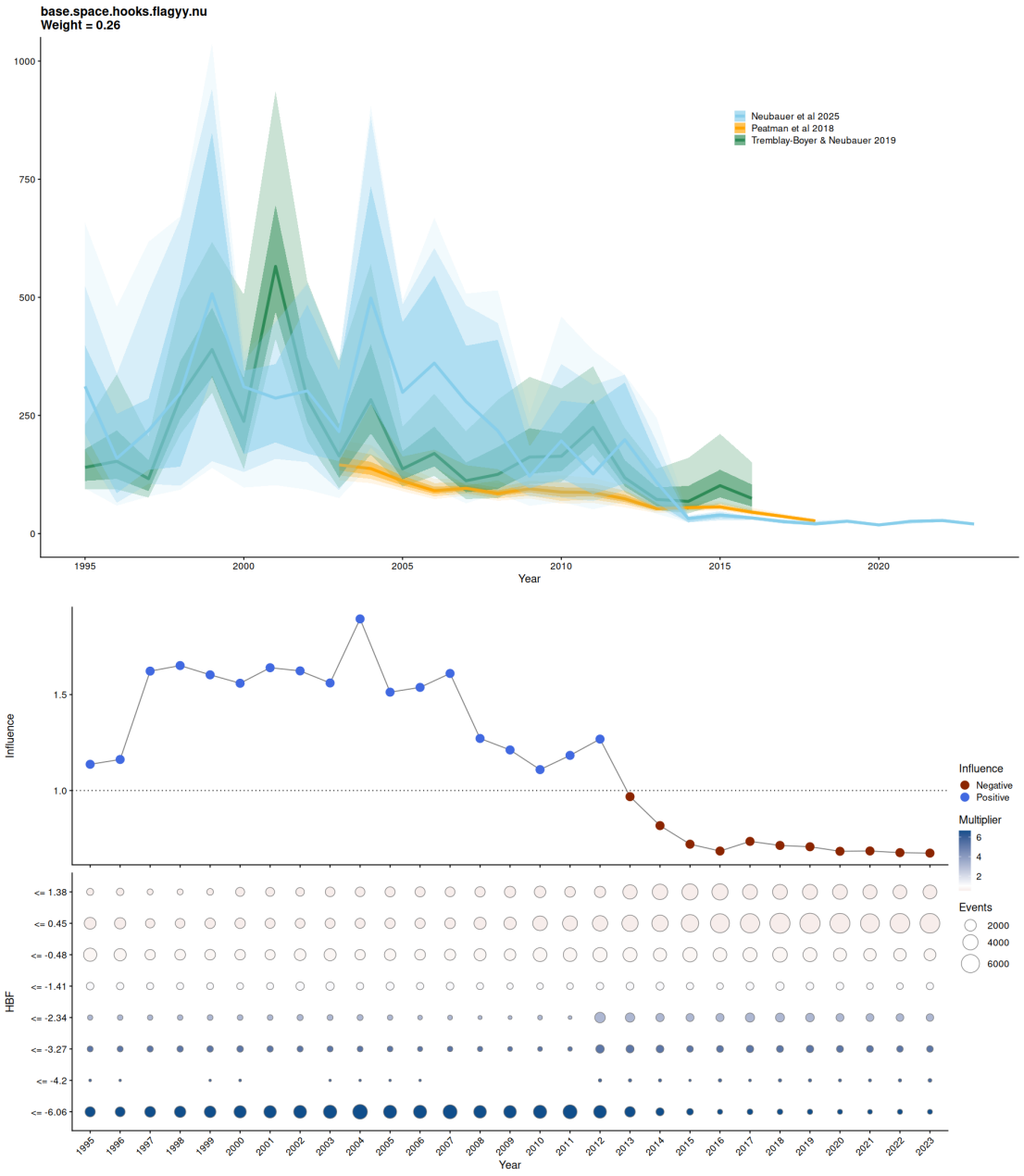

Figure A-1: Comparison of catch reconstruction predictions from three alternative studies (top panel); the blue estimate uses similar assumptions about reported hooks-between-floats (HBF; reported zeros are true HBF) as the green estimate. The bottom panel shows the influence of assumed HBF on predictions when reported zeros for HBF are treated as data. Note, that this catch time-series was not considered reliable and was therefore not used, as zero HBF records were judged to be missing data or errors, as opposed to true records of HBF.